Matthias Gilgien

Characterisation of Skiers' Mechanics, Course Setting and Terrain Geomorphology in World Cup Alpine Skiing using Global Navigation Satellite Systems

Injury Risk, Performance and Methodological Aspects

DISSERTATION FROM THE NORWEGIAN SCHOOL OF SPORT SCIENCES • 2014

ISBN nr 978-82-502-0500-0

Table of contents

Acknowledgements

This thesis was undertaken in the Department of Physical Performance at the Norwegian School of Sport Sciences, Oslo, Norway and was funded by the Norwegian School of Sport Sciences and the International Skiing Federation (FIS).

The thesis was conducted in collaboration with the Department of Sport Science and Kinesiology, University of Salzburg, Austria; the Group for Snow Sports at the WSL – Insitute for Snow and Avalanche Research SLF, Davos, Switzerland, the Laboratory of Movement Analysis and Measurement at the Ecole Polytechnique Federal Lausanne, Switzerland and the Institute of Geodesy and Photogrammetry at ETH Zurich, Zurich, Switzerland.

Firstly, I would like to thank my supervisiors Prof. Dr. Erich Müller and Prof. Dr. Jan Cabri who gave me the opportunity, means and support to complete my thesis in this multi-center project. It is known that field measurements in winter sports are challenging to conduct. But collecting data in World Cup competitions is where science and the real world meet. It was great to have your guidance and backing whenever needed.

Secondly, I would like to thank my co-workers in the FIS ISS project core group, Dr. Jörg Spörri, Dr. Josef Kröll and Dr. Julien Chardonnens, and my master students and scientific assistants Philip Crivelli, Cynthia Unholz and Geo Boffi for a fantastic team work and adventure 24/7, literally.

Further, I would like to thank the persons who have contributed to the project in additionen to the ones mentioned above: Prof. Dr. Alain Geiger, Benjamin Hinterberger, Christian Josef, Fabian Wolfsperger, Hansueli Rhyner, Patrick Thee, Per Haugen, Dr. Philippe Limpach, Rüdiger Jahnel, Robert Kenner, Dr. Robert Reid, Ron Kipp, Prof. Dr. John Seifert.

And last but most I thank my family and friends for their support and for allowing me to hide behind a screen for 4 years. Grazie fitg grondamain spezialmain: Ellen, Ruth, Urs, Sabine, Manuel and Barbara, WG - GS und alli GS and GS-inne.

List of papers

This thesis is based on the following papers, which are referred to in the text by their Roman numerals:

Paper I. Determination of the centre of mass kinematics in alpine skiing using differential Global Navigation Satellite System.

Paper II. Determination of external forces in alpine skiing using a differential Global Navigation Satellite System.

Published in Sensors (Physical Sensors), Basel (http://www.mdpi.com/1424-8220/13/8/9821).

Paper III. The effect of different Global Navigation Satellite System methods on positioning accuracy in sports applications.

Paper IV. Course setting and terrain characteristics in World Cup Alpine Skiing.

Paper V. External forces in World Cup Alpine Skiing for the disciplines Giant Slalom, Super-G and Downhill.

Paper VI. Mechanical parameters related to injury risk in World Cup alpine skiing – a comparison between the competition disciplines.

Published in British Journal of Sports Medicine under the title: Mechanics of turning and jumping and skier speed are associated with injury risk in men's World Cup alpine skiing: a comparison between the competition disciplines (http://bjsm.bmj.com/content/48/9/742.full).

Abbreviations

Differential. GNSS method using data from two GNSS units. Correction signals from a stationary unit are used to enhance the accuracy of a moving unit.

DTM. Digital terrain model.

GDOP. Geodetic Dilution of Precision

GNSS. GNSS is the umbrella term for global navigation satellite systems, while the more widely used term GPS is the name of the American global navigation satellite system. The current study makes use of both the Russian (GLONASS) and the American (GPS) system. We therefore use GNSS as the collective term for both.

INS. Inertial Navigation Systems

PDOP. Position Dilution of Precision

PP. Postprocessing

RTK. Real Time Kinematic

Standalone. GNSS method using data only from one receiver to calculate position and speed.

Summary

This study was undertaken to characterize course setting, terrain geomorphology and skier mechanics in World Cup (WC) alpine skiing. Since there was no existing appropriate methodology to capture skier mechanics across large capture volumes under WC racing conditions in speed disciplines, a novel method was invented. The method was based on a global navigation satellite system (GNSS) and was tailored to assess position, velocity, acceleration and external forces while causing minimal interference to the athlete. The method was assessed in a field study against an independent reference system and found valid to assess skier position, velocity, acceleration and external forces in WC alpine skiing. Furthermore, the position results of five different geodetic GNSS methods were compared to an independent reference system. The comparison revealed that differential GNSS applying GPS and GLONASS satellite systems and the satellite signal frequencies L1 and L2 was the only configuration which consistently yielded postion results that were accurate enough to capture alpine skiing under WC conditions.

The motion capture method was applied in male WC alpine skiing competitions in the disciplines giant slalom (GS), Super-G (SG) and downhill (DH). Seven GS, five SG and five DH races were assessed in this study. The GNSS device was carried by one forerunner per race and collected data for entire runs. Prior to the races, course setting and terrain geomorphology were captured using static differential GNSS. The captured positions were used to compute digital terrain models (DTM) of the race courses including gate positions. The DTM, the skiers' GNSS trajectory and the method developed in the first part of the study were used to compute the position, velocity, acceleration and external forces of the forerunner.

The captured data from WC races were used to comprehensively and quantitatively characterize skier mechanics, course setting and terrain geomorphology for the disciplines GS, SG and DH in male WC alpine skiing. The study revealed that variability in course setting was introduced by the horizontal gate distance and that the horizontal gate distance tended to decrease with decreasing terrain inclination in GS. Gates were set close to terrain transitions. Terrain was on average steepest in GS followed by SG and DH. Extreme terrain inclination changes along the skiers' trajectory per unit time skiing were overrepresented in DH, while extreme changes per unit distance were overrepresented in GS. Mean speed was found to be 17.7 m/s in GS, 23.8 m/s in SG and 25.6 m/s in DH. Skiers skied straight (turn radius > 125m) for approximately 45% (DH), 20% (SG) and 7% (GS) of the time. The median ground reaction force was found to be 1.46 BW in GS, 1.42 BW in SG and 1.21 BW in DH. The median air drag force was 0.07 BW in GS, 0.09

BW in SG and 0.13 BW in DH. Ski–snow friction was the main contributor to energy dissipation in GS and SG, while in DH the contribution of air drag and ski–snow friction was approximately equal.

The data on skier mechanics were used to assess if the differences in injuries per 1000 runs between disciplines could be explained by differences in skier mechanics between disciplines. This investigation showed that WC alpine skiing is approximately equally dangerous, per unit of time, for all disciplines. In contrast, the skiers' mechanical characteristics were significantly different between disciplines. Therefore, it is likely that the causes and mechanisms of injury are different for the specific disciplines. In SG and DH, injuries might be mainly related to higher speed and jumps, while injuries in the technical disciplines might be related to a combination of turn speed and turn radius resulting in high loads.

1 Introduction

1.1 Problem Outline

Alpine skiing is a well-recognized competition sport and is part of the Olympic program. The International Skiing Federation (FIS) organizes World Championships, World Cup and Continental Cups. Races are held in four main competition disciplines: Slalom (SL), giant slalom (GS), super-G (SG) and downhill (DH). The sport suffers from an extensive injury problem and is considered a high-risk sport. Therefore the FIS established a network of scientific institutions comprising the Injury Surveillance System (ISS). The members of the ISS were commissioned to assess epidemiology, injury mechanisms and risk factors and to invent preventive measures to reduce the extent of the injury problem. The identification process for injury risk factors revealed that speed and the relationship between speed and course setting were major risk factors. Therefore, FIS commissioned the Department of Sport Science and Kinesiology at the University of Salzburg, Austria, and the Department of Physical Performance at the Norwegian School of Sport Sciences to assess that topic from a mechanical perspective. Since quantitative data on course setting, terrain geomorphology and skier mechanics in WC alpine skiing were lacking, these relationships could not be assessed immediately. Quantitative data on course setting, terrain geomorphology and skier mechanics had to be captured to allow an assessment of the relationship between the three factors. Hence, the current study was designed to quantify course setting, terrain geomorphology and skier mechanics of male WC alpine skiing for the disciplines GS, SG and DH. In addition, there was no existing motion capture system tailored and validated to assess skier mechanics in WC alpine skiing conditions and for speed disciplines. Therefore a Global Navigation Satellite System (GNSS)-based method was invented and validated to simultaneously capture point mass kinematics, mechanical energy and kinetics in WC alpine skiing.

1.2 Research Context

The FIS Medical Committee established the Injury Surveillance System (ISS) prior to the 2006/07 World Cup season and commissioned the Oslo Sports Trauma Research Center (OSTRC) to systematically investigate epidemiology in World Cup racing. Following the injury prevention sequences of (Van Mechelen, Hlobil, & Kemper, 1992), the extent of the injury

problem in terms of the frequency and severity of injuries was analysed (Florenes, Bere, Nordsletten et al., 2009; Bere, Florenes, Nordsletten et al., 2013). In a second step, injury mechanisms (Bere, Florenes, Krosshaug et al., 2011a; Bere, Mok, Koga et al., 2013) were investigated. Based on the information on both epidemiology and injury mechanics, the factors that led to injuries were investigated qualitatively using video material from World Cup races (Bere, Florenes, Krosshaug et al., 2013; Bere, Florenes, Krosshaug et al., 2011b).

The Department of Sport Science and Kinesiology of the of University of Salzburg, Austria, became a part of FIS ISS and was commissioned to assess mechanical and biomechanical risk factors in WC alpine skiing. To establish a basis for mechanical and biomechanical assessments, expert stakeholders' opinions on injury risk factors were assessed (Spörri, Kröll, Amesberger et al., 2012). Analysis of the expert interviews revealed that the following five items were perceived as the most important factors leading to injuries in alpine ski racing: (1) Ski–binding–boot system, (2) Changing snow conditions, (3) Speed and course setting aspects, (4) Physical fitness, (5) Speed in general.

The results of this study were used as the basis for deciding which injury risk factors should be assessed from a biomechanical or purely mechanical perspective. Item 1 (ski–binding–boot system), item 2 (changing snow conditions) and the combination of item 3 (speed and course setting aspects) and 5 (speed in general) were assessed in three different projects. The entire project was led by the Department of Sport Science and Kinesiology, University of Salzburg, Austria, in close cooperation with the FIS from 2010 onward.

The Group for Snowsports at the WSL – Insitute for Snow and Avalanche Research SLF, Davos, Switzerland, was commissioned to assess Item 2 (changing snow conditions) in cooperation with the University of Salzburg. Item 1 (ski–binding–boot system) was assessed by the Department of Sport Science and Kinesiology, University of Salzburg, in cooperation with the Ecole Polytechnique Federal Lausanne and the Norwegian School of Sport Sciences. Items 3 (speed and course setting aspects) and 5 (speed in general) were assessed in a cooperative project involving the University of Salzburg, the Norwegian School of Sport Sciences, the WSL – Insitute for Snow and Avalanche Research SLF and the Ecole Polytechnique Federal Lausanne.

This thesis was established within the framework of the FIS ISS and the project topic addressed risk factor items 3 (speed and course setting aspects) and 5 (speed in general).

1.3 Research Goals

- Development and validation of a GNSS technology-based measurement system to simultaneously assess skier position, speed, mechanical energy and external forces in WC alpine skiing for the disciplines GS, SG and DH (papers I - III).
- Establishment of a quantitative understanding of WC alpine skiing in the disciplines GS, SG and DH with respect to terrain geomorphology and course setting (paper IV) and skier mechanics (paper V).
- Investigation of whether differences in injury incidences between disciplines can be explained by differences in skiers' mechanics (paper VI).

1.4 Research Structure

The study was conducted in two separate parts. Figure 1 illustrates the research structure. Part one included the development and validation of the GNSS technology-based measurement system. The first step in this section was the development and validation of the method to assess skier position, speed and acceleration (point mass kinematics). The second step included the assessment of different GNSS position computation methods to find the method which was most suitable for application in WC skiing conditions. In part three, a method to assess external forces (kinetics) was developed and validated. Part one was completed in an experiment in April 2011 in Kühtai, Austria.

The methods developed in part one were applied in part two to assess skier mechanics in WC alpine skiing. In part two, WC alpine skiing was monitored in field measurements at actual WC events. Terrain geomorphology and course setting were captured prior to the WC races. Data for the assessment of skier mechanics were collected in competition by one skier who was equipped with the GNSS based system that was developed and validated in part one. Data were collected at WC races during seasons 2010/11 and 2011/12. Data analyses were conducted in parallel and after data collection until summer 2013.

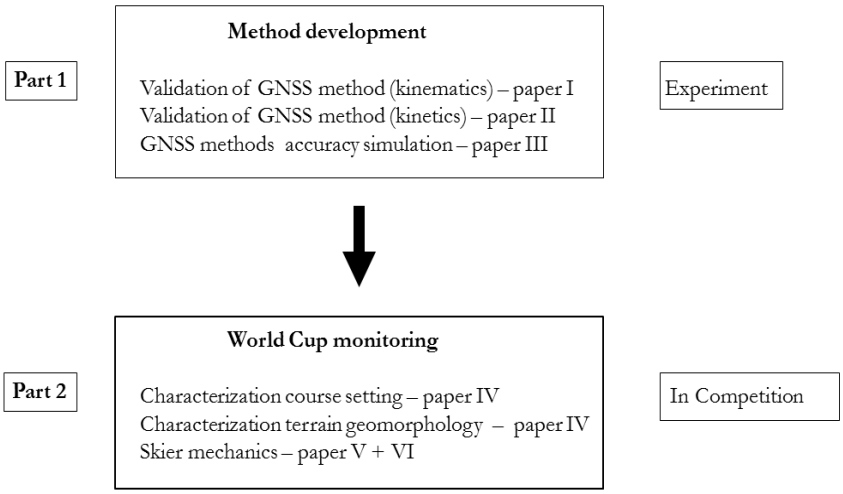

Figure 1. Structure of the research design.

1.5 State of the Art

The state of the art chapter is divided into two parts. The first part (motion capture in alpine skiing) gives an overview of the current literature which is relevant to part 1 of the study. In the second part of the chapter the state of the art on injury prevention in alpine ski racing is outlined to present the background for part 2 of the study.

1.5.1 Motion capture in alpine skiing

1.5.1.1 Kinetics

1.5.1.1.1 Ground reaction force

In alpine skiing, bipedal ground reaction forces are measured using force platforms mounted between binding and ski (Niessen, Müller, Wimmer et al., 1998; Wunderly, Hull, & Maxwell, 1988; Nakazato, Scheiber, & Müller, 2011; Lüthi, Federolf, Fauve et al., 2004; Wunderly & Hull, 1989) or capacitive pressure insoles placed in the ski boots (Nakazato et al., 2011; Lüthi et al., 2004; Holden, Parker, & Walsh, 2004; Krüger & Edelmann-Nusser, 2009). It was shown that pressure insoles yield valid results when applied in ordinary sports shoes with a low shaft (Gurney, Kersting, & Rosenbaum, 2008; Hurkmans, Bussmann, Selles et al., 2004; Orlin & McPoil, 2000). However the internal measurement validity of pressure insoles applied in ski boots is limited due to forces being transferred through the boot shaft (Nakazato et al., 2011; Stricker,

Scheiber, Lindenhofer et al., 2010; Lüthi et al., 2004; Holden et al., 2004). The advantage of the insole method however is that kinesthetic perception is minimally altered compared to skiing without this measurement device (Nakazato et al., 2011) and hence, the method can be applied in racing.

The measurement precision and internal validity is substantially better when using force plates mounted between ski and binding (Lüthi et al., 2004), but kinesthetic perception is altered (Nakazato et al., 2011). The application of force plates in competition or competition-like skiing is not recommended due to the altered kinesthetic perception and for safety reasons (Lüthi et al., 2004). A new approach incorporating a force plate between boot and binding (Moritz, Haake, Kiefmann et al., 2006; Kiefmann, Krinninger, Lindemann et al., 2006) might provide a better compromise between internal and external validity than the two approaches discussed above, since skiers can use their own skis. Measurement precision is better than with insoles, where skiers also use their own skis.

The summed ground reaction forces of both legs are calculated by subtraction of air drag force and gravity from the resultant force. For reconstruction of the air drag force and the resultant force, video-based photogrammetric systems (Reid, 2010; Gilgien, Reid, Haugen et al., 2009; Schiestl, Kaps, Mossner et al., 2006) or GNSS-based models are used (Supej, Saetran, Oggiano et al., 2012).

1.5.1.1.2 Air drag

Air drag is challenging to measure in the field (Barelle, Ruby, & Tavernier, 2004), since skiers continuously change posture. The effect of body posture on air drag was assessed by wind tunnel testing (Savolainen & Visuri, 1994; Luethi & Denoth, 1987; Barelle et al., 2004). In the field, determination of air drag is based on the reonstruction of body posture. The reconstruction of full body segment models is based on photogrammetric methods (Reid, 2010; Meyer, Le Pelley, & Borrani, 2011), or a combination of GNSS and inertial measurement units (Brodie, Walmsley, & Page, 2008). One study based the air drag model on body extension using a GNSS and a terrain model (Supej et al., 2012).

1.5.1.2 Kinematics

1.5.1.2.1 Video based photogrammetry

Multiple video camera-based photogrammetric systems are used to capture and reconstruct full body kinematics. (Schiestl et al., 2006; Mossner, Kaps, & Nachbauer, 1996; Nachbauer, Kaps, Nigg et al., 1996; Mossner, Kaps, & Nachbauer, 1995; Reid, 2010; Spörri, Kröll, Schwameder et al., 2012b; Spörri, Kröll, Schwameder et al., 2012a; Supej & Holmberg, 2010; Supej, Nemec, & Kugovnik, 2005; Supej, Kugovnik, & Nemec, 2005; Supej, Kugovnik, & Nemec, 2004a; Supej, Kugovnik, & Nemec, 2004b; Klous, Müller, & Schwameder, 2010; Lüthi et al., 2004; Schiefermüller, Lindinger, Raschner et al., 2004; Müller & Schwameder, 2003; Pozzo, Canclini, Cotelli et al., 2001; Müller, Bartlett, Raschner et al., 1998; Müller, 1994). The sporting reality in space and time is recreated from several synchronized two-dimensional video pictures. A transfomation algorithm (Schiestl, 2005a; Schiestl, 2005b; Brewin & Kerwin, 2005; Yeadon & King, 1999) is applied to relate the two-dimensional pictures to 3-D space using calibration points in the area of investigation. Time synchronization is accomplished using hardware gen-locks (Klous et al., 2010), software gen-locks based on least squares methods, or using the precise atomic clock of GNSS devices (Meyer, Bahr, Lochmatter et al., 2011). The advantage of video-based photogrammetry is its precision (Klous et al., 2010), but analyses are limited to a few turns and require extensive processing time.

1.5.1.2.2 Infrared camera - passive marker photogrammetry

The standard method for indoor full-body kinematic motion capture is the infrared passive marker method (Robertson, Caldwell, Hamill et al., 2004). Compared to video-based photogrammetry, infrared camera-based systems have the advantage that no digitisation process is needed, the frame rate is usually higher and the camera calibration is more time-efficient. The major drawback of infrared camera-based systems with respect to outdoor applications is their sensitivity to interference from daylight (Atha, 1984). As a consequence, measurements have to be undertaken during the night and the scenery must be illuminated using artificial light. The cameras are temperature-sensitive and need to be heated (Lindinger, 2007). Competition situations are difficult to capture due to the requirement of having reflective markers on the athletes. Snow spray from the skis might cause reflections, making it difficult to sort the true marker reflections from the ones caused by snow spray (Lindinger, 2007).

1.5.1.2.3 Global Navigation Satellite Systems

GNSSs are used to determine the kinematics of athletes in outdoor environments. Due to signal degradation by the United States Department of Defense, the use of non-differential GPS was difficult until May 2000, the date when signal degradation was abandoned. The scrambled signal had to be corrected by a differential measurement, using two receivers placed close together (Terrier, Ladetto, Merminod et al., 2000). The reduction of the error from the scrambled GPS signal, the introduction of the Russian GNSS system, called GLONASS, and the Wide-Angle Augmentation System and European Geostationary Navigation Overlay Service reduced the need for differential GNSS measurements for certain applications. With these enhancements and simplification of the measurement process, the number of applications of GNSS as an analysis tool in sports has increased during the last 10 years (Aughey, 2011).

GNSS is applied in alpine skiing to capture the skier's trajectory, considering the skier as a point mass (Terrier, Turner, & Schutz, 2005; Waegli & Skaloud, 2007; Supej & Holmberg, 2011; Limpach & Skaloud, 2003; Ducret, Ribot, Vargiolu et al., 2004b; Ducret, Ribot, Vargiolu et al., 2004a; Gilgien, Singer, & Rhyner, 2010; Huber, Spitzenpfeil, Waibel et al., 2012). The advantage of GNSS systems compared to photogrammetric methods for motion capture is their efficiency across large capture volumes. However, skiers are represented as a point mass only and accuracy has not so far been assessed with reference systems.

1.5.1.2.4 Inertial Navigation Systems

Accelerometers, gyroscopes and magnetometers are the most common components used in Intertial Navigation Systms (INS). INS can directly measure acceleration and orientation alterations over time. By time integration of these measures, velocities and positions can also be computed in order to complete the spectrum of kinematic measures. INS can be used to track the kinematics of single segments and when incorporated in a system can also track full body movement. The practicability of such systems with regard to outdoor applications is very high (Muthukrishnan, 2009). Linear or angular acceleration determination may be more precise than optical systems, as long as good components are used (Kruger & Edelmann-Nusser, 2010). However, INS's velocity and position precision suffer from drift with time (Muthukrishnan, 2009; Waegli, 2009). Therefore drift has to be controlled by implementing biomechanical constraints in the algorithms. In gait, the foot plant is used to adjust the measures for drift. In movements without unambiguous static instances, drift elimination is a more demanding issue.

Therefore, the activity-specific drift constraints have to be defined and implemented for every specific application (Chardonnens, Favre, Gremion et al., 2012). If using magnetometers, INSs are at risk of suffering interference from magnetic disturbances from metallic structures or power lines (Muthukrishnan, 2009). In general, the accuracy of INS depends strongly on the components used, the biomechanical constraints and the calibration procedure (Muthukrishnan, 2009). Applications of INS in alpine skiing are conducted in combination with GNSS systems. Single INS units are used to enhance the GNSS trajectory accuracy (Waegli & Skaloud, 2009; Skaloud & Limpach, 2003). Multiple INS systems are used to reconstruct the skier segment kinematics. The kinematics are attached to a global skier trajectory which is captured using a GNSS (Brodie et al., 2008; Supej, 2010; Kruger & Edelmann-Nusser, 2010). Such systems allow a time-efficient analysis and enable the extension of motion capture to large volumes, compared to video-based photogrammetric systems. Only one such system for the determination of angles has been strictly validated against an independent reference system (Kruger & Edelmann-Nusser, 2010).

1.5.1.3 Global Navigation Satellite System technology in alpine skiing

The application of GNSS to capture alpine skiing performance faces specific challenges mainly related to satellite signal obstruction due to the alpine terrain. When conducting experiments, locations with minimal satellite signal obstruction can be chosen and the data acquisition can be timed to periods with good satellite coverage. However, when capturing data in World Cup races, constraints can include signal obstruction by terrain, vegetation and buildings (start house) and the measurement system has to be adjusted to meet the prevailing conditions.

For the proper reception of GNSS signals, a direct line of sight between satellites and antenna is needed. Measurements taken in obstructed surroundings can therefore face the problem of reduced signal reception. Reduced signal reception has a negative influence on the accuracy of GNSS positioning, since accuracy is dependent on the number of received signals and the spatial distribution of the satellites in the sky. Geometric dilution of precision (GDOP) is the quality measure of the geometric satellite distribution. GDOP determines how sensitive measurement precision is to changes in the satellite constellation. The effect of the number of received satellite signals on positioning dilution of precision (PDOP) and measurement precision are illustrated in Figure 2 for data from a giant slalom WC race in Adelboden (January 2012). The differential trajectory solutions for elevation masks of 5 degrees (red) and 30 degrees (blue) were computed. With the elevation mask manipulation, the effect of satellite signal shading on the resulting

number of satellites in view, PDOP and root mean square error of the position were computed. The graphs in Figure 2 illustrate that positioning precision is dependent on the number of satellites in view and the PDOP. In this example, precision decreased by a factor of 4 when the number of satellites in view decreased from about 11 to 7, and the PDOP increased by a factor of 8.

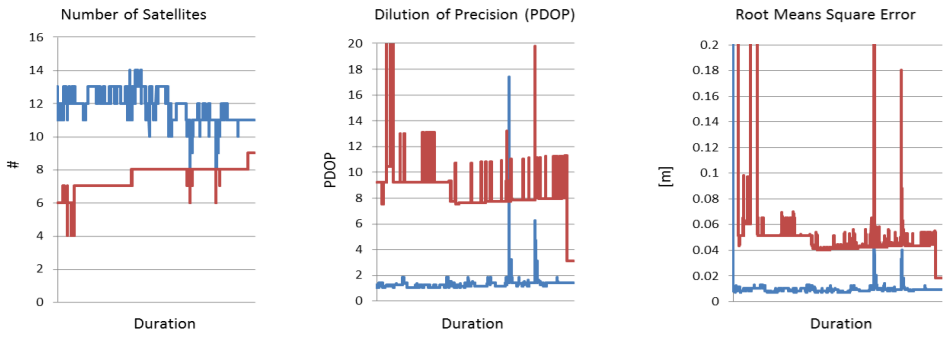

Figure 2. Simulation of satellite shading due to obstruction for an elevation mask of 5 degrees (blue) and 30 degrees (red). The kinematic data are taken from an alpine skiing World Cup race. Left: the number of satellites in view. Middle: Position Dilution of Precision (PDOP). Right: Root Means Square Error of position estimate.

1.5.1.3.1 Strategies to avoid poor signal reception due to obstruction

1.5.1.3.1.1 Choice of Satellite systems

To keep the precision of GNSS measurements high when measuring in obstructed areas it is recommended to use antennas and receivers which can receive signals from several satellite systems to increase the number of satellites in view. The American GPS system consists today of 32 satellites. Without local obstruction at least 8 satellites should be in view from all locations on the planet. Four satellites are the minimum needed to allow the computation of a position solution. Russia (GLONASS), China (Beidou, Compass), India (IRNSS), Japan (QZSS), France (DORIS), and Europe (Galileo) are other regional and global satellite navigation systems which are operative or planned. GLONASS currently includes 24 satellites. Combining GPS and GLONASS thus increases the chances of receiving enough satellite signals when measuring in obstructed areas. When measuring on north-facing slopes, as is often the case in alpine skiing, the use of GLONASS is especially recommended, since the trajectories of the GLONASS satellites are generally more in the north than the GPS satellite flight paths. In 2019 the European GNSS Galileo (http://www.gsa.europa.eu/go/home/galileo/programme/) will be up and

running. The trajectories of the Galileo satellites will be centered over Europe and are therefore expected to decrease the obstruction problem in Europe (Kumar & Moore, 2002).

1.5.1.3.1.2 Number of measured carrier phase frequencies

GNSS satellites transmit several signals in the microwave range. The two signals which are normally used are designated L1 and L2. Standard geodetic low-cost devices usually use one carrier phase frequency (L1, at 1575.42 MHz, wavelength 19.05 cm) to send the navigation information from the satellite to the receiver. More advanced receivers also receive the navigation information on a second frequency (L2, 1227.60 MHz, wavelength 24.45 cm). The carrier signal propagation velocity through the ionosphere is dependent on the wavelength. Therefore disturbances in the ionosphere can be identified and corrected for when two wavelengths, L1 and L2, are used (Pireaux, Defraigne, Wauters et al., 2010). The effect of the frequency choice on measurement precision is substantial for long base-line measurements. High-end receivers usually use both frequencies, while low-end receivers normally use L1 alone (Waegli & Skaloud, 2009).

1.5.1.3.1.3 Processing methods

Stand-alone: When using the so called stand-alone methodology only one receiver is needed to compute position and speed. Typically the athlete carries a compact unit combining antenna and receiver in one piece. This system has the advantage that the measurement is simple to conduct (Terrier et al., 2000).

Differential: To conduct a differential measurement at least two GNSS units are needed. One unit is mounted on the moving athlete (rover), as in the stand-alone method, while the other units (base stations) are placed as close as possible to the sporting area. The base stations are immobile. The fact that they are stationary is used to identify the measurement errors in the raw signal. These raw signal errors are used to correct the measurements of the rover unit on the athlete. Transfer of the correction signal to improve the positioning and velocity solution of the rover can be done either in real time by means of a GSM or radio link [Real-Time Kinematic (RTK)] or by post-processing (PP) after the measurement is taken. The usage of the differential method leads to a substantial improvement of precision in the measurement of both position and speed. The differential method is thus mainly used in sports in which position precision within 1m is needed over time to distinguish trajectories, as is the case in alpine skiing. The drawback of the differential method is price and weight, including the additional weight of the communication link if the RTK mode is chosen.

Differential processing software: Many software packages designed for differential solution computation are tailored for static applications. Dynamic applications face particular challenges and some software packages may be more suitable than others for finding good positioning solutions for dynamic applications. In some situations a complete loss of GNSS signal reception cannot be avoided, such as in start houses with solid roofs prior to the start of racing, or when travelling under bridges. A certain number of measurements, and the time from the time point when signals are available, are needed until the ambiguities can be solved and a fixed solution can be computed. The reacquisition time for fixed solutions is dependent on signal reception, hardware and software. The difference between software packages is illustrated in data from the downhill World Cup race in Wengen 2011. A total GNSS signal reception outage occurred due to passage under a bridge. Software "X" could compute differential solutions only on the positive time axis and needed nearly 5.8 seconds or about 150m distance for the reacquisition of a fixed positioning solution. Software "Y" on the other hand was able to solve positioning ambiguities in both directions in time, and could tighten the gap to 0.86s or about 25m. (See illustration below, adapted from Boffi, G., 2011. Kinematik bei Skiabfahrten, Semester project, ETH Zürich). If gaps occur in the measurement time series, spline filters are powerful to bridge short gaps (Limpach & Skaloud, 2003; Skaloud & Limpach, 2003) caused by loss of fixed solutions.

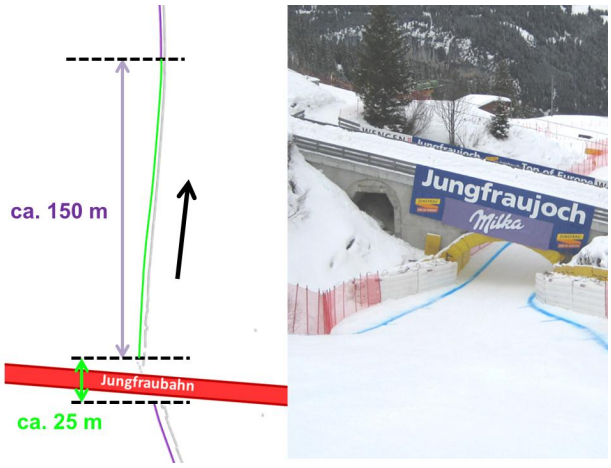

Figure 3. Passage under a bridge in the alpine skiing World Cup downhill race in Wengen caused a total outage of satellite signal reception. The illustration on the left shows the solutions of two geodetic post-processing softwares. Method "Y" was able to solve positioning ambiguities in both directions in time and thus tightened the data gap for a fixed solution down to 25m. The green trajectory indicates the range where only method "Y" was able to compute fixed solutions. Method "X" computed differential solutions in the positive time direction only, resulting in a gap of 150m. The lilac line indicates the section where both methods had fixed solutions. The grey trajectory is the stand-alone solution. The black arrow indicates skiing direction.

1.5.1.3.1.4 GNSS receivers and antennas

Receivers tailored for static applications often exclude measurements if they are associated with high accelerations. Such receivers cause measurement outages when high accelerations occur. For dynamic applications, filter settings have to be adjusted to prevent the interpretation of high accelerations as measurement errors. Large differences were found between receivers from different manufacturers in terms of time required to compute fixed solutions (Limpach & Skaloud, 2003). Hence it seems that certain receivers are more suitable for use in dynamic applications than others. Also antennas were shown to have substantial input on measurement accuracy (Tranquilla & Collpits, 1989).

1.5.1.4 Lack of knowledge

In most studies CoM kinematics was estimated using a GNSS antenna mounted on the skier's back (Supej and Holmberg, 2011; Supej, 2010; Gilgien, Singer, and Rhyner, 2010). A potential drawback of the mounting point on the skier's back might be satellite signal shading by the skier's own body. Skaloud and Limpach (2003), Lachapelle (2009) and Brodie (2008) had mounted the antenna on the helmet of the skier. In order to overcome the limitation generated by the fact that in both approaches the GNSS antenna was not placed at the location of the CoM, modelling methods (Supej et al., 2012) and methods devicing INS to reconstruct segment movements (Supej, 2010; Kruger & Edelmann-Nusser, 2010; Brodie et al., 2008) were proposed to determine the CoM kinematics. However, these previous GNSS-based methods have not been strictly validation against reference systems for the determination of CoM kinematics and the reconstruction of external forces. Also, many methods might not be sutiable for WC speed discipline conditions. Hence, a GNSS based system for the capture of skier mechanics in World Cup racing conditions had to be developed and validated against an independent reference system. Also different types of GNSS processing methods are applied in alpine skiing. It is not clear which methods are sufficiently accurate for applications in alpine skiing. Hence a comparison and validation of different methods is needed.

1.5.2 Injury prevention in World Cup alpine skiing

1.5.2.1 Epidemiology

Competitive alpine skiing is considered a sport with high injury rates (Florenes et al., 2009; Spörri et al., 2012). The injury risk for recreational skiers has been well documented but epidemiology

on competitive alpine skiing was rare until the International Skiing Federation (FIS) installed the FIS Injury Surveillance System (ISS) in 2006 (Florenes et al., 2009). Florenes et al. (2009) reported an injury rate of 36.7 per 100 World Cup (WC) athletes per season. During competition the incidence was 9.8 injuries per 1000 runs and injury rates were found to be dependent on the discipline (for males: slalom: 7.5 injuries per 1000 runs; giant slalom: 12.8; super-G: 14.5; and downhill: 19.3). More than 30% of all injuries were classified as serious injuries and led to abstinence from training and competition for more than 28 days. A recent study found an increased injury risk for male compared to female athletes (Bere et al., 2013). Severe injuries imply not only acute medical conditions, but also those that may hinder the athlete from returning to the sport and may increase the risk of re-injury. Moreover, long-term adverse health effects are possible, such as a higher prevalence of early osteoarthritis (Myklebust & Bahr, 2005). The most frequently injured body part was the knee, and rupture of the anterior cruciate ligament (ACL) was the most frequent diagnosis (Florenes et al., 2009). No gender-specific difference was found for ACL injury risk (Bere et al., 2013). The most frequent injury mechanisms leading to ACL injuries in WC ski racing were found to be "slip-catch" (Bere et al., 2013), "dynamic snowplough" and "landing back weighted" (Bere et al., 2011b).

1.5.2.2 Injury risk factors

Despite the amount of literature dealing with injury prevention in alpine skiing in general, the factors which lead to injuries in competitive alpine skiing are not well understood. A reason for that might be that they seem to be multifactorial (Bahr & Krosshaug, 2005; Meeuwisse, 1994). The results of a qualitative study where experts' and stakeholders' opinions on injury risk factors were investigated support the multifactorial nature of causes for injuries in alpine ski racing (Spörri et al., 2012). The study found five main risk factor categories: 1) System: ski, binding, plate and boot; 2) Changing snow conditions; 3) Physical aspects of the athletes; 4) Speed and course setting aspects; and 5) Speed in general (Spörri et al., 2012). Another recent study qualitatively investigated the causes of 69 accidents which lead to injuries (Bere et al., 2013). It was found that injuries occured most often while turning or landing from a jump. Most of the injuries to the upper body and head were a result of crashing. The majority of knee injuries happened during skiing. Gate contact and contact with safety nets/material occured less frequently. Forty-six percent of all injuries occurred in the final fourth of the race. The study highlighted high-energy impacts to the body when crashing in speed disciplines. The causes of ACL injuries were also analysed qualitatively (Bere et al., 2011b). The main reasons for ACL

accidents were assumed to be skier technique and strategy, visibility, and snow and piste conditions.

1.5.2.2.1 Speed and injury risk

The interview study conducted at the Department of Sport Science and Kinesiology, University of Salzburg (Spörri et al., 2012) revealed the following expert stakeholder opinions on the relationship between speed and injury risk. The experts' opinion on the item "speed in general" was that: 1) high speed led to shorter response times if terrain and course changed at high rates; 2) athletes had more time to anticipate and react to new situations if speed was lower; 3) high speed was dangerous if speed was constantly high over a long period of time, since athletes' senses of speed were altered and this resulted in a loss of concentration; 4) crashes were more harmful if skiers crashed at higher speeds; 5) technical mistakes had less fatal consequences at lower speed.

It was speculated that speed was responsible for the increased injury risk in speed disciplines, since the injury incidence per number of runs seemed to increase with the respective speeds in the disciplines (Florenes et al., 2009). However, a comprehensive assessment of speed in WC alpine skiing is lacking to date. Speed measurements are available so far from experimental studies in GS (Spörri et al., 2012b; Spörri et al., 2012a; Supej et al., 2012) and SL (Supej, Kipp, & Holmberg, 2010; Reid, 2010).

There is a lack of knowledge concerning the relationship between speed and injury risk: no comprehensive speed data is available for WC skiing. Current knowledge is based on experimental setups in SL and GS, while data for the disciplines Super-G (SG) and Downhill (DH) are lacking.

1.5.2.2.2 Speed, course setting and injury risk

An interview study conducted at the Department of Sport Science and Kinesiology, University of Salzburg (Spörri et al., 2012) revealed the following expert stakeholder opinions on the relationship between speed, course setting and injury risk. The experts' opinion on the item "speed and course setting aspects" was that: 1) speed in combination with small turn radii led to high forces in carved turns; 2) speed in turns had increased over the years and hence skiing in turns had become more risky; 3) course setting adjustments should be used to reduce speed in turns; 4) speed reduction by course setting was only efficient if skiers were forced to skidd; 5) as long as turns could be carved no substantial speed reduction was expected; 6) small turn radii and

high speed might cause increased forces and expose skiers to another type of injury risk; 7) speed should be reduced substantially ahead of key sections but not along the entire course; 8) course setters should introduce more tactical aspects forcing athletes to decide how they should govern speed.

It was recently shown that course setting alters skier mechanics (Reid, 2010; Spörri et al., 2012b; Supej & Holmberg, 2010) in SL and GS. Spörri et al. (2012b) showed that course setting affected skier mechanical parameters which are related to injury risk. Spörri et al. (2012b) further showed that increasing the horizontal gate distance resulted in: 1) no significant differences for turn speed for the entire turn, but a speed reduction towards the end of the turn; 2) a slight increase of the radial force at the beginning and a significantly higher force at the end of the turn; 3) an increased inward leaning and decreased fore/aft movement after gate passage. The study concluded that increasing the horizontal gate distance might not be an efficient tool to reduce speed, but could cause increased fatigue as a result of increased radial forces and increased risk of out-of-balance situations with respect to backward and inward leaning. Hence course setting might not only affect speed, but also force and mechanical energy.

1.5.2.3 Lack of knowledge

There is a lack of knowledge concerning the relationship between skier mechanics, course setting and injury risk. World Cup courses may consist of a large range of different terrain geomorphologies and course settings. It is therefore unknown to what extent the experimental findings on the relationship between course setting and skier mechanics in SL and GS (Reid, 2010; Spörri et al., 2012b; Supej & Holmberg, 2010) can be generalized to WC situations. In SG and DH, knowledge on the relationship between course setting and skier mechanics is entirely lacking. With respect to course setting, national teams collect statistics on gate distances, but do not include the entire geometry of course setting. Terrain is also likely to have an effect on skier mechanics. Terrain characteristics however are unknown, other than the altitude drop and course length from start to finish. Knowledge on skier mechanics (speed, force, mechnical energy) is limited to experimental setups in SL and GS and one section of a downhill WC race (Schiestl et al., 2006).

2 Methods

2.1 GNSS method development and validation

In paper I – III a GNSS based method is presented and compared against an independent measurement system to assess validity of different GNSS computation methods, position, speed, acceleration and the external forces acting on the skier. Papers I – III are based on a field experiment and have common data and partly common methods.

2.1.1 Measurement protocol

Six male athletes (former World Cup or current Europa Cup skiers) were enrolled for this study. For each athlete two runs were collected, simultaneously using the reference video-based system and the GNSS system. The Giant Slalom course consisted of twelve gates set at an average distance of 27.2m apart with an offset of 8m. For the analysis, one turn cycle was recorded. The start and end of the turn was defined according to Supej, Kugovnik and Nemec (2003). In total, twelve runs were recorded. The experimental conditions were typical for World Cup races: the snow surface was injected with water and the mean terrain inclination in the area of investigation (i.e., between gates seven and eight) was 26°. A picture of the experimental setup is shown in Figure 4. The data was collected on four different days (3 runs each day) from 29.3 – 1.4.2011 at approximately 0700h (UTC time) each day. The location of the data collection was Kühtai, Austria (WGS 84 coordinates: X: 4261800; Y: 830500; Z: 4659400). This study was approved by the Ethics Committee of the Department of Sport Science and Kinesiology at the University of Salzburg.

2.1.2 Geodetic network

The coordinates of the control points, video cameras and gates were determined by geodetic tachymeter surveys in a local coordinate system (LCS). The positions of the cameras and the control points were determined prior and after the experiment on each day. The position of the tachymeter was controlled frequently during the data collection, using the fixpoints 1 and 2 and the base stations as connection points. The position of the tachymeter, the fixpoints and the base stations were computed differentially using GNSS every day prior and past each data collection session. The geodectic network is shown in Figure 5.

Global GNSS positioning of the network was achieved using the GNSS software Justin (Javad, San Jose, USA) GNSS measuremtns of several 8 hours for each point and reference data from the Austrian Positioning Service (APOS, Wien, Austria). The differential GNSS measurements were determined in the global coordinate system WGS84 (Universal Transverse Mercator zone 32, Northern Hemisphere. The coordinates of the reconstructed body landmarks, control points, video cameras and gates were transformed from the local, tachymeter measurements based coordinate system (LCS) to the global WGS84 coordinate system. The spatial matching of the coordinate systems was based on the two GNSS base stations at the start, the position of the tachymeter and two landmarks on the bottom of the slope, outside the area of investigation. The matching of the two coordinate systems was accomplished using the Helmert least square resection method (Sheynin, 1995), using Leica Geo Office (Leica Geosystems, Heerbrugg, Switzerland). The coordinate system matching was accomplished both before and after the motion capture period. To account for drift the difference between the solution before and the solution after the motion capture period was distributed by time interpolation. The mean difference of the resection at a reference point was below 0.9 cm in the horizontal and below 1.3 cm in the vertical component, with standard deviations of 0.3 cm and 0.4 cm, respectively.

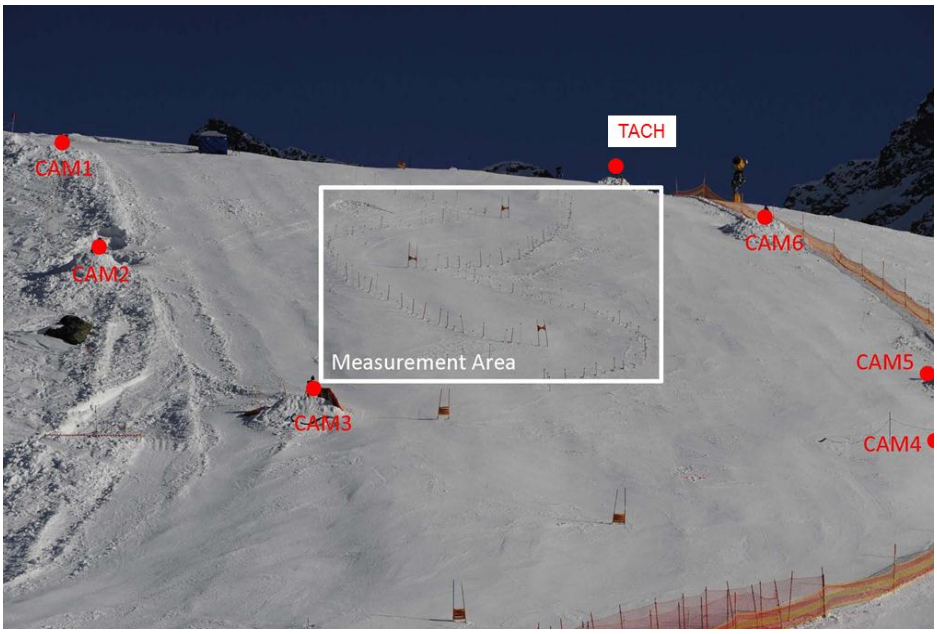

Figure 4. Location of the experimental setup of the validation studies paper I and II. Video camera locations are indicated with "CAM". The tachymeter location is marked with "TACH". The area covered by the video based 3D kinematics was accomplished is marked with a white frame. Photo: Philippe Chevalier.

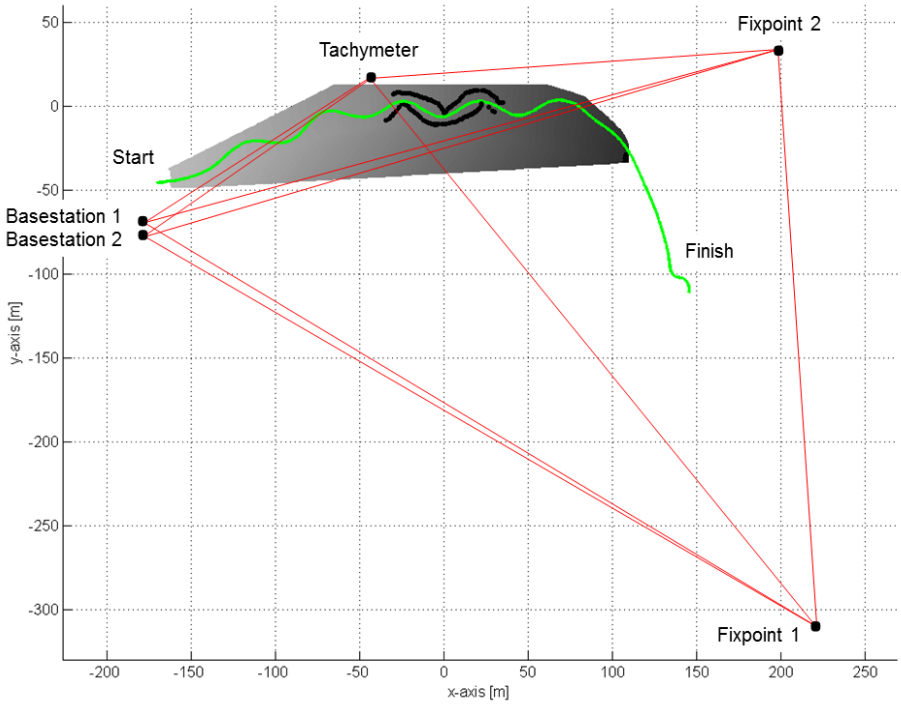

Figure 5. Overview over the geodetic measurement setup. A skier trajectory is drawn in green, the digital terrain model is given in gray. The gray scale is darker with decreasing altitude. Fixpoints 1 and 2, the tachymeter position and the GNSS basestations are marked with black dots. The GNSS network in drawn in red. The black dots along the skier trajectory represent the calibration points used for the video based photogrammetry.

2.1.3 Digital terrain model

The geomorphology of the slope (i.e., snow surface) was determined by terrestrial surveying with a tachymeter (Leica TPS 1200, Leica Geosystems AG, Heerbrugg, Switzerland). The surveyed points were triangulated following Delaunay's method (de Berg, Otfried, van Kreveld et al., 2008), gridded (grid spacing of 0.3m), and low-pass filtered using bi-cubic splines (Gilgien, Reid, Haugen et al., 2008). The terrain model was transformed from the local coordinate system (LCS) to the global WGS84 coordinate system.

2.1.4 Skiers' GNSS antenna position

The GNSS measurement system was composed of an antenna mounted on the helmet of the athlete (G5Ant-2AT1, Antcom, USA) and a GPS/GLONASS dual frequency (L1/L2) receiver (Alpha-G3T, Javad, USA) recording position signals at 50Hz and carried in a small cushioned

backpack. To enable differential positioning, two base stations were located at the start of the course and equipped with antennas (GrAnt-G3T, Javad, USA) and Alpha-G3T receivers (Javad, USA). The second base station was used for redundancy. As a first step, accurate absolute global positions of the GNSS base stations were computed with the geodetic GNSS software Justin (Javad, San Jose, USA), using reference data from the Austrian Positioning Service (APOS, Wien, Austria). The differential GNSS measurements were determined in the global coordinate system WGS84 (Universal Transverse Mercator zone 32, Northern Hemisphere).

The kinematic positions of the skier's GNSS antenna were computed in post-processing with the geodetic GNSS software GrafNav (NovAtel Inc., Canada), using the L1 and L2 carrier phase signals of the GPS and GLONASS satellite systems. In average 13 satellites were used for the GNSS solution computation. Fixed ambiguity solutions were achieved throughout the entire course for all skiers. Each component of the antenna positions was then low-pass filtered based on cubic spline filtering according to Skaloud and Limpach (2003), applying a tolerance factor of 0.5 for the horizontal components and 0.7 for the vertical component. The filtered positions yielded the three-dimensional position vector $\boldsymbol{P}_{GNSS,ANT.}$ Based on the obtained trajectory vectors ($\boldsymbol{P}_{GNSS,ANT}$) the velocity and acceleration vectors ($\boldsymbol{V}_{GNSS,ANT}$ and $\boldsymbol{A}_{GNSS,ANT}$) were derived according to Gilat and Subramaniam (2008).

2.1.5 GNSS based skiers' center of mass position

A biomechanical model was developed to compute the CoM position, velocity and acceleration using the GNSS antenna mounted on the helmet of the athlete, assuming that the skier's movements can be represented by an inverted pendulum (Morawski, 1973; Supej et al., 2012). During a turn, the pendulum is deflected from its neutral position due to the lateral inclination of the skier. It was assumed that external forces are the cause of this movement. The pendulum inclination direction vector (**L**) was modelled by a linear combination of the accelerations acting on the skier according to equation 1 where $\mathbf{A}_{GNSS,radial}$ is the radial acceleration vector derived from the antenna position ($\mathbf{P}_{GNSS,ANT}$) according to Gilat and Subramaniam (2008); $\mathbf{g}_N$ corresponds to the gravity vector projected in plane **N** containing the antenna position and normal to the velocity vector $\mathbf{v}_{GNSS,ANT}$; $\mathbf{P}_{GNSS->N}$ is the vector between the antenna position and its successive projection ($\mathbf{P}_N$), first on the snow surface then on plane **N**; D corresponds to the minimum turn radius divided by the instantaneous turn radius calculated following the method of Reid (2010). The pendulum modelling along with its projection into plane **N** normal to the velocity vector was tailored to compensate for both lateral and fore-aft inclinations of the skier.

The factor D was introduced in equation 1 to take into account the derivative artifacts in the radial acceleration computation.

$$\boldsymbol{L} = \frac{-\boldsymbol{A_{GNSS,radial}} + \boldsymbol{g_N}}{\|-\boldsymbol{A_{GNSS,radial}} + \boldsymbol{g_N}\|} \cdot D + \frac{\boldsymbol{P_{GNSS \to N}}}{\|\boldsymbol{P_{GNSS \to N}}\|} \cdot (1 - D) \quad (1)$$

The CoM position vector of the GNSS ($\mathbf{P}_{\mathbf{GNSS,CoM}}$) corresponded to 53% of the vector **L** from the antenna position to its snow surface intersection. The 53% value was obtained as an average value for the entire turn cycle from the dataset of Reid (2010). The construction of $\mathbf{P}_{\mathbf{GNSS,CoM}}$ is illustrated in Figure 6. Then the CoM position vector was low-pass filtered (second-order Butterworth filter; cut-off frequency of 4 Hz). Similarly to the GNSS antenna kinematics, the GNSS CoM velocity ($\mathbf{V}_{\mathbf{GNSS,CoM}}$) and acceleration ($\mathbf{A}_{\mathbf{GNSS,CoM}}$) vectors were obtained from the time differentiation of the GNSS CoM position vector ($\mathbf{P}_{\mathbf{GNSS,CoM}}$) (Gilat and Subramaniam, 2008).

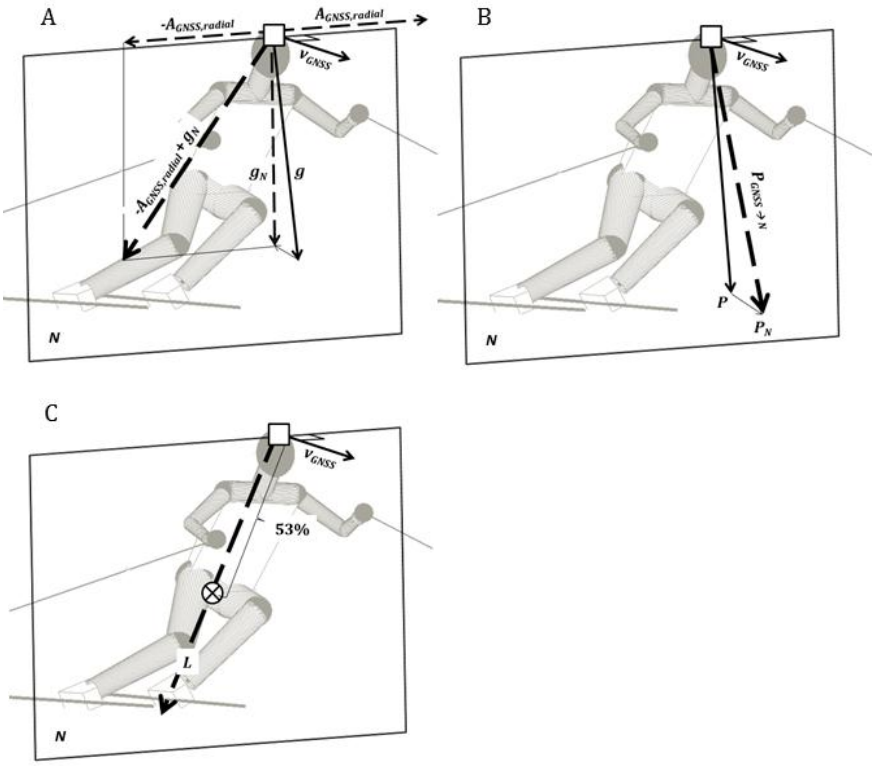

Figure 6. Illustration of the pendulum modelling: A) antenna (□), radial acceleration ($A_{GNSS,radial}$), gravity vector (g) projected in the N plane (g_N); B) successive projection of the antenna position on the snow surface (P) then on the plane N (P_N); C) The combination of illustration A and B along with equation 1 leads to the illustration C: CoM position (⊗) and direction vector of the pendulum modelling (L). The CoM position corresponds to 53% of L from the antenna to its snow surface intersection.

2.1.6 Reference measurement system

The photogrammetric reconstruction of body landmarks of the reference system was not part of my work, but was accomplished by Dr. Jörg Spörri, University of Salzburg, Department of Sport Science and Kinesiology, Hallein-Rif, Austria. The work which was conducted by Dr. Jörg Spörri is therefore marked in italic: *Six panned, tilted and zoomed HDV cameras (Sony, PMW-EX3) at 50 Hz and a DLT-based panning algorithm by Drenk (1994) were used to capture the skiers' kinematics over one turn within a twelve turn giant slalom turn section. Camera images were calibrated and synchronised using a gen-lock signal. Twenty-two joint centres and landmarks on the skier's body (head, neck, right and left (r/l) shoulder, (r/l) elbow, (r/l) hand, (r/l) stick's tail, (r/l) hip, (r/l) knee, (r/l) ankle, (r/l) ski's tip and tail), as well as the GNSS antenna (*$\boldsymbol{P}_{REF,ANT}$*) were manually digitised and their position was reconstructed in the 3D space. Position data were low-pass filtered using a second-order Butterworth filter; cut-off frequency between 2 and 4 Hz determined according to the Jackson Knee method (Jackson, 1979). Thereafter, a segment length normalisation technique (Smith, 1994) was applied to adjust the computed segment lengths to the measured lengths of the skier's segments. In terms of accuracy, the method used was found to have a mean resultant photogrammetric error of 23mm with a standard deviation of 10mm as in an earlier study (Klous, Müller, and Schwameder, 2010).*

CoM position of the reference system ($\mathbf{P}_{\mathbf{REF,CoM}}$) was computed using the body segment model of Zatsiorsky (2002) with adjustments of (de Leva, 1996) and considering the athlete's equipment. For the CoM and ANT the velocity ($\mathbf{V}_{\mathbf{REF,CoM}}$ and $\mathbf{V}_{\mathbf{REF,ANT}}$) and acceleration vectors ($\mathbf{A}_{\mathbf{REF,CoM}}$ and $\mathbf{A}_{\mathbf{REF,ANT}}$) were computed according to Gilat and Subramaniam (2008). The GNSS system and the reference system were time-synchronised using an electronic gen-lock between the video-basedand the GNSS system.

2.1.7 Accuracy assessment for position, velocity and acceleration

The position, velocity, and acceleration of the CoM and antenna obtained from the GNSS system were compared for the twelve turn cycles to the corresponding values of the CoM obtained from the reference system (i.e., $\boldsymbol{P}_{GNSS,CoM}$ vs. $\boldsymbol{P}_{REF,CoM}$, $\boldsymbol{P}_{GNSS,ANT}$ vs. $\boldsymbol{P}_{REF,CoM}$, and so on for the velocity and acceleration). This characterisation allowed an assessment of the performance of the proposed method with and without the effect of the pendulum modelling. In addition, to characterise the raw performance of the GNSS measurement system, the position, velocity, and acceleration of the antenna obtained from the GNSS system and the reference system were compared ($\boldsymbol{P}_{GNSS,ANT}$ vs. $\boldsymbol{P}_{REF,ANT}$, and so on for the velocity and acceleration). For each turn cycle the mean (offset) and standard-deviation (precision) of these vectorial difference amplitudes

were calculated. Thereafter the mean and standard deviations were averaged over the twelve turn cycles. In the following, these difference measures are named vectorial amplitude average mean and vectorial amplitude average SD. The vectorial amplitude average mean describes the systematic difference (offset) between the measurement systems, while the vectorial amplitude average SD describes the random difference (precision). In addition, the position difference was also decomposed into a component tangent to the trajectory (fore-aft component), radial (lateral component), and normal to the snow surface (inferior-superior component). Mean and maximum values of the velocity and acceleration amplitude were extracted for each turn cycle and then the mean and standard deviation of their differences were computed as for the turn cycle analysis. These difference measures are named in the following turn mean and turn maximum. The normality of the data was verified prior to applying parametric statistics using the Lilliefors test ($p<0.05$).

2.1.8 Position accuracy assessment of different GNSS methods

In paper III different GNSS methods were compared against an independent reference system for one turn and against the most valid method for an entire run. Further, time to fix differential GNSS ambiguities is assed for each method.

The kinematic position solutions for the skier antenna positions were computed for five different GNSS methods (Table 1). Method *A* was a differential phase solution that included both GPS and GLONASS satellite signals and the signal frequencies L1 and L2. Method *B* was similar to method *A*, but using frequency L1 only. Method *C* was similar to method *A* except that GPS signals only were used. Method *D* was similar to *C* but using frequency L1 only. Method *E* was a non-differential code solution using only GPS code signals (the software was choosing among the code signals P1, P2, C2, C5 and C/A. In order to simulate measurement environments with different grades of satellite signal obstruction, each GNSS method was computed for circular elevation angles of 10°, 30° and 40° on top of the masking caused by the topography. The elevation angles were adjusted in the post-processing software. Hence, 5 methods were used, with 3 different satellite signal obstruction conditions each. The method names are written in italic (*A* – *E*), while the position vectors of the skier trajectory are written in italic and bold (***A*** – ***E***).

Table 1. Composition of the 5 GNSS methods applied in study 1 and 2.

Method	GNSS		Frequency		Processing	
	GPS	**GLONASS**	**L1**	**L2**	**Differential**	**Nondifferential**
A	X	X	X	X	X	
B	X	X	X		X	
C	X		X	X	X	
D	X		X		X	
E	X		Code			X

2.1.8.1 Comparison with independent reference system (step 1)

The GNSS antenna trajectory solutions $\boldsymbol{A}$– $\boldsymbol{E}$were compared to $\boldsymbol{P_{GNSS,ANT}}$ every 0.02s within turn 7 using GPS time as reference time. $\boldsymbol{P_{GNSS,ANT}}$ was time interpolated to the GPS time points to allow spatial comparison at the corresponding point in time. The spatial differences between $\boldsymbol{P_{GNSS,ANT}}$ and the GNSS position solutions were expressed as vector norms (XYZ) and decomposed in the z-direction (Z) and the horizontal component (XY). For each run the mean difference, standard deviation (SD) of the difference and the median of the difference were calculated. Subsequent to the analysis of each trajectory, these measures were averaged across the 12 runs for each component. The results for the differential methods used for $\boldsymbol{A}$ – $\boldsymbol{D}$ were expressed for the periods in which differential solutions were computable. The timespans in which the methods were unable to compute solutions were illustrated in histograms, along with the spatial differences between methods for the periods when solutions could be computed.

2.1.8.2 Position accuracy assessment of entire runs and time to acquire fixed solutions (step 2)

In step 2, the same GNSS data as in step 1 were used, but, in contrast, the data from the entire run (12 turns) were assessed. The analysis of the spatial differences started shortly after the start gate when the individual skiers reached a speed of 2 m/s (using the Doppler-speed measurement of method *A*). The analysis ended when the skiers passed the last gate. The analysis in step 1 revealed that method *A* under the condition 10° ($\boldsymbol{A_{10}}$) was the most accurate and consistent (see results step 1). Consequently, $\boldsymbol{A_{10}}$ served as the reference method in step 2 Using the same approach as in step 1, the spatial differences between $\boldsymbol{A}$ – $\boldsymbol{E}$ and $\boldsymbol{A_{10}}$ were calculated each 0.02s from start to finish for the elevation masks 10°, 30° and 40°. GNSS measurements were started (warm start) on average 69s (minimum 53s, maximum 92s) before skiers reached the speed of 2

m/s. Between the start of the differential GNSS measurement and the time point when skiers left the start gate, skiers stood in a upright position in an open area with no obstacles other than the topography affecting satellite signal reception.

The time to acquire a differential positioning solution was assessed at measurement start. The time from the start of the GNSS measurement to the instant of fixing integer ambiguities was calculated for methods *A* to *D* (method *E* was non-differential). The mean and SD of the times to fix integer ambiguities was calculated for the 12 trials. The number of trials which reached a fixed solution at least once during the run were counted.

2.1.9 Computation of external forces using the GNSS based system

In paper II a method for the determination of external forces is presented and validated against the independent reference system. The new method and the reference system were based on the kinematic data from paper I.

The resultant force ($\boldsymbol{F}_{RES,GNSS}$) and the gravitational force ($\boldsymbol{F}_{G}$) were calculated using the skier's mass (including equipment) and the $\boldsymbol{P}_{GNSS,CoM}$ acceleration and gravitational acceleration respectively. The air drag force ($\boldsymbol{F}_{D,GNSS}$) was computed according to Equation (1), where ϱ is the air density. Air density was calculated from temperature and air pressure measurements taken at a meteorological station mounted along the slope. The effect of air humidity was neglected. The line of action of the drag force was assumed to be opposite to $\mathbf{v}_{GNSS}$. The ambient wind velocity field ($\mathbf{v}_{WIND}$) was based on two meteorological stations positioned on the top and the bottom part of the slope respectively. Wind speed was lower than 0.6 m/s during the measurement and at about right angles to the main course direction. The drag area $(C_DA)_{BARELLE}$ was computed by adapting the model of Barelle (2004) (Barelle et al., 2004), where the drag area was expressed as a function of reduced body extension (D) and arm position. For this study the arms were omitted from the model, and only the body extension was considered. Barelle (2004) computed D (the distance between neck and feet) as the projections of the segment lengths L_1 (leg), L_2 (thigh) and L_3 (chest) into the frontal plane using the angles θ_1, θ_2 and θ_3 (Equation (2)). In the GNSS method dataset D was computed along the vector between the feet position ($\boldsymbol{P}_{SKI}$) and the GNSS antenna position ($\boldsymbol{P}_{GNSS,ANT}$). The length of D was determined by the reduction of the distance between $\boldsymbol{P}_{SKI}$ and $\boldsymbol{P}_{GNSS,ANT}$ by 17% to accommodate for the distance between $\boldsymbol{P}_{GNSS,ANT}$ and the neck in order to follow the definition of Barelle (2004) (Figure 7a). Drag area was computed according to Equation (3).

$$F_{D,dGNSS} = \frac{\rho \cdot (-v_{dGNSS} + v_{WIND})^2}{2} \cdot (C_D A)_{BARELLE} \quad (1)$$

$$(C_D A)_{BARELLE} = 0.0003 \cdot (L_1 \cdot \sin\theta_1 + L_2 \cdot \sin\theta_2 + L_3 \cdot \sin\theta_3) - 0.026 \quad (2)$$

$$(C_D A)_{BARELLE} = 0.0003 \cdot D - 0.026 \quad (3)$$

$$F_{GRF,GNSS} = F_{RES,GNSS} - F_G - F_{D,GNSS} \quad (4)$$

The ground reaction force ($\boldsymbol{F_{GRF,GNSS}}$) was calculated according to Equation (4) and therefore includes all components of the ground reaction force: The ski friction force ($\boldsymbol{F_{F,GNSS}}$) is the component of $\boldsymbol{F_{GRF,GNSS}}$ in the tangent direction to the direction of motion. $\boldsymbol{F_{F,GNSS}}$ therefore measures the braking effect of the entire ski manipulation (loading, angulation, angle of attack, etc.) and interaction with the snow on the $\boldsymbol{P_{GNSS,CoM}}$ in the global spatial reference frame and might thus be relevant for performance related analysis. The direction of $\boldsymbol{F_{F,GNSS}}$ was defined as the vertical projection along the gravitational vector of $\mathbf{v_{GNSS}}$ onto snow surface ($\boldsymbol{v_{GNSS}}$'). The negative component of $\boldsymbol{F_{F,GNSS}}$ (-$\boldsymbol{F_{F,GNSS}}$) was computed by projecting $\boldsymbol{F_{GRF,GNSS}}$ normal onto $\boldsymbol{v_{GNSS}}$'. $\boldsymbol{F_{F,GNSS}}$ was finally determined as the inverse of (- $\boldsymbol{F_{F,GNSS}}$) (Reid, 2010) (Figure 7b).

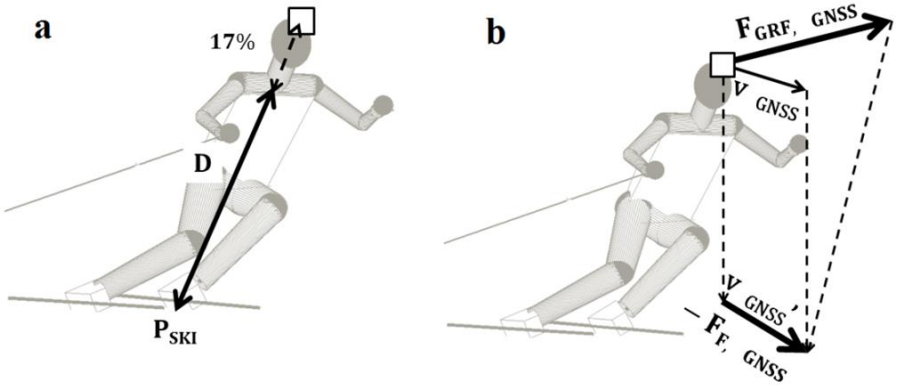

Figure 7. (a) Illustration of the reduced skier amplitude (D) applied for the drag area calculation. P_{GNSS} (□), intersection point of the pendulum and the snow surface (P_{SKI}); (b) Illustration of the ski friction force (F_F) calculation. The direction of F_F is defined by the vertical projection of the velocity vector (v_{GNSS}) onto the snow surface (v_{GNSS}'). F_F is finally calculated by projection of the ground reaction ($F_{GRF,GNSS}$) onto v_{GNSS}'.

2.1.10 Computation of external forces using the reference system

The resultant force ($\boldsymbol{F}_{RES,REF}$) and the gravitational force ($\boldsymbol{F}_{G}$) were calculated using the skier's mass (including equipment) and the ($\boldsymbol{a}_{CoM}$) acceleration and gravitational acceleration respectively. The air drag force ($\boldsymbol{F}_{D,REF}$) was computed according to Equation (5). The drag area ($(C_DA)_{MEYER}$) was computed by applying the "GM1" model of Meyer *et al.* (Meyer et al., 2011) to the video-based segment kinematics method (Equation (6)), where UpH is the body length, A_F is the frontal area, and H and W are the skier's instantaneous height and width. The frontal area was calculated using the orthonormal projection of the skier's silhouette on the plane normal to $\mathbf{v}_{COM}$. The silhouette was generated by attaching geometric bodies to the reconstructed body landmarks and line segments. The frontal area (A_F) was technically determined by counting the pixels within the skier's silhouette (Brodie et al., 2008; Reid, 2010; Gilgien, 2008). H and W were computed from segment kinematics in the frontal plane. The air drag model was found valid with respect to wind tunnel testing. ($R^2 = 0.972$, $p < 0.001$, SD of the dragarea = 0.016) with wind-tunnel tests (Meyer et al., 2011). The ground reaction force ($\boldsymbol{F}_{GRF,REF}$) was calculated according to Equation (7). $\boldsymbol{F}_{GRF,REF}$ was decomposed into the component parallel to the direction of motion ($\boldsymbol{F}_{F,REF}$) with the same method as in the GNSS method, but using $\mathbf{v}_{CoM}$ instead of $\mathbf{v}_{GNSS}$.

$$F_{D,REF} = \frac{\rho \cdot (v_{COM} + v_{WIND})^2}{2} \cdot (C_D A)_{MEYER} \tag{5}$$

$$(C_D A)_{MEYER} = 0.046 - 0.155 \cdot UpH + 0.649 \cdot A_F + 0.181 \cdot H + 0.039 \cdot W \tag{6}$$

$$F_{GRF,REF} = F_{RES,REF} - F_G - F_{D,REF} \tag{7}$$

2.1.11 Accuracy assessment of external forces determined by the GNSS based method

For comparison of the GNSS based method and the reference system, each trial was time-normalized. The GNSS-based method was then compared with the reference system for the vector amplitude of the ground reaction force ($\boldsymbol{F}_{GRF} = \boldsymbol{F}_{GRF,REF} - \boldsymbol{F}_{GRF,GNSS}$), the ski friction ($\boldsymbol{F}_{F} = \boldsymbol{F}_{F,REF} - \boldsymbol{F}_{F,GNSS}$), the air drag force ($\boldsymbol{F}_{D} = \boldsymbol{F}_{D,REF} - \boldsymbol{F}_{D,GNSS}$) and the resultant force ($\boldsymbol{F}_{RES} = \boldsymbol{F}_{RES,REF} - \boldsymbol{F}_{RES,GNSS}$). The vectorial differences between the GNSS-based method and the reference system were calculated for each time point of each trial. For each trial the offsets of these vectorial differences were calculated. Thereafter the offsets were averaged over the twelve

trials and named average vectorial difference offset (AVD-Offset). In order to obtain a precision measure for between-measurement system comparisons (GNSS and reference system) the standard deviation (precision, SD) of the vectorial differences was calculated for the entire turn cycle for each trial separately and then averaged across the twelve trials. This precision measure was named average vectorial difference between SD (AVD-Offset-Between-SD). To assess the precision of the GNSS method for relative comparisons between skiers and/or different turns (within-measurement system precision) the SD of the twelve trials was calculated at each time point across the turn cycle (instantaneous AVD-Within-SD) and then averaged for all time points across the turn cycle. This precision measurement was called the average vectorial difference within SD (AVD-Within-SD). The described SD and offset procedures were performed for: (a) the entire turn cycle and (b) the turning phase, the section of the turn where the turn radius of the reference system was below 30 m (Spörri et al., 2012b) except for AVD-Within-SD. The average vectorial difference offsets and SD's were also expressed in relation to the respective turn mean forces in order to put the measurement errors into perspective with the size of the forces. These differences were expressed in percentage and computed as division of the vectorial difference offset or SD and the turn mean force of the reference system. Mean force and maximal force were extracted for each trial and averaged across the twelve trials with both the GNSS method and the reference system for each force. The differences between the GNSS and the reference system of the turn cycle mean and turn cycle maxima computation were assessed by calculation of the mean error and the SD between the methods. The normality of the data was verified prior to applying parametric statistics using the Lilliefors test ($p < 0.05$).

2.2 Application of the GNSS based method in World Cup giant slalom, super-G and downhill

2.2.1 Measurement protocol

Seven WC giant slalom (GS) races, (14 runs in total at Sölden, Beaver Creek, Adelboden, Hinterstoder, Crans Montana), 4 super-G (SG) races, (4 runs in total at Kitzbühel, Hinterstoder, Crans Montana) and 5 downhill (DH) races, (16 runs in total at Lake Louise, Beaver Creek, Wengen, Kitzbühel, Åre) were monitored during the WC season 2010/11 and 2011/12. For paper IV and V 5 super-G races were analysed. The additional race was held in Åre. This study

was approved by the Ethics Committee of the Department of Sport Science and Kinesiology at the University of Salzburg.

2.2.2 Digital terrain model

During the days prior to the race the geomorphology of the snow surface was captured by several members of the project group. The terrain geomorphology (i.e., snow surface) was determined by static differential GNSS (Alpha-G3T receivers with GrAnt-G3T antenna (Javad, USA) and a Leica TPS 1230+ (Leica Geosystems AG, Switzerland). The GNSS antenna were mounted on a rover pole and the vertical offset was adjusted in the post – processing. Both systems used the GPS and GLONASS satellites and the frequencies L1/L2 to compute differential positioning solutions. The differential position solutions were computed in post-processing using the geodetic GNSS software Justin (Javad, San Jose, USA) and a GNSS base station located at the start of the races at a spot with minimal satellite signal obstruction. In races in Switzerland and Austria also RTK solutions were applied for the Leica receiver. All GNSS computations were accomplished in the Universal Transverse Mercator coordinate system (WGS84). In order to reconstruct the terrain geomorphology in sufficient detail, in average 0.3 points per m^2 were measured but more points in terrain transitions and fewer in uniform terrain. The surveyed point cloud was triangulated applying the Delaunay method (de Berg et al., 2008) and gridded on a rectangular grid (grid spacing of 0.3m). The vertical grid component was finally low-pass filtered using bi-cubic spline functions (Gilgien et al., 2008; Hugentobler, 2004) and represented as a digital terrain model (DTM) in MATLAB (MATLAB Inc., Natick, USA). Also fence positions and types of fences were captured along the slope.

2.2.3 Forerunner GNSS antenna trajectory

The forerunner's trajectory was captured using a differential global navigation satellite system (GNSS). One male forerunner (age: 25.1±3.6 year, mass: 86.1±10.0 kg) per race captured date. Forerunners were part of the official forerunner group and started as first forerunner prior to the respective race. The GNSS antenna (G5Ant-2AT1, Antcom, USA) was mounted on the skier's helmet and a GPS/GLONASS dual frequency (L1/L2) receiver (Alpha-G3T, Javad, USA) recorded position signals at 50Hz. The receiver was carried in a small cushioned backpack (Figure 8). The total weight of the measurement equipment carried by the skier was 940g (receiver 430g, backpack 350g, antenna 160g). Differential position solutions of the skier trajectory were computed using the data from two base stations (antennas (GrAnt-G3T, Javad, USA) and Alpha-

G3T receivers (Javad, USA)) (Figure 9) and the geodetic post-processing software GrafNav (NovAtel Inc., Canada).

Figure 8. Forerunner equipped with a GNSS receiver in a cushioned camelbag. The receiver is connected with a cable to a GNSS antenna mounted on the helmet.

2.2.4 Characterisation of course setting in World Cup alpine skiing

In paper IV course setting in male WC alpine skiing is quantified for the disciplines GS, SG and DH. Paper IV further describes how course setting is related to terrain inclination and terrain transitions. Finally the study describes the extent skiers are exposed to different terrain inclinations.

2.2.4.1 Course setting geometry

Course setting was captured prior to each race. For the speed disciplines and the first runs in giant slalom the courses were usually captured the day before races. For giant slalom the second run was captured as soon as the course was set. Course setting was captured using the same GNSS method as the snow surface (Figure 10).

The position of each gate and the terrain geomorphology were determined according to the method described above. The course setting was characterized, similar to the method used by Spörri et al. (2012b), by three distances: the gate distance, and the horizontal and the vertical gate distances. Gate distance is the linear distance from turning gate to turning gate. The horizontal

distance is the distance between gate (i) and the normal projection of gate (i) on the vector from gate (i-1) to gate (i+1).

Figure 9. Two GNSS base stations mounted at the start of the downhill race in Lake Louise. Antennas in green mounted on tripods, the receivers and batteries protected in black boxes.

Figure 10. Capturing gate position using a GNSS rover with the antenna mounted on a rover pole.

The vertical distance is the distance from gate (i-1) to the projection of (i) onto the vector between (i-1) and (i+1). For illustration see Figure 11. If two consecutive gates (i and i+1) defined one turn, both were projected on the vector from gate (i-1) and (i+2) to compute the horizontal gate distance. The gate with the largest horizontal gate distance was chosen to represent the turn. Gate distance and vertical gate distance were calculated for the respective gates. The median gate distance and the median horizontal distance were deviced to calculate the median change in direction from gate (i-1) to gate (i) and gate (i+1).

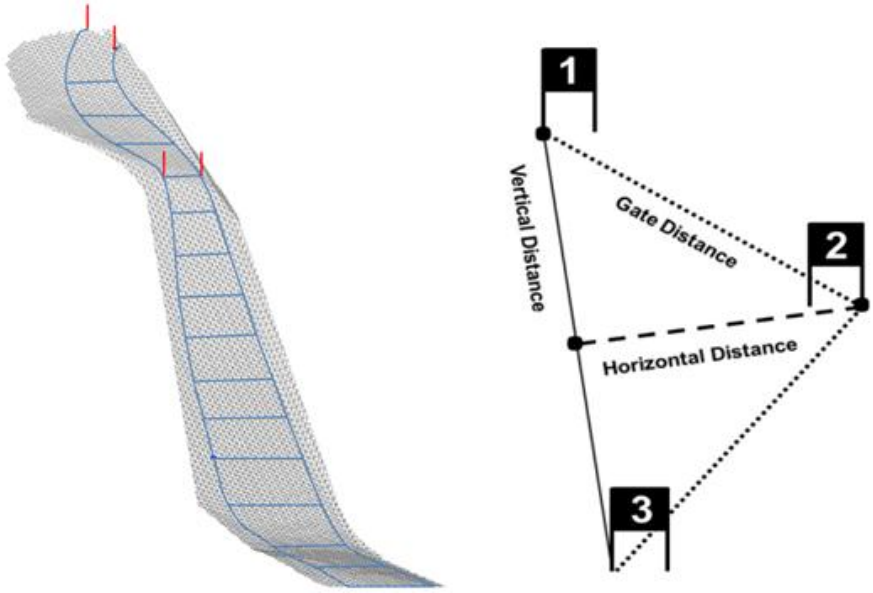

Figure 11. Left side: Illustration of the digital terrain model and course setting at the "Mausefalle" in the downhill race in Kitzbühel, Austria. Right side definition of gate distance, horizontal and vertical gate distance.

2.2.4.2 Terrain inclination

To calculate terrain inclination the skier trajectory was projected normal to the DTM (P_S). The terrain inclination angle was calculated as the angle between the gradient vector and the horizontal plane at every point of P_S. Figure 12 illustrates a typical DTM from which terrain inclination measures were derived.

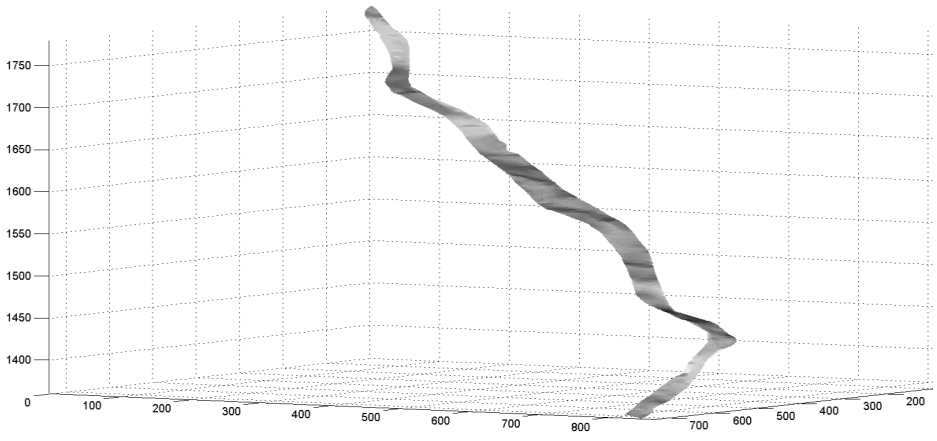

Figure 12. Digital terrain model of the WC giant slalom slope "Chuenisbergli", Adelboden, Swizterland. The gray shading illustrates the terrain inclination. The brighter the grayscale is the steeper is the terrain.

2.2.4.3 Terrain inclination in relation to course setting

The course setting was characterized, similar to the method used by Spörri et al. (2012b), by three distances: the gate distance, and the horizontal and the vertical gate distances. Gate distance is the linear distance from turning gate to turning gate. The horizontal distance is the distance between gate (i) and the normal projection of gate (i) on the vector from gate (i-1) to gate (i+1). The vertical distance is the distance from gate (i-1) to the projection of (i) onto the vector between (i-1) and (i+1). If two consecutive gates (i and i+1) defined one turn, both were projected on the vector from gate (i-1) and (i+2) to compute the horizontal gate distance. The gate with the largest horizontal gate distance was chosen to represent the turn. Gate distance and vertical gate distance were calculated for the respective gates. The computation method for angles α, β and θ is illustrated in Figure 13. The median gate distance and the median horizontal distance were used to calculate the median change in direction from gate (i-1) to gate (i) and gate (i+1).

To assess the association between 1) the horizontal gate distance and the terrain inclination and 2) the gate distance and the terrain inclination, a Spearman correlation was used and significance was tested ($p = 0.01$).

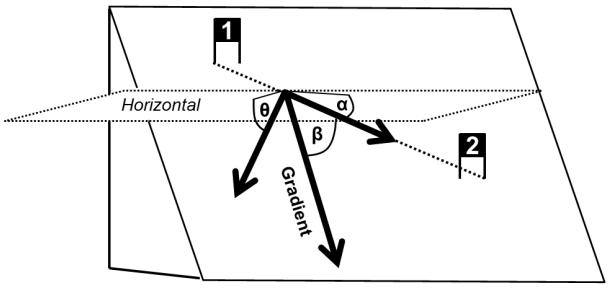

Figure 13. Illustration of the parameters describing the relationship between terrain and course setting: Terrain inclination in course direction (a), Angle between course direction and the gradient (β) and terrain inclination normal to course direction (θ).

2.2.4.4 Course Setting relative to terrain transitions

It was calculated how far gates were set from terrain transition (concave and convex) apices. Convex terrain transitions are terrain transitions where terrain is bulging outward (bump). Concave terrain transitions are transitions where terrain is hollowed inward (compression). The apex point of a terrain transition was calculated following a specific procedure: (1) The deflection

points (DP) of the skier trajectory before and after the gate (i) were projected normal to the DTM (pDP) and a plane was spanned by the pDPs and gravity; (2) The projection of the skier trajectory onto the DTM (P_S) was projected onto the plane spanned by pDP and gravity. The maximal distance of the projected P_S to the vector between the two pDP was defined as the terrain transition apex; (3) The distance from the terrain transition apex to the gate (i) was calculated and named (DTTG convex and DTTG concave). The calculation procedure for the distance from a terrain apex to the corresponding gate is illustrated in Figure 14. The median distance and interquartile range (IQR) of the distance were calculated for all data and only the DTTG which were smaller than 10m for both convex and concave terrain transitions.

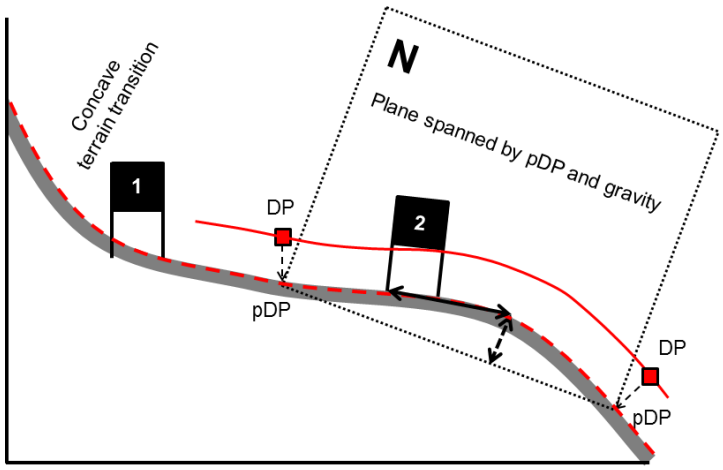

Figure 14. Illustration of terrain transition apex determination and the distance calculation between terrain transition apex and gate. The skier trajectory is shown in red with the deflection points of the trajectory (DP). The DPs were projected (pDP) normal onto the DTM (profile in dark grey) as well as the skier trajectory. The two pDPs and gravity span a plane. The terrain transition apex is where the arrows meet. The arrow with the dashed line represents the maximal distance to the vector between the pDPs. The solid arrow indicates the distance between the terrain apex and the gate.

2.2.4.5 Terrain inclination relative to the skier trajectory

For terrain inclination, parameters were calculated relative to the course setting as shown, but also in relation to skier trajectory. For that purpose the skier trajectory was projected normal to the DTM (P_S). The terrain inclination in the skier direction (parallel to P_S), the terrain inclination in the direction normal to P_S, and the angle between P_S and the gradient were computed in the same way as the terrain inclination in the course direction (α), terrain inclination normal to course direction (θ) and the angle between course direction and the gradient (β) but using P_S.

The instantaneous terrain inclination change along the skier trajectory was computed along the projection of the skier trajectory onto the DTM (P_S). Terrain inclination was calculated for every position of P_S as the angle between the vector spanned by two consecutive points of P_S and the horizontal plane. The change in terrain inclination along P_S was computed both as the change in inclination per unit of distance travelled, as well as the change in inclination per unit of time skiing. The change in terrain inclination per unit of distance travelled was calculated to characterize the terrain along the skier's trajectory. The change in terrain inclination per unit of time travelled was calculated to characterize the rate at which skiers face terrain inclination alterations along their path.

2.2.4.6 Statistical analysis

The number of gates analysed was 572 in GS, 210 in SG and 271 in DH. Normality of data was tested using a Lilliefors test ($\alpha = 0.05$). Most parameters were found not to be normally distributed. Hence, non-parametric statistics were applied to all parameters. Median and IQR were computed for all parameters and disciplines. The relative sizes of GS and SG compared to DH were computed from the medians of each discipline and were expressed as % of DH medians. The medians of the disciplines were tested for significant difference from each other for all parameters using an ANOVA, Kruskal – Wallis test ($\alpha = 0.01$), followed by a Friedman's test ($\alpha = 0.01$) when differences were found in the ANOVA. It was tested pairwise if the distributions of the three disciplines were statistically equal using a two-sample Kolmogorov-Smirnov test ($\alpha = 0.01$). The distributions of terrain inclination change per distance and the terrain inclination change in relation to time were assessed in detail for the largest 5% and smallest 5% values. For terrain inclination change per distance it was tested if the distributions were larger or smaller for all values larger than 1.3°/m and smaller than -1.2°/m using a two-sample Kolmogorov-Smirnov test ($\alpha = 0.01$). For terrain inclination change in relation to time it was tested if the distributions were larger or smaller for all values larger than 19°/s and smaller than -21°/s using a two-sample Kolmogorov-Smirnov test ($\alpha = 0.01$). The relationships between terrain inclination and gate distance and horizontal gate distance respectively were assessed with a linear model and the Spearman correlation coefficient was computed to assess its strength. A Wilcoxon signed rank test ($\alpha = 0.05$) was applied to test if distance from gate to terrain transition apex and terrain inclination changes were significantly different from zero. A Wilcoxon rank sum test and a two-sample Kolmogorov-Smirnov test ($\alpha = 0.01$) were applied to test if the medians and distributions were different between: 1) terrain inclination in skier direction and terrain inclination in the

course direction, 2) terrain inclination normal to skier direction and terrain inclination normal to the course direction, and 3) the angle between skier direction and gradient and the angle between course direction and gradient. It was tested if distributions were similar between disciplines using a two sample Kolmogorov – Smirnov test ($\alpha = 0.01$) and testing two disciplines consecutively.

2.2.5 Characterisation of skiers' mechanics in World Cup alpine skiing

Paper V was undertaken to comprehensively describe the distributions of ground reaction forces and their components and air drag forces within and between the disciplines GS, SG and DH, the dependence of the external forces on turn radius and their significance with respect to energy dissipation. In paper VI it was assessed if the differences in injury incidences per 1000 runs between competiton disciplines can be explained by differences in skiers' mechanics.

2.2.5.1 Parameter computation

CoM position, speed, velocity, acceleration, ground reaction force, air drag force and resultant force were calculated by the methods presented in paper I and II using the GNSS antenna trajectory and the snow surface. Turn radius was calculated using a geometrical approach (Reid, 2010). The antenna trajectory of the skier, the DTM and the method described in paper II were used to calculate the resultant force ($\boldsymbol{F}_{RES}$), air drag force ($\boldsymbol{F}_{D}$), the ground reaction force ($\boldsymbol{F}_{GRF}$), speed and turn radius were reconstructed. $\boldsymbol{F}_{GRF}$ was decomposed into the component normal to the snow surface ($\boldsymbol{F}_{GRF\ Vert}$) in the tangent direction to the skiers' trajectory ($\boldsymbol{F}_{GRF\ Friction}$) and orthogonal to $\boldsymbol{F}_{GRF\ Vert}$ and $\boldsymbol{F}_{GRF\ Friction}$ in the radial direction ($\boldsymbol{F}_{GRF\ Radial}$).

$\boldsymbol{F}_{GRF\ Vert}$ was computed as the component of $\boldsymbol{F}_{GRF}$ parallel to the snow surface normal unit vector at the skiers' location. $\boldsymbol{F}_{GRF\ Friction}$ was computed as described in paper II and represents the total ski–snow friction in the tangential direction to the trajectory. The ski–snow friction coefficient (c_f) was computed from $\boldsymbol{F}_{GRF}$ and $\boldsymbol{F}_{GRF\ Friction}$. $\boldsymbol{F}_{GRF}$, $\boldsymbol{F}_{GRF\ Vert}$, $\boldsymbol{F}_{GRF\ Friction}$, $\boldsymbol{F}_{GRF\ Radial}$, $\boldsymbol{F}_{D}$ and c_f were illustrated in relation to the turn radius for each discipline. The turn radius was divided into sections of 2m. Each single data point was assigned to its corresponding turn radius section. Force and speed values were then assigned as a function of their turn radius to a turn radius section. The mean value of each section was calculated for all forces and speeds and expressed as a function of the mean turn radius of the section. The relationship was plotted for sections with a minimum of 100 data points only. Further, instantaneous energy dissipation due to ski–snow friction $E_{DISS\ (FGRF\ Friction)}$ and air drag $E_{DISS\ (FD)}$ were computed according to equations 8 and 9. The

relative contribution of $E_{DISS\ (FGRF\ Friction)}$ and $E_{DISS\ (FD)}$ to the total instantaneous drag (sum of $E_{DISS\ (FGRF\ Friction)}$ and $E_{DISS\ (FD)}$) were expressed as percentages of total instantaneous energy dissipation.

Using speed and the skier's mass the skier kinetic energy (E_{kin}) was computed. The impulse of $\boldsymbol{F_{GRF}}$ and $\boldsymbol{F_D}$ were calculated for the entire race and added (I_{GRF+D}) as shown in equation 10. I_{GRF+D} might account for the major part of the processes causing fatigue. The race time was measured with the official race timing system.

The jump frequency per race (J_f), air time (J_t) and distance (J_d) per jump were determined from the skier trajectory and the DTM. The time of take-off was determined from the distance over ground and the touch-down from the peak of the vertical acceleration. J_d and J_t were computed from the spatial and temporal difference between take-off and touch-down locations.

$$\mathbf{E_{DISS\ (F_{GRF\ Friction})}} = \int F_{GRF\ Friction}(t) \cdot v(t) \cdot dt \tag{8}$$

$$\mathbf{E_{DISS\ (F_D)}} = \int F_D(t) \cdot v(t) \cdot dt \tag{9}$$

$$I_{GRF+D} = \int_{Start}^{Finish} F_{GRF} \cdot dt + \int_{Start}^{Finish} F_D \cdot dt \tag{10}$$

2.2.5.2 Statistical analysis

The data from 572 GS turns, 210 SG turns and 271 DH turns were used for this analysis. Normality of data was tested using a Lilliefors test ($\alpha = 0.05$). No parameter was found to be normally distributed, so non-parametric statistics were applied to compare parameters between disciplines for all parameters. Median and IQR were computed for all parameters and disciplines. The relative size of GS and SG compared to DH were computed from the medians of each discipline and were expressed as % of DH medians. The medians of the disciplines were tested using an ANOVA, Kruskal – Wallis test ($\alpha = 0.01$), followed by a Friedman's test ($\alpha = 0.01$) if differences were found in the ANOVA. For the computation of the median and IQR of turn radius, only radius values smaller than 150m were considered. The distribution within and between the disciplines was visualized using histograms. It was tested if distributions were similar between disciplines using a two sample Kolmogorov – Smirnov test ($\alpha = 0.01$) and testing two disciplines consecutively.

2.2.6 Differences in injury rate and skiers' mechanics between the disciplines giant slalom, super-G and downhill

In paper VI it was assessed if the differences in injury incidences per 1000 runs between competiton disciplines can be explained by differences in skiers' mechanics. In the GS discipline each single run was included in the analysis. In DH official competition training runs were also used. If several DH runs were measured in one race location they were treated as repeated measures in the analysis. At each race one forerunner, who was part of the official forerunner group, was equipped to collect data for this study.

2.2.6.1 Epidemiologic parameters

Epidemiologic injury data from the FIS ISS injury surveillance system (Florenes et al., 2009) were used to compute exposure-time independent injury rates. Exposure time was defined as the average race time per discipline and was calculated as the mean of all race medians involving all racers who finished the race. The data for the exposure time analysis were taken from the fis-ski.com webpage and represented the same two seasons (2006/7 and 2007/8) in which the injury data was collected. Finally, exposure-time normalized incidence rates, injuries per hour, were computed for each discipline as the (number of injuries in WC races) / (average run time * number of runs in WC races) and were compared to the skier's mechanical characteristics.

2.2.6.2 Statistical analysis

For Ekin, I_{GRF+D}, run time, J_f, J_t, and J_d, the mean and SD were calculated within each discipline and compared as a percentage of the DH values. The medians of each discipline were compared using a Kruskal - Wallis test ($\alpha = 0.01$). The distributions between and within disciplines were illustrated in histograms for speed, turn radius and $\boldsymbol{F_{GRF}}$. Straight skiing was defined by a minimum turn radius of 125m for all disciplines. To compare turn characteristics between the disciplines, the phases with substantial direction change were defined and analyzed based on a maximal turn radius criterion: 30m in GS (Spörri et al., 2012b) and proportional criteria for SG (75m) and DH (125m). The mean of the turn means was calculated for turn speed, turn $\boldsymbol{F_{GRF}}$ and turn radius within each discipline. The extreme values (minimum for turn radius, maximum for turn speed and $\boldsymbol{F_{GRF}}$) were calculated for each single turn and the values of the turns with the 10% most extreme values were averaged within each discipline. The median of each discipline was compared using a Kruskal - Wallis test ($\alpha = 0.01$).

3 Results and Discussion

3.1 GNSS method development and validation

3.1.1 Assessment of position, velocity and acceleration accuracy

3.1.1.1 Results

The CoM position, velocity and acceleration were calculated for twelve runs and were analysed for the assessment. The position differences of the antenna obtained from the GNSS and the reference system were 0.00±0.04 m (Table 2). Comparing the GNSS antenna position and the pendulum model as an approximation of the CoM, the pendulum model had substantially smaller positioning differences to the reference CoM position (Table 2): 0.09±0.12 m using the pendulum model, 0.69±0.34 m without using the pendulum model). The differences were mainly reduced in lateral and inferior-superior direction (Table 2).

Table 2 Average mean and average standard deviation (SD) of position differences for the turn cycles (N=12). The position differences are in m. $P_{GNSS,CoM} - P_{REF,CoM}$ is the difference between the CoM approximation of the pendulum model ($P_{GNSS,CoM}$) and the CoM of the reference system ($P_{REF,CoM}$). $P_{GNSS,ANT} - P_{REF,CoM}$ is the difference between the antenna position computed by the GNSS method ($P_{GNSS,CoM}$) and the CoM of the reference system ($P_{REF,CoM}$). $P_{GNSS,ANT} - P_{REF,ANT}$ is the difference between the antenna position computed by the GNSS method ($P_{GNSS,ANT}$) and the antenna position computed by video-based 3D kinematics ($P_{REF,ANT}$).

Turn cycle differences		$P_{GNSS,CoM} - P_{REF,CoM}$	$P_{GNSS,ANT} - P_{REF,CoM}$	$P_{GNSS,ANT} - P_{REF,ANT}$
Vectorial amplitude	Mean	0.09	0.69	0.00
	SD	0.12	0.34	0.04
Fore-aft	Mean	0.07	0.07	0.00
	SD	0.03	0.03	0.01
Lateral	Mean	0.02	0.05	0.00
	SD	0.1	0.32	0.02
Inferior-superior	Mean	0.05	0.69	0.00
	SD	0.06	0.09	0.04

For velocity, the pendulum modelling also showed a smaller vectorial amplitude average mean difference (0.08m/s) than without modeling (0.20 m/s), while the precision (vectorial amplitude average standard deviation) did not decrease (i.e., 0.19 m/s with modelling vs. 0.16 m/s without modelling) (Table 3). When analysing the pattern of the differences, it can be seen that the maximum error in the pendulum modelling occurred during the first third of the turn cycle. When comparing the turn maximum values of velocity the offset and precision were improved with the pendulum model (Table 3). It is worth noting that the standard deviation of the antenna velocity between the GNSS and the reference system was 0.12 m/s, representing the precision of the reference method (Table 3).

The vectorial amplitude mean and standard deviation of the differences in acceleration were slightly lower using the pendulum model (Table 3). While the offset was minimally improved (0.22 m/s^2 with pendulum model vs. -0.34 without pendulum model) the precision increased to a larger extent (1.28 m/s^2 vs. 1.92 m/s^2). When analysing the pattern differences, the maximum vectorial amplitude difference was noticed during the last quarter of the turn cycle with or without pendulum model. For the turn mean and maximum values of acceleration a smaller offset and a better precision was found using the pendulum model except for the precision of the turn mean (Table 3).

Table 3 Average mean and average standard deviation (SD) of velocity and acceleration differences for the turn cycles and for the typical extracted features (mean and maximum value of a turn) (N=12). The velocity and acceleration differences are in m/s and m/s², respectively. $V_{GNSS,CoM}$ - $V_{REF,CoM}$ and $A_{GNSS,CoM}$ - $A_{REF,CoM}$ are the differences between the CoM approximation of the pendulum model and the CoM of the reference system. $V_{GNSS,ANT}$ - $V_{REF,CoM}$ and $A_{GNSS,ANT}$ - $A_{REF,CoM}$ are the differences between the antenna computed by the GNSS method and the CoM of the reference system. $V_{GNSS,ANT}$ - $V_{REF,ANT}$ and $V_{GNSS,ANT}$ - $V_{REF,ANT}$ are the differences between the antenna computed by the GNSS method and the antenna computed by video-based 3D kinematics.

Turn cycle differences		$V_{GNSS,CoM}$-$V_{REF,CoM}$	$V_{GNSS,ANT}$-$V_{REF,CoM}$	$V_{GNSS,ANT}$-$V_{REF,ANT}$
Vectorial amplitude	Average mean	0.08	0.2	0.01
	Average SD	0.19	0.16	0.12
Turn mean and maximum	Turn mean	0.06	0.19	0
	SD of turn mean	0.05	0.05	0.02
	Turn maximum	0.06	0.08	-0.03
	SD of turn max.	0.13	0.16	0.07

		$A_{GNSS,CoM}$-$_{REF,CoM}$	$A_{GNSS,ANT}$-$A_{REF,CoM}$	$A_{GNSS,ANT}$-$A_{REF,ANT}$
Vectorial amplitude	Average mean	0.22	-0.34	-0.57
	Average SD	1.28	1.92	0.48
Turn mean and maximum	Turn mean	0.01	0.42	0.47
	SD of turn mean	0.43	0.23	0.22
	Turn maximum	0.06	0.08	-0.03
	SD of turn max.	0.13	0.16	0.07

3.1.1.2 Discussion

The findings of the current study indicate that the proposed GNSS method is valid for the assessment of CoM velocity and acceleration and some lower validity for the estimation of the CoM position. As long as the investigated differences are smaller than the precision boundaries requested by the research question, the proposed method can be considered as technically valid.

With respect to CoM velocity and acceleration, in an earlier study using a video-based system, Spörri et al. (2012b) found differences of 0.3-0.5 m/s and of 2.6 m/s² when comparing the CoM kinematics of different course settings. The reported offset and precision of the proposed pendulum model was within the range of these discriminative meaningful changes (0.08±0.19 m/s and 0.22±1.28 m/s²). Even the velocity and acceleration offset and the precision of the GNSS antenna (without pendulum model) might be sufficient for various applications, since it

was found to be 0.20±0.16 m/s and -0.34±1.92 m/s^2. The velocity and acceleration errors of the model might be mainly caused by the position modeling of the CoM approximation methods and derivative artifacts. The derivative artifacts might result from the fact that in order to calculate velocity and acceleration, for both GNSS and reference systems, derivation operations are required. This may increase the signal-to-noise ratio. Another reason might be that body segment movements (e.g., body extension of turn initiation and completion) were not directly considered in the proposed modeling. Maximum error was observed during the turn transitions (0 – 20% and 80 – 100% of the turn cycle). These turn phases are known to involve extensive body segment movements (Müller & Schwameder, 2003). Another interesting finding was that the offset and standard deviation of the turn mean and maximum velocity and acceleration were rather small. This indicates that the comparison of turn mean and turn maximum values between turns based on both the pendulum model and directly from the GNSS antenna can be considered to be valid.

With respect to CoM position, in an earlier study using video-based systems, Schiefermüller et al. (2004) observed CoM position differences of 0.1 m between different skiing techniques. Considering this value as the range of meaningful changes, the reported precision of the proposed pendulum model (0.09±0.12 m) was larger than the range found by Schiefermüller et al. (2004). Consequently, there might be some limitation of the proposed method when analyzing trajectories with small, but still substantial spatial differences as they are in giant slalom or slalom. In this case the use of camcorder-based 3D kinematics might be indispensable. However, the precision requirements with respect to position for the relative comparison between skiers / runs might be reduced for the speed disciplines (i.e. super-g and downhill), where spatial differences in trajectories are expected to be larger. The position error of the pendulum model in inferior-superior direction might be mainly influenced by the 53% value to affix the CoM approximation along the pendulum. This value was obtained from a dataset in slalom and might be some different for the use in giant slalom. However, based on the current data it was found that if a value of 56% instead of 53% would be used the position error in inferior- superior direction would be reduced by 5cm. Moreover, this adjustment would increase the SD in lateral direction by 1.5 cm.

3.1.1.3 Methodological considerations

Generally, it has to be stressed that the validity found in this study is reliable for the specific GNSS method and modelling and the specific setup (giant slalom on an even slope) of the

current study. If different GNSS methods are used the validity of the antenna kinematics is likely to be different. The number of satellites in view might have effect on the goodness and stability of the positioning solution. Thus, the combination of several satellite systems such as GPS and GLONASS might be advantageous, when measuring in obstructed locations. Further the number of GNSS signal frequencies, the differential processing algorithm, the measurement frequency, the filtering technique and the used hardware might be significant for the goodness of the GNSS antenna data. Furthermore, the pendulum model might perform differently when it is applied in disciplines other than giant slalom or on non-even terrain. When skiing over convex terrain transitions the pendulum model might underestimate the skier lateral inclination if skiers are actively unweighting. In the case that the skiers are air born the pendulum model is unable to predict the CoM position in vertical direction, since the body extension cannot be limited by the intersection of the pendulum with the terrain. The body extension has to be estimated for the phases when the skiers are air born. If the terrain model is not reconstructed in detail, the pendulum length can be under or overestimated. In slalom the difference between head and CoM acceleration is larger, than in giant slalom and the CoM and head trajectories are less in parallel compared to giant slalom (Gilgien, M., Reid, R., Haugen, P., Kipp, R., and Smith, G., 2010). Therefore, it can be expected, that the pendulum model faces bigger challenges when being applied in slalom and that its validity is poorer than in giant slalom. At the same time the limits of meaningful changes might be smaller in slalom. Consequently, the use of alternative methods for the reconstruction of CoM kinematics might be indispensible for slalom. In contrast, for the speed disciplines the limits of meaningful changes might be larger and the head and CoM kinematics might be more identical than in giant slalom.

In a previous study using GNSS methodology along with a pendulum model for the reconstruction of the CoM kinematics in alpine skiing (Supej et al., 2012) the antenna was mounted on the skier's back. Using this mounting point the reconstruction of the CoM kinematics might be simpler, since the kinematics of the back is closer to the kinematics of the CoM (Meyer, 2012). But on the other hand, a GNSS antenna mounted on the skier's helmet, as it was used for the current study, eliminates satellite signal shading by the skier's body. This may, therefore, avoid large positioning errors due to loss of the differential GNSS solution in obstructed terrain. Hence, the measurement location with its satellite signal shading characteristics might guide the user in the choice of method.

3.1.2 Position accuracy assessment of different GNSS methods

Paper III compares five different GNSS methods to an independent reference system for one turn. In a second step the most valid method from the first analysis is used as reference to compare different methods for an entire run. Further also time to acquire differential solutions is assessed.

3.1.2.1 Results

3.1.2.1.1 Comparison with the independent reference system (step 1)

The results revealed that: a) the position differences generally increased with increasing elevation angle; b) the position differences (mean and median) and SD were larger in the Z dimension than in the XY dimension; c) method *E* had the largest position difference mean, median and SD of all methods in all conditions; d) in the conditions 10° and 30° the position differences (mean and median) were smallest for method *A*, followed by *C*, *B*, *D* and *E*; e) the differences (mean and median) in the condition 40° were smallest for method *A*, followed by *C*, *B* and *E*, while method *D* was unable to compute a differential solution; f) method *A* was the only method with mean and median XYZ differences smaller than 7 cm in all elevation angle conditions; g) in the 10° condition methods *A* – *C* had mean and median XYZ differences smaller than 2 cm and SDs smaller than 4 cm.

The histograms shown in Figure 15 illustrate the norm of the spatial differences (XYZ) along with the proportions of time when no solutions could be computed with the respective methods (NaN). For the condition of 10°, all differential methods were able to fix integer ambiguities for the entire turn. Method *D* consisted of differences smaller than 5 cm and in the range of 2-3 m. Method *E* had no differences smaller than 0.5 m or larger than 10m. For the condition of 30°, method *A* had only fixed solutions and position difference mean and median were smaller than 5 cm. The fraction of the data without solution (NaN) was largest for method *D,* followed by *E*, *C* and *B*. For method *B* and *D* approximately 80% and 70% of the differences respectively were smaller than 5cm, while the remainders were in the order of meters. Method *E* had most differences in the range of 2 – 15 m. For the condition of 40°, the fraction of the data without solution (NaN) was largest for method *D* (no solution) followed by *E*, *C*, *B* and *A*. Method *A* had differences smaller than 10cm for more than 75% of the time. Method *B* had most differences in the range of 1-10m. Compared to method *B*, method *C* had a larger fraction with

differences smaller than 0.5m and periods of no solution. Method *E* had no solution for about 70% of the time and all differences were larger than 1m.

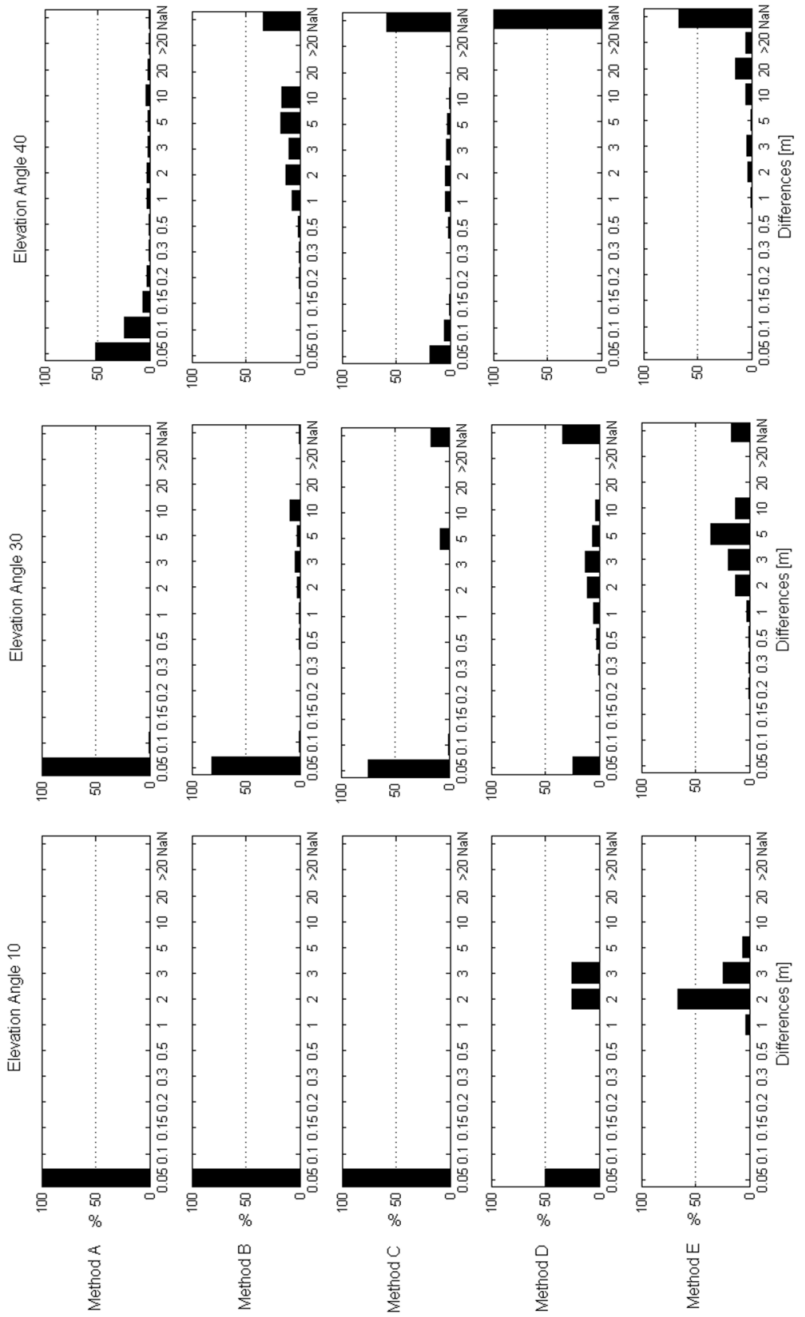

*Figure 15. Histograms of the position difference norms (XYZ) between the trajectories of methods A – E (**A_1** – **E_1**) and the reference trajectory (**P_{REF}**) for the elevation masking conditions 10°, 30° and 40°. On the horizontal axis, NaN indicates the amount of time when no solution could be computed.*

3.1.2.1.2 Position accuracy assessment of entire runs and time to acquire fixed solutions (step 2)

Table 4 indicates that the differences were slightly smaller in step 2, where the entire run was considered, than in study 1, where the analysis was based on a specific section only. Using the entire run, more trajectories managed to compute a fixed ambiguities solution (Table 5, left side). The histogram of the differences for step 2 differed insignificantly from the results in the histograms in study 1.

Table 4. Mean, Median and SD of the spatial differences between the skier trajectory solution $\boldsymbol{A_2 - E_2}$ *and the solution of method A in the condition 10°. XYZ represents the difference norm in 3 dimensions, XY the difference norm in the horizontal plane and Z in the vertical direction.*

	Mean XYZ [m]			**Mean XY [m]**			**Mean Z [m]**		
Elev. Angle	10°	30°	40°	10°	30°	40°	10°	30°	40°
Method *A*	-	0.02	0.37	-	0.02	0.12	-	0.02	0.35
Method *B*	0.02	0.95	4.29	0.01	0.5	1.3	0.01	0.8	3.98
Method *C*	0.02	0.48	0.85	0.01	0.35	0.31	0.01	0.34	0.76
Method *D*	0.96	1.22	NaN	0.49	0.37	NaN	0.79	1.08	NaN
Method *E*	1.86	3.42	11.66	1.06	1.79	2.99	1.3	2.62	11.19

	Median XYZ [m]			**Median XY [m]**			**Median Z [m]**		
Elev. Angle	10°	30°	40°	10°	30°	40°	10°	30°	40°
Method *A*	-	0.02	0.02	-	0.02	0.06	-	0.02	0.06
Method *B*	0.01	0.02	1.23	0.01	0.03	3.43	0.01	0.03	3.43
Method *C*	0.01	0.02	0.03	0.01	0.02	0.07	0.01	0.02	0.07
Method *D*	0.03	0.22	NaN	0.03	0.16	NaN	0.03	0.16	NaN
Method *E*	1.07	1.54	2.97	1.15	2.39	11.81	1.15	2.39	11.81

	SD XYZ [m]			**SD XY [m]**			**SD Z [m]**		
Elev. Angle	10°	30°	40°	10°	30°	40°	10°	30°	40°
Method *A*	-	0.05	1.54	-	0.04	0.49	-	0.05	1.47
Method *B*	0.04	2.37	3.43	0.04	1.25	0.9	0.04	2.03	3.46
Method *C*	0.04	1.39	1.4	0.04	1.02	0.5	0.04	0.97	1.33
Method *D*	1.04	1.68	NaN	0.59	0.52	NaN	0.91	1.66	NaN
Method *E*	0.69	1.51	6.73	0.47	1.11	1.79	0.98	1.66	6.63

Attention: When reading the accuracy results, it is important to keep in mind that the differences from the reference system are valid only for the time periods with differential solutions. For the periods without differential solution the accuracy was substantially reduced compared to the accuracy of the respective navigated position solutions.

The timespans from (warm) start of the differential GNSS measurement until ambiguities were fixed are given in the right hand side of table 5. The mean time to fix the ambiguities was below 1.2s for method *A* in all conditions and for method *B* and *C* in the 10° condition. Method *C* required less time (mean) to fix the integer ambiguities than method *B*. Method *D* was slowest to fix integer ambiguities and was unable to do so in the 40° condition.

Table 5. The number of trajectories (out of 12) for which a fixed ambiguities solution was computed at least once during the run is shown on the left. The duration from GNSS measurement start to the instant a fixed ambiguities solution was computed for the first time is shown on the right.

	Number of trajectories with fixed solution			**Time to fix [s] mean ± SD**		
Elev. Angle	10°	30°	40°	10°	30°	40°
Method *A*	12	12	12	0.06±0.10	0.06±0.06	0.56±1.52
Method *B*	12	12	9	1.1±1.1	13.58±20.50	43.70±20.24
Method *C*	12	10	7	0.34±0.88	4.62±11.12	27.94±66.18
Method *D*	12	8	-	19.96±2.26	51.54±46.54	-
Method *E*	-	-	-	-	-	-

3.1.2.2 Discussion

The elevation angles 10°, 30° and 40° were chosen to simulate realistic signal obstruction conditions for WC alpine ski racing. Positioning dilution of precision (PDOP) was determined by forerunners skiing real WC races, using method *A*. The measurements in the WC races revealed that PDOP of 1.5 to 2.0 occurred 76% of the time, PDOP between 2 and 5 for 19% of the time and PDOP above 5 for approximately 5% of the time for method *A*. These measures are in agreement with the findings of other studies (Lachapelle, Morrison, Ong et al., 2009; Lachapelle, Morrison, & Ong, 2009). During the experiment for this simulation a mean PDOP of 1.9 was found for an elevation angle of 30° and a mean PDOP of 7.8 for the 40° elevation angle condition. Hence, the 10° elevation angle condition represented conditions without any

additional obstruction, as would be the case on glaciers for example, while the 30° and 40° conditions represented ordinary and extreme WC racing conditions respectively.

In order to be able to detect relevant functional differences, the accuracy requirements for position data in alpine skiing must be in the range of a few centimetres in slalom and giant slalom (Spörri et al., 2012a), but might be larger in the speed disciplines super-G and downhill.

Hence, the results of study 1 and 2 showed that GNSS measurements in WC races should be accomplished using both GPS and GLONASS and frequency L1 and L2 (method *A*). If measuring in areas with little satellite signal obstruction, for example on glaciers, GLONASS or frequency L2 can probably be dropped, if high-end devices are used. But under real WC competition conditions, where topography and trees are obstructing the satellite signal, both accuracy of the fixed solutions and the amount of fixed solutions decreased, if either frequency L2 (method *B*) or GLONASS (method *C*) was dropped. Comparing method *B* and *C,* the use of frequency L2 increased the accuracy of the fixed solutions in method *C*, possibly as a result of the reduction of disturbances in the ionosphere (Pireaux et al., 2010). However, using method C the share of data with fixed integer ambiguities was smaller than for method *B*. The increased amount of fixed integer ambiguity for method *B* compared to method *C* might be the result of a better satellite signal constellation since geometrical dilution of precision (GDOP) was increased for method *B*. The effects of satellite signal frequencies and satellite systems on the share of fixed integer ambiguities and accuracy found in this study are in line with the literature (Lachapelle et al., 2009).

Since obstruction can lead to loss of differential solutions, the time to fix integer ambiguities and quickly regain acceptable accuracy is crucial (Skaloud & Limpach, 2003). This study showed that time to fix integer ambiguities was shorter when both frequencies (L1 and L2) were used instead of L1 only. Hence, integer ambiguity fixing is a second reason to use frequency L1 and L2 when measuring alpine ski racing under ordinary conditions. However, it is known that time to fix integer ambiguities also depends on the GNSS equipment (Skaloud & Limpach, 2003) and might deviate when different GNSS devices are used. If different receivers, antennae and processing software are applied, positioning accuracy may also differ, especially if low-cost devices are used. Initial comparison of non-differential low-cost devices applying L1 and GPS resulted in substantially larger differences to method *A* than the ones presented for method *E* in this study.

The findings of this study might not only be applicable to the sport of alpine skiing, but also to other sports held in surroundings with variable GNSS signal obstruction. Furthermore, the

results of the 10° condition might be applicable to all kinds of sports allowing favorable GNSS measurement conditions. Buildings, vegetation and topography might mask satellite signals in a manner which is comparable to the conditions known in alpine ski racing (30° and 40° condition). Hence, a broad variety of GNSS operators might benefit from an enhanced understanding of the significance of GNSS methods on their outcomes.

3.1.2.3 Methodological considerations

The current study has several limitations, which may influence the results of the method comparisons: (1) the accuracy of the photogrammetric reference system was found to be 23mm ± 10mm for well-defined points. Additional uncertainty might be added in the digitalization of the antenna GNSS antenna center. (2) The resection method used for the matching of the reference system with the GNSS measurements had a mean difference of 16 mm. The SD of the difference was ± 5mm. (3) The reference system of step 2 is not independent. It is therefore theoretically possible that method *A* had a larger difference from the true trajectory than one of the other methods.

3.1.3 Computation of external forces using the GNSS based system

The GNSS system based forces were compared to the forces of the reference system for twelve trials.

3.1.3.1 Results

Table 6 shows the results of the assessment. The average vectorial difference offset obtained from the GNSS and the reference system was largest for $\boldsymbol{F}_{GRF}$ but substantially smaller for $\boldsymbol{F}_{F}$ and $\boldsymbol{F}_{D}$. The average vectorial difference offset for $\boldsymbol{F}_{GRF}$ and $\boldsymbol{F}_{D}$ was smaller for the turning phase when the turn radius was below 30 m than for the entire turn cycle both in absolute values and relative to the size of the respective turn cycle mean and turning phase mean forces. The average vectorial difference offset of $\boldsymbol{F}_{F}$ was larger for the turning phase than the turn cycle. The precision offsets for comparison within the GNSS system (AVD-Within-SD) for $\boldsymbol{F}_{GRF}$ and $\boldsymbol{F}_{F}$ were less than half of the precision offsets between the GNSS and the reference system (AVA-Between-SD) while this was nearly unchanged for $\boldsymbol{F}_{D}$. During the turning phase when the turn radius was below 30 m the AVA-Between-SD was reduced in both absolute and relative terms compared to the entire turn cycle for $\mathbf{F}_{\mathbf{GRF}}$ and $\mathbf{F}_{\mathbf{F}}$ but not for $\boldsymbol{F}_{D}$. Comparing the typical features of turn cycles, the differences in the turn mean were substantially smaller than the AVD-Within-

SD and AVD-Between-SD for all forces. The maximum values were underestimated for all forces with the largest error for $\boldsymbol{F_{GRF}}$. The upper parts of Figures 16-17 illustrate $\boldsymbol{F_{GRF}}$ and $\boldsymbol{F_F}$ obtained from the reference and the GNSS method in time-normalized format across the examined turn cycle. The lower parts of Figures 16-17 show the progression of the vectorial difference and its AVD-Within-SD for $\boldsymbol{F_{GRF}}$ and $\boldsymbol{F_F}$ graphically. All three forces have a variability of the offset. The largest offsets occur in the initiation and completion phase for $\boldsymbol{F_{GRF}}$.

Table 6 Average vectorial difference offset, between and within standard deviation (SD) and percent difference of the ground reaction force ($\boldsymbol{F_{GRF}}$), ski-snow friction ($\boldsymbol{F_F}$) and air drag ($\boldsymbol{F_D}$) for the entire turn cycle and the turning phase (turn radius < 30 m). Comparisons of the turn mean and maximum values (typical feature of turn cycle) are given in the bottom part of the table (N = 12).

Differences		$\mathbf{F_{GRF}}$	$\mathbf{F_F}$	$\mathbf{F_D}$
Average Vectorial Difference (AVD) for Turn Cycle	Offset [N]	−25.8	1.3	−6.4
	Offset [%]	−1.9	0.3	−8.9
	Offset-between SD [N]	151.7	96.2	6.1
	Offset-between SD [%]	11	26.3	8.5
	Within SD [N]	63.2	41.5	7
	Within SD [%]	4.6	11.4	9.8
Average Vectorial Difference (AVD) for Turning Phase	Offset [N]	7.7	−16.6	3.1
	Offset [%]	0.5	−3.8	4.8
	Offset-between SD [N]	124.2	81.3	5.8
	Offset-between SD [%]	7.5	18.5	9.1
Typical Turn Cycle Feature	Mean [N]	−22.2	1.1	−4.4
	SD of Mean [N]	24	6.8	2.9
	Maxima [N]	−71.7	−23.2	−18.7
	SD of Maxima [N]	63.1	76.2	5.8

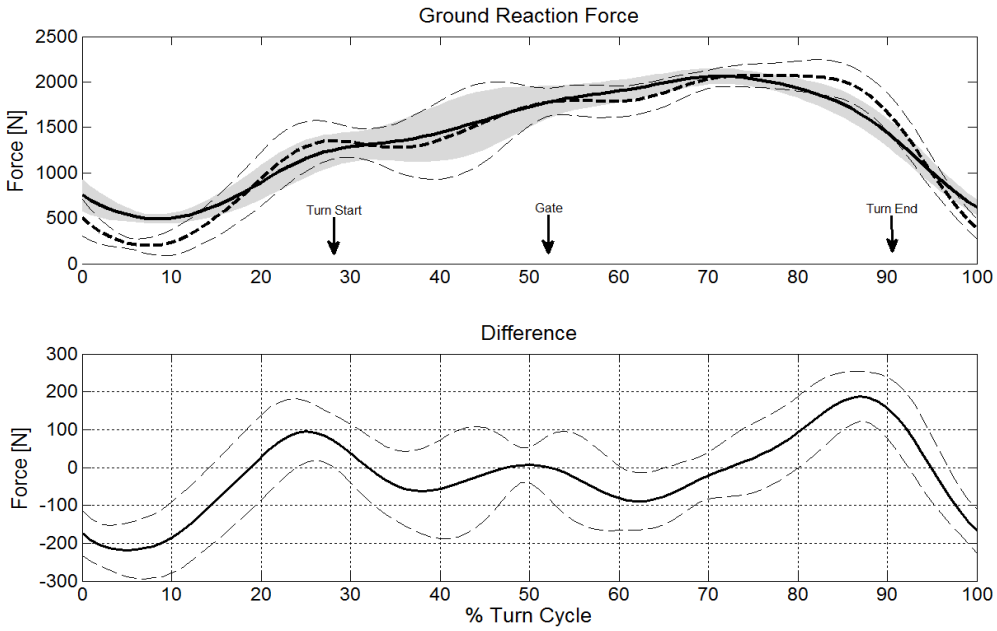

Figure 16. Comparison of the ground reaction force computed from the GNSS method ($\boldsymbol{F}_{GRF,GNSS}$, solid line) and the reference system ($\boldsymbol{F}_{GRF,REF}$, thick dashed line) with their standard deviations ($\boldsymbol{F}_{GRF,GNSS}$, gray area; $\boldsymbol{F}_{GRF,REF}$, thin dashed lines) in the upper part of the graph. The bottom part of the graph shows the instantaneous average vectorial difference (solid line) and its instantaneous AVD-Within-SD (dashed lines) across the turn cycle. Gate passage and the points where the turn radius is less than 30 m are marked as turn start and turn end.

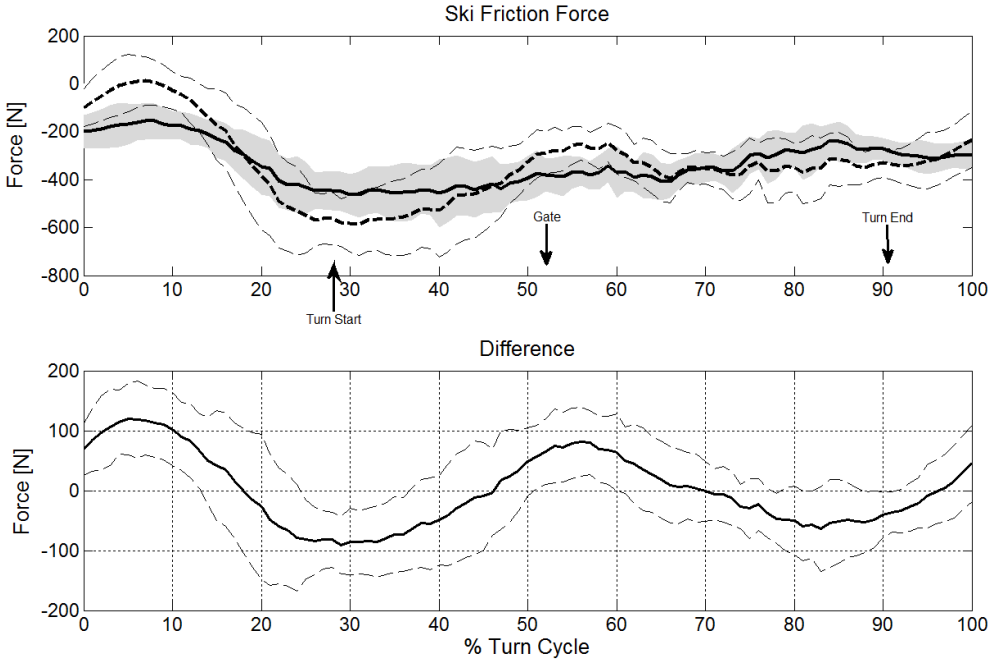

Figure 17. Comparison of the ski friction force computed from the GNSS method ($\boldsymbol{F}_{F,GNSS}$, solid line) and the reference system ($\boldsymbol{F}_{F,REF}$, thick dashed line) with their standard deviation ($\boldsymbol{F}_{F,GNSS}$, gray area; $\boldsymbol{F}_{F,REF}$, thin dashed lines) is provided in the upper part of the graph. The bottom part of the graph shows the instantaneous average vectorial difference (solid line) and instantaneous AVD-Within-SD (dashed lines) across the turn cycle. Gate passage and the points where the turn radius is less than 30 m are marked as turn start and turn end.

3.1.3.2 Discussion

A repeatable instantaneous vectorial difference pattern was observed between the GNSS method and reference system for $\boldsymbol{F}_{GRF}$, $\boldsymbol{F}_{F}$ and $\boldsymbol{F}_{D}$ (Figures 16-17). These patterns oscillated above and below zero and therefore the instantaneous AVD-offsets and the turn mean error compensate across the entire turn cycle and thus differ little from the reference values. Similarly the instantaneous average vectorial difference of $\boldsymbol{F}_{F}$ followed a harmonic pattern around zero (Figure 17) and was approximately compensated in the phase before and after gate passage. Therefore, the offsets of the section before gate passage (−2 N) and after gate passage (5 N) were also small. These findings suggest that comparisons of turn means between skiers or between different turns are valid as long as they are larger than these precision (SD) boundaries of the method.

The AVD-Offset-Between-SDs represent the precision of the GNSS method with respect to the reference system in predicting the absolute values of the forces at random time points in the turn

cycle. These were relatively large for $\boldsymbol{F_{GRF}}$ and $\boldsymbol{F_F}$ but were reduced both in absolute values and relative to the acting forces in the turning phase, when the turn radius was below 30 m.

Because the instantaneous vectorial difference patterns were repeatable for the twelve trials, the AVD-Within-SDs were relatively small: smaller than the AVD-Offset-Between-SDs for $\boldsymbol{F_{GRF}}$ and $\boldsymbol{F_F}$ but about equal for $\boldsymbol{F_D}$. The AVD-Offset-SDs describe the precision within the GNSS method and therefore apply for relative comparisons between skiers or turns when both components are determined with the GNSS method. In a study investigating slalom skiing (Reid, 2010) it was found that the ground reaction force was 253 N higher at gate passage on a course with a 10 m gate distance compared to a course with a 13 m gate distance. The AVD-Within-SD of the GNSS method for $\boldsymbol{F_{GRF}}$ was 63 N and thus the GNSS method is valid to identify such discriminative meaningful changes for the ground reaction force. Similarly the air drag was increased, at 15 N at gate passage in the 13 m course (Reid, 2010), while the AVD-Within-SD for $\boldsymbol{F_D}$ was 7 N. As long as the AVD-Within-SD's are smaller than the differences to be investigated, the method is valid for identifying discriminative meaningful changes at random instances in a turn cycle.

The GNSS method underestimated the turn cycle maxima of all three forces. However, the offset and SD were acceptable with respect to the size of the maximal ground reaction forces (Babiel, Hartmann, Spitzenpfeil et al., 1997; Federolf, Fauve, Luthi et al., 2004). Air drag might be maximal in the initiation phase of the turn, when skiers are in a relatively extended body position (Lachapelle et al., 2009). It is likely that skiers had their arms abducted in that phase of the turn cycle and that these contributed to $\boldsymbol{F_D}$. The underestimation of both maximum and AVD-offset in that phase of the turn may thus partly be caused by the lack of inclusion of the arms in the GNSS method.

The AVD-offset of $\boldsymbol{F_{GRF}}$ might be caused by the offset in the resultant force, since the offset of the resultant force follows a similar pattern (see results of $\boldsymbol{F_{RES}}$ in the electronic supplementary information) and is substantially larger than the offset of the air drag force. Consequently, the offsets in the first and the last phase of the turn of $\boldsymbol{F_{GRF}}$ might be caused by deficient CoM reconstruction in the GNSS method. Thus the offset and precision values presented in this study may be valid for the applied GNSS method and CoM modelling, but may be different for other methods.

3.1.3.3 Methodological considerations

The attachment of the measurement device on the head leads to exclusion of the high frequency ground reaction force components. The skier's body acts as a damper (Babiel et al., 1997) and the measurement frequency of the GNSS of 50 Hz is too low to capture the remaining high frequency components transmitted to the head. The same phenomenon is present for the reference system applied in this study. A previous study (Lüthi et al., 2004) showed that CoMs reconstructed from video-based 3D kinematic motion capture systems lack the high frequency components due to damping by the lower extremities and the low capture frequency. However, the overall course of the ground reaction force was well reconstructed. Therefore, our reference system seems valid to assess the low frequency component of the ground reaction force. For the assessment of high frequency components or left and right leg ground reaction force information, other types of measurement systems should be applied, such as pressure insoles (Nakazato et al., 2011; Lüthi et al., 2004; Holden et al., 2004; Krüger & Edelmann-Nusser, 2009; Klous, Müller, & Schwameder, 2008), force plates (Niessen et al., 1998; Wunderly et al., 1988; Nakazato et al., 2011; Lüthi et al., 2004; Wunderly & Hull, 1989; Federolf, Scheiber, Rauscher et al., 2008) or accelerometers (Chardonnens et al., 2012). The air drag force model might be improved by adding a model for the arms.

3.2 Application of GNSS methods in World Cup giant slalom, super-G and downhill

3.2.1 Characterisation of course setting in World Cup alpine skiing

3.2.1.1 Results

Median, interquartile range (IQR), significance of the difference between discipline medians and distributions and % of DH for GS and SG are presented in Table 7. Whether the medians and distributions were significantly different between the disciplines or not is indicated in own columns of Table 7. Race length, vertical drop and all gate distance parameters were significantly different and increased from GS to SG and DH. GS consisted of significantly more gates and direction changes per race than SG. The median change in direction of the course per turn was approximately equal for GS (31.5°) and SG (30.3°). The coefficient of variation (CV) was larger for horizontal gate distance than gate distance and vertical gate distance for all disciplines. In Figure 18 the distributions within and between disciplines are shown for gate distance and

horizontal gate distance. Terrain inclination was significantly different between all disciplines adn steepest for GS, followed by SG and DH.

*Table 7. Median, interquartile range (IQR) and significance level of the difference between discipline medians and distributions for all parameters, and percentage of DH for GS and SG. DH represents 100% for the relative measure. Differences between medians and distributions were significant between all disciplines if indicated with * and were significantly different between GS and SG when marked with 1, significantly different between GS and DH if marked with 2 and significantly different between SG and DH if marked with 3. If no parameter was significantly different the column is empty. Columns marked with – indicate, that the measure was not computed.*

	Absolute Values (median and IQR)			**Significance**		**% of DH**	
	GS	**SG**	**DH**	**Median**	**Distr.**	**GS**	**SG**
Race length [m]	1437±65	2293±204	3499±501	*	*	41	66
Vertical drop [m]	407±23	598±38	859±112	*	*	47	69
# Gates / Race	53.8±3.4	44.3±3.3	41.5±6.5	1,2	*	130	106
Direction changes	51.2±3.5	40.8±4.0	-	1	1	-	-
Gate Distance [m]	26.24±2.25	49.48±5.69	79.10±37.27	*	*	33	63
Horizontal Gate Distance [m]	7.47±2.93	12.39±10.13	28.96±26.88	*	*	31	52
Vertical Gate Distance [m]	25.12±2.42	48.05±6.76	73.72±34.12	*	*	34	65
CV Gate Distance	0.09	0.11	0.47	-	-	18	24
CV Vertical Gate Distance	0.10	0.14	0.46	-	-	21	30
CV Horizontal Gate Distance	0.39	0.82	1.13	-	-	35	72
Terrain Inclination [°]	-17.8±7.0	-16.6±6.9	-13.6±7.7	*	*	131	121
DTTG Convex (<10m) [m]	1.61±4.79	-0.00±8.43	0.57±10.28			-	-
DTTG Concave (<10m) [m]	1.39±4.20	-0.92±6.67	0.00±5.07	1,2	1,2	-	-
Terrain Incl. in Course Direction [°]	-17.2±8.8	-16.2±6.4	-14.3±6.1	*	*	120	113
Terrain Incl. in Skier Direction [°]	-15.4±10.6	-14.3±11.0	-11.0±9.3	*	*	140	130
Terrain Incl. Normal to Course Dir. [°]	-8.2±6.0	-6.9±6.1	-8.9±8.5	2,3	*	92	77
Terrain Incl. Normal to Skier Dir. [°]	-6.3±6.2	-5.2±6.1	-5.9±7.4	2,3	*	107	86
Angle bw. Grad. & Course Dir.[°]	22.3±12.6	22.3±18.0	31.9±24.0	2,3	2,3	69	69
Angle bw. Grad. & Skier Dir. [°]	23.2±24.0	22.5±28.4	34.7±35.5	2,3	*	66	64
Terrain Inclination Change [°/m]	0.025±0.620	-0.009±0.436	0.008±0.468		*	-	-
Terrain Inclination Change [°/10s]	0.003±0.046	0.001±0.041	0.002±0.054		*	-	-

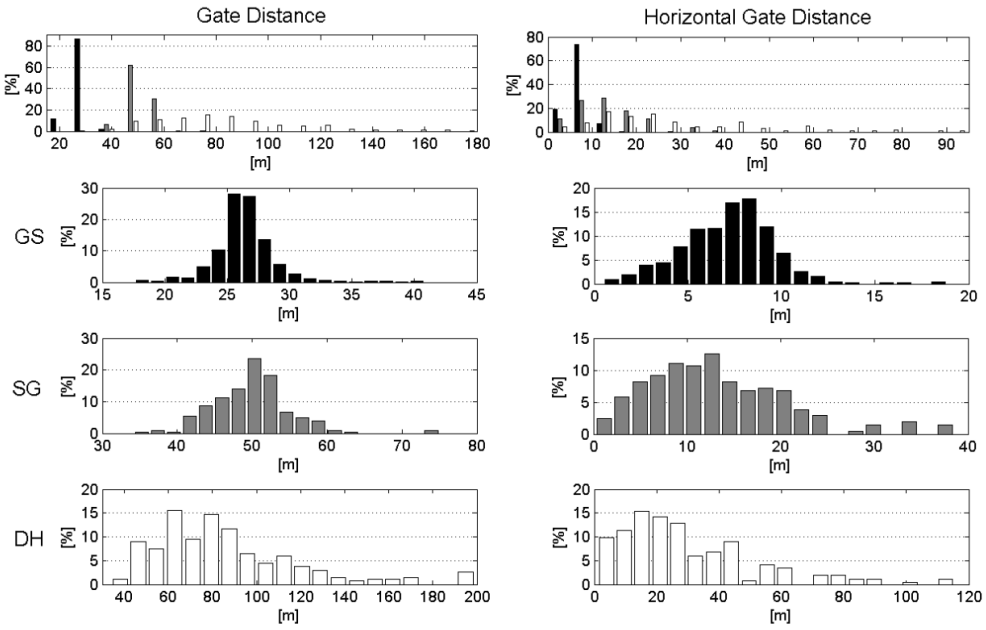

Figure 18. Course setting characteristics. The left-hand column shows gate distance and the right-hand column indicates horizontal gate distance. The uppermost histograms illustrate the differences between disciplines and the lower histograms represent each discipline alone. GS is shown in black, SG in gray and DH in white.

Figure 19 shows the course setting characteristics as a function of terrain inclination. Spearman's Rho's were small for all relationships, but largest for horizontal gate distance in GS. There was a tendency to a shorter gate distance as the terrain became steeper in GS and SG. In GS the horizontal gate distance increased with the steepness of the terrain inclination. Horizontal gate distance approximately doubled when terrain inclination increased from -10° to -30° in GS.

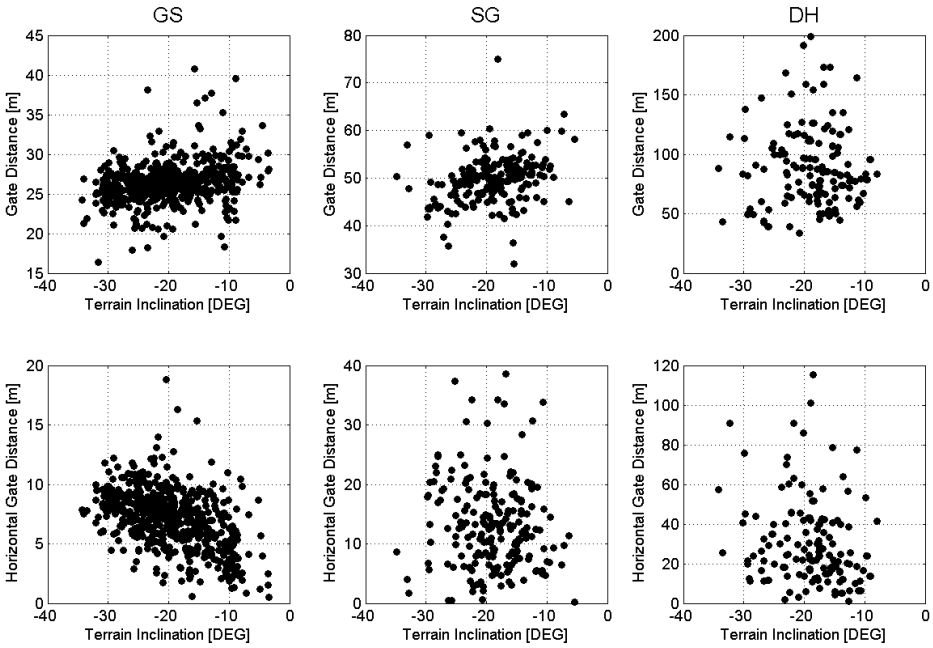

	GS	SG	DH
Terrain Inclination - Gate Distance			
Intersection	28.47	55.05	83.31
Inclination	0.11*	0.28*	-0.08
Spearman's Rho	0.26	0.33	-0.04
Terrain Inclination - Horizontal Gate Distance			
Intersection	3.64	11.34	11.4
Inclination	-0.18*	-0.1	-0.92*
Spearman's Rho	-0.47	-0.08	-0.31

* Significance level is 0.01

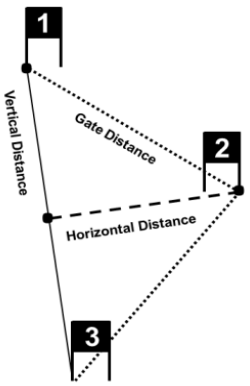

Figure 19. Scatterplots of the relationship between 1) terrain inclination and horizontal gate distance and 2) terrain inclination and gate distance for all disciplines. Statistics of the relation between terrain inclination and gate distances (gate distance and horizontal gate distance) are shown in the table.

Table 7 reveals that terrain inclination in the skier's direction and terrain inclination in the course direction were steepest for GS, followed by SG and DH. Terrain inclination normal to skier direction, terrain inclination normal to course direction, angle between skier direction and gradient and angle between course direction and gradient were larger for DH than GS and SG, while they were equal for GS and SG and distributions were different for all parameters and disciplines except the angle between course direction and the gradient for GS and SG.

Terrain inclination in skier direction was significantly smaller than terrain inclination in course direction and terrain inclination normal to skier direction was significantly smaller than terrain inclination normal to course direction in all disciplines. The angle between skier direction and gradient was significantly smaller than the angle between course direction and gradient for GS only. The histograms of these parameters are illustrated in Figure 20. All distributions were significantly different between skier and course direction.

The median of terrain inclination change along P_S per meter skiing and relative to time were not different from zero. For the terrain inclination change along P_S per meter skiing it was found that GS was significantly overrepresented compared to SG for values larger than 1.3°/m and values smaller than -1.2°/m, while GS and DH and SG and DH were not significantly different in their distribution of data in those ranges. For the terrain inclination change along P_S per second skiing it was found that DH was significantly overrepresented compared to SG and GS for values larger than 19°/s and values smaller than -21°/s, while the distributions for GS and SG and were not significantly different from each other.

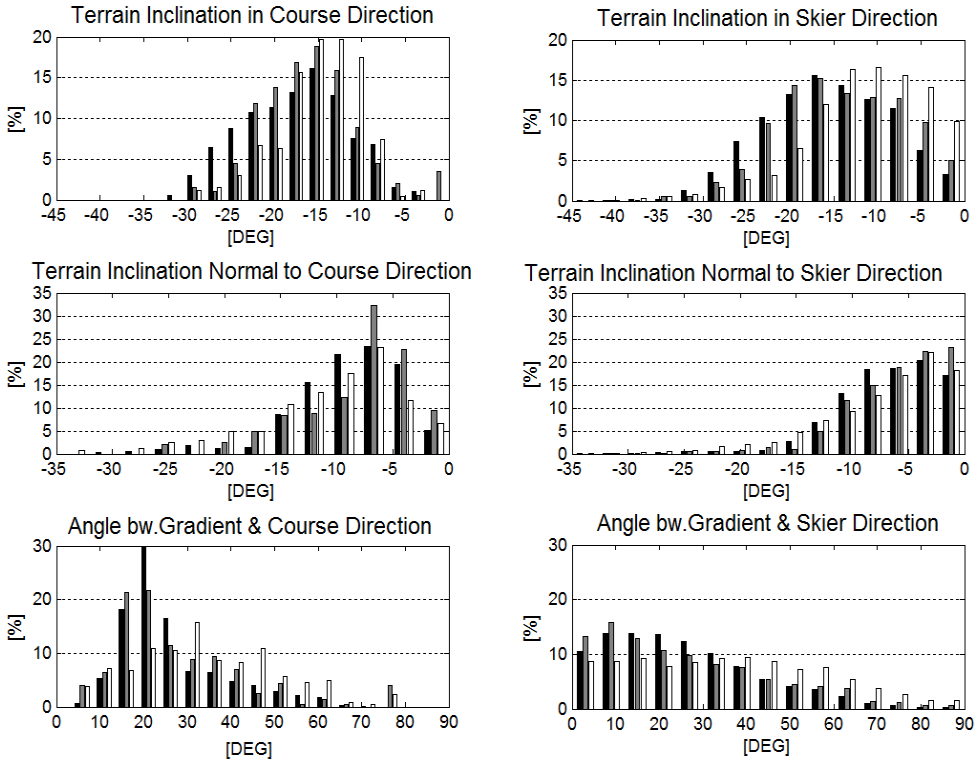

Figure 20. Terrain inclination features relative to course setting are presented in the left column. Terrain inclination features relative to the projection of the skier trajectory on the DTM are in the right column. The distributions for GS are shown in black, for SG in gray and for DH in white.

3.2.1.2 Discussion

This study showed that: 1) the differences between course setting characteristics were significant between disciplines; 2) the horizontal gate distance included more variability than gate distance and vertical gate distance for all disciplines, 3) the horizontal gate distance tended to increase with increasing terrain inclination in GS; 4) there was a weak tendency that gate distance decreased slightly with increasing terrain inclination in GS and SG; 5) gates were set close to terrain transitions (convex and concave) in GS and SG and for concave terrain transitions in DH; 6) the median terrain inclination was steeper in GS and SG than DH; 7) in DH skiers skied traverse to the gradient direction and faced extreme terrain inclination changes per time skied to slightly larger extent than in the other disciplines.

The FIS regulations (16. 7. 2013) define a range of direction changes, respective to the number of gates. The number of direction changes is dependent on the altitude drop from start to finish and has to be in the range of 11-15% of the vertical drop in meters in GS. Applying the FIS regulation and the median vertical drop per race found in this study, the range of direction changes for a typical GS race is 41 to 61 direction changes. The number of direction changes usually set is about in the middle of the range (51) determined by the FIS regulations for an average race. The given range is quite large and following the rules with respect to the number of direction changes is usually not a challenge for course setters. However, it might make sense to keep the range large, since course length and vertical drop vary between race locations and the rules have to cover all cases. Very steep and short races might challenge the lower limit. Flat and long courses might be in the upper range of allowed number of direction changes. Once it is established whether course setting can help prevent injuries, it might be useful to investigate if more specific regulations which take into account the steepness of the slope could contribute to make courses safer.

For male SG the regulations define the minimum number of gates and respective changes of direction at 7% of the vertical drop in meters. A minimum of 35 gates must be set as long as the vertical drop of the course is larger than 450m. The distance between the turning poles of two successive gates must be at least 25 m in normal situations. Using the data from this study, the numbers of direction changes are set close to the minimum given by the regulations.

The coefficients of variation (CV) in gate distance and vertical gate distance were found to be small compared to the CV for the horizontal gate distance in all disciplines. Hence variability in course setting geometry was regulated mainly by the horizontal gate distance, while gate distance and vertical gate distance were fairly constant. An explanation for the constant gate distances might be that course setters control the gate distance with distance measurement devices probably to ensure that the gate distance regulation is followed and courses are set rhythmically. This study also showed a tendency for horizontal gate distance to increase with increasing terrain inclination in GS. In GS and SG, there was a weak tendency toward shorter gate distance when terrain inclination increased. These measures were probably taken to force the skier to turn more often and to a larger extent in steep sections in order to control speed when the component of gravity accelerating the skier was large due to the steep terrain. Controlling speed might be an important issue, since high speed is recognized as an important injury risk factor (Spörri et al., 2012; Florenes et al., 2009) and increased horizontal gate distance has been suggested as a measure to control speed (Spörri et al., 2012b) in GS. However, external force has also been

suggested to be an injury risk factor (Spörri et al., 2012b; Spörri et al., 2012) and force was found to vary with course setting (Spörri et al., 2012b; Reid, 2010). Hence it might be worthwhile to investigate the effect of increased horizontal gate distance and/or shorter gate distances on skier speed and forces in different types of terrain.

It was found that gates were usually set close to terrain transitions in all disciplines. The reason for setting gates close to convex terrain transitions might be to ensure gates are fully visible. Avoiding gates which are hidden behind convex terrain transitions might help in avoiding accidents (Bere et al., 2013). In GS, gates were usually set 1 to 2m behind the terrain transition apex, so that the gate was still visible to the athlete but could provide guidance about where the course was leading after the terrain transition. Other safety and competition considerations might also play a role. Turning in terrain transitions might increase the demands on skier technique (balance, timing) and strength compared to uniform terrain. Hence, it would be worthwhile to investigate the effect of course setting at terrain transitions with respect to performance and safety aspects.

The study showed that more than 85% of the time, terrain inclination change per meter of distance skied was less than 1° for all disciplines and hence alpine skiing courses are held on mostly uniform terrain regardless of the discipline. GS included to larger extent of extreme terrain inclination change per meter than GS and SG. In DH, rapid terrain inclination changes per unit time occured to larger extent than in GS and SG. This might be due to the higher speed in DH (paper V and VI). Whether the abrupt terrain inclination changes (per unit time) in DH can be associated with the increased injury risk in DH (Florenes et al., 2009) might be worth investigating.

Significant differences between disciplines were found in the extent to which terrain was tilted, not only in the lateral direction to the course direction but also in the direction the skier was skiing. It is probable that tilted terrain sets higher demands for balance, but it is unknown whether the increased amount of tilted terrain in speed disciplines can be associated with increased injury risk in the speed disciplines (Florenes et al., 2009).

3.2.1.3 Methodological considerations

To investigate the relationship between course setting and terrain inclination, gate distance and horizontal gate distance were used, since gate distance is the distance which is directly and indirectly regulated via the number of direction changes per metre of altitude drop from start to

finish by FIS regulations, and measured by distance measurement devices by practitioners when setting courses. Gate distance and horizontal gate distance are not linearly independent, but they were chosen for the analysis since they make sense in practice and since there is an association between gate distance and vertical gate distance (Spearman's Rho was found to be 0.94 for GS, 0.91 for SG and 0.96 for DH).

3.2.2 Characterisation of skier mechanics in World Cup alpine skiing

3.2.2.1 Results

3.2.2.1.1 Point mass kinematics

The distributions within and between disciplines for speed and turn radius are shown in Table 8 and Figure 21. DH had the largest mean turn radius, while GS had the smallest mean turn radius. Straight skiing (turn radius of >125m) occurred for approximately 45% of the time in DH, 20% of the time in SG and 7% of the time in GS. Kinetic energy for GS, SG and DH are shown in Table 8.

*Table 8. Mean and SD values of the absolute values for all disciplines and the relative values for GS and SG compared to DH for speed, kinetic energy and turn radius. * The value of DH is equal to 100%.*

	Mean ± SD in absolute values			**% of DH ***	
	GS	**SG**	**DH**	**GS**	**SG**
Speed [m/s]	17.7±2.3	23.8±2.7	25.6±4.3	69	93
E_{KIN} [BW·m]	15.5±4.0	27.9±6.1	32.7±10.7	47	85
Turn Radius < 150m [m]	40.6±31.6	66.8±38.8	90.3±43.5	45	74

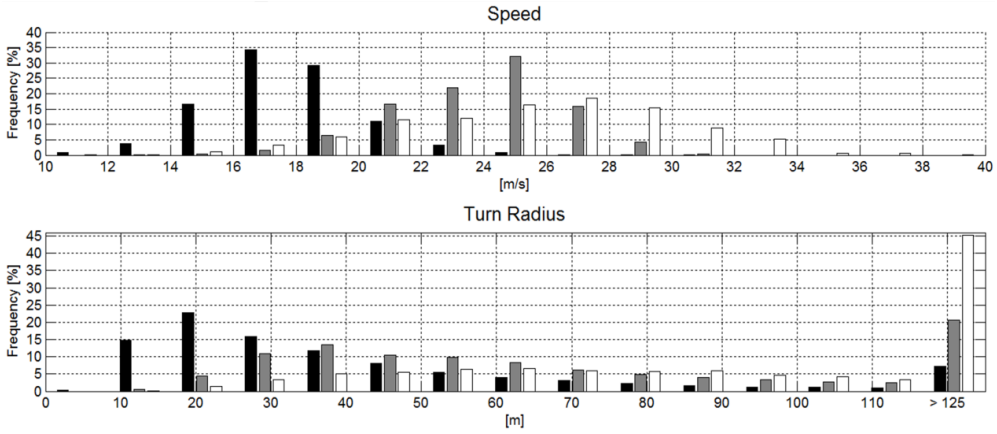

Figure 21. Histograms for speed and turn radius. GS is shown in black, SG in gray and DH in white.

3.2.2.1.2 External forces

For the forces median, IQR and the percentage values for GS and SG in relation to DH are given in Table 9. The medians were significantly different ($\alpha = 0.01$) between disciplines for all parameters except for $\boldsymbol{F_{GRF\ Vert}}$ between GS and DH and for $E_{DISS\ (FGRF\ Friction)}$ between GS and SG. The $\boldsymbol{F_{RES}}$ median was 46% larger for GS and 42% larger for SG compared to DH. GS and SG had also a larger IQR than DH. The histogram in Figure 22 illustrates that $\boldsymbol{F_{RES}}$ was larger than 1.5BW for less than 10% of the run time in DH, while for GS and SG the $\boldsymbol{F_{RES}}$ was larger than 1.5BW for approximately 30% and 25% of the time respectively. The median $\boldsymbol{F_D}$ was largest for DH, followed by SG and GS, and was approximately twice as large for DH compared to GS. IQR was largest for DH, followed by SG and GS. In DH, $\boldsymbol{F_D}$ was larger than 0.2 BW for approximately 25% of the time, while this magnitude occurred for less than 2% of the time in GS. The median $\boldsymbol{F_{GRF}}$ was 22% larger for GS and 15% larger for SG compared to DH. The IQRs were largest for GS, followed by SG and DH. In GS skiers skied for more than 40% of the time with $\boldsymbol{F_{GRF}}$ larger than 1.5 BW, while in DH a value above 1.5BW was achieved less than 20% of the time. The differences between the median of $\boldsymbol{F_{GRF\ Vert}}$ between GS and DH were the only differences between disciplines, and were not significant. Despite the similarities in the medians, the IQR was substantially larger for GS and SG compared to DH. DH was under-represented in both the low and high force ranges. $\boldsymbol{F_{GRF\ Friction}}$ median was doubled for GS compared to DH and 52% larger for SG compared to DH. The IQR was largest for GS, followed by SG and DH.

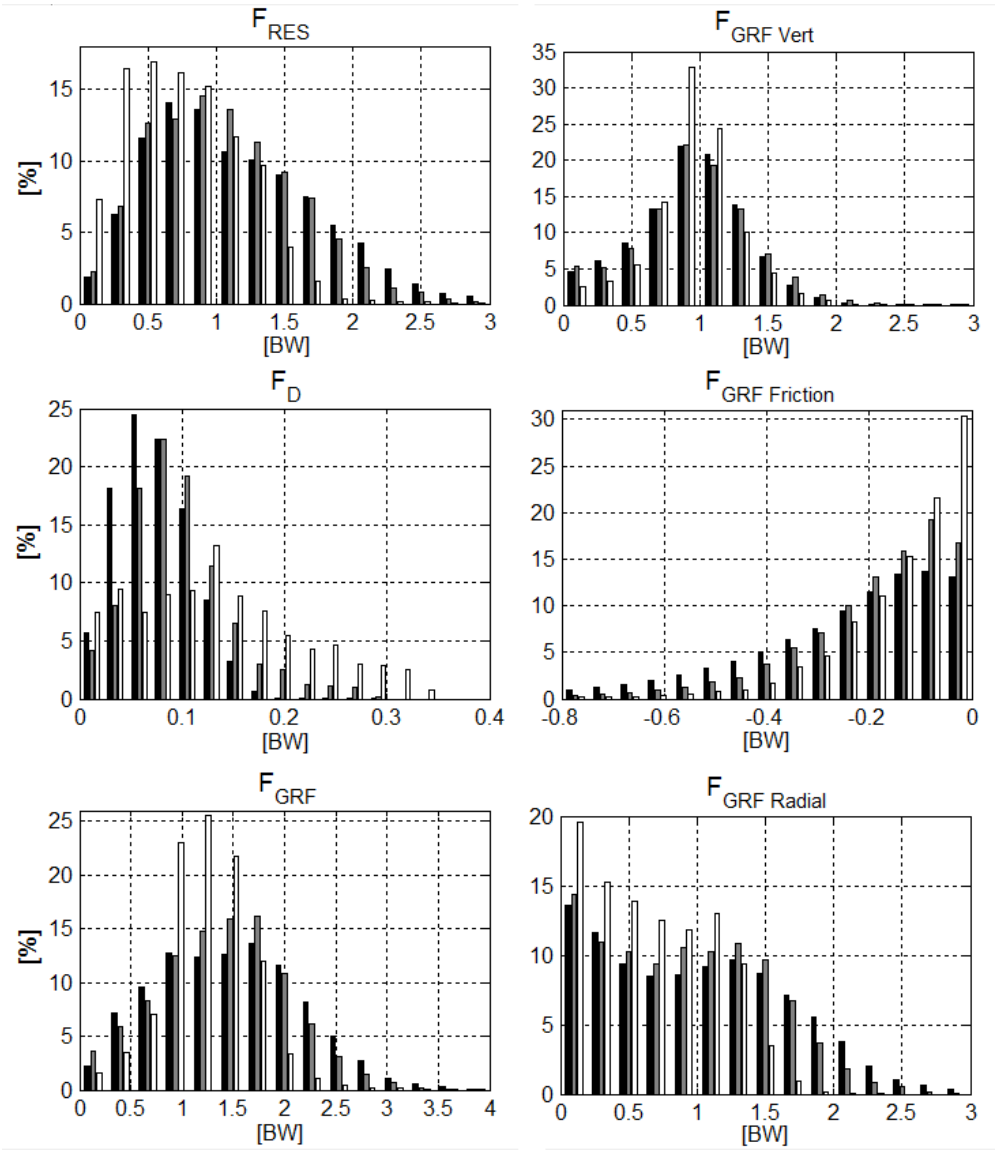

*Figure 22. Histograms of the force distributions within and between disciplines for resultant force, air drag force, ground reaction force (**F_{GRF}**), and the vertical, friction and radial components of the ground reaction force. GS is plotted in black, SG in gray and DH in white.*

The median of the $F_{GRF\ Radial}$ component was 54% larger for GS compared to DH and 45% larger for SG compared to DH. Also the IQR increased from DH to SG and GS. In GS skiers skied with $F_{GRF\ Radial}$ larger than 1.5 BW for approximately 20% of their time, while in DH skiers spent less than 3% of their time in this force range. Also all distributions were significantly different from each other.

*Table 9. Median and interquartile range (IQR) of the absolute values for all disciplines and the relative values for GS and SG compared to DH. * The value of DH is equal to 100%.*

	Absolute values Median ± IQR			**% of DH ***	
	GS	**SG**	**DH**	**GS**	**SG**
F_{RES} [BW]	1.04±0.88	1.01±0.77	0.71±0.63	146	142
F_D [BW]	0.07±0.05	0.09±0.06	0.13±0.12	57	71
F_{GRF} [BW]	1.46±1.04	1.42±0.86	1.21±0.53	122	115
$F_{GRF\ Vert}$ [BW]	0.96±0.50	0.97±0.51	0.96±0.32	101	101
$F_{GRF\ Friction}$ [BW]	-0.20±0.27	-0.15±0.19	-0.10±0.15	202	152
$F_{GRF\ Radial}$ [BW]	0.96±1.11	0.90±0.97	0.62±0.77	154	145

3.2.2.1.3 External forces and ski – snow friction coefficient in relation to turn radius

Figure 24 illustrates F_{GRF}, $F_{GRF\ Vert}$, $F_{GRF\ Friction}$, $F_{GRF\ Radial}$ and F_D in relation to turn radius for GS, SG and DH. For all disciplines F_{GRF}, $F_{GRF\ Vert}$, $F_{GRF\ Friction}$, and $F_{GRF\ Radial}$ decreased with increasing turn radius, while F_D and speed increased. For a given turn radius above 50m F_{GRF}, $F_{GRF\ Vert}$, $F_{GRF\ Friction}$, and $F_{GRF\ Radial}$ were largest for DH followed by SG and GS. For a given turn radius smaller than 50m, the magnitude of $F_{GRF\ Friction}$ was largest for SG. A qualitative inspection of the speed graph revealed that speed decreased substantially for turn radii lower than 20m in GS, 40m in SG and 50m in DH. The c_f is illustrated in Figure 23. For turn radii larger than 45m c_f was smallest for DH, followed by SG and GS. For turn radii smaller than 45m c_f was smallest for SG but still largest for GS, with large variations for GS.

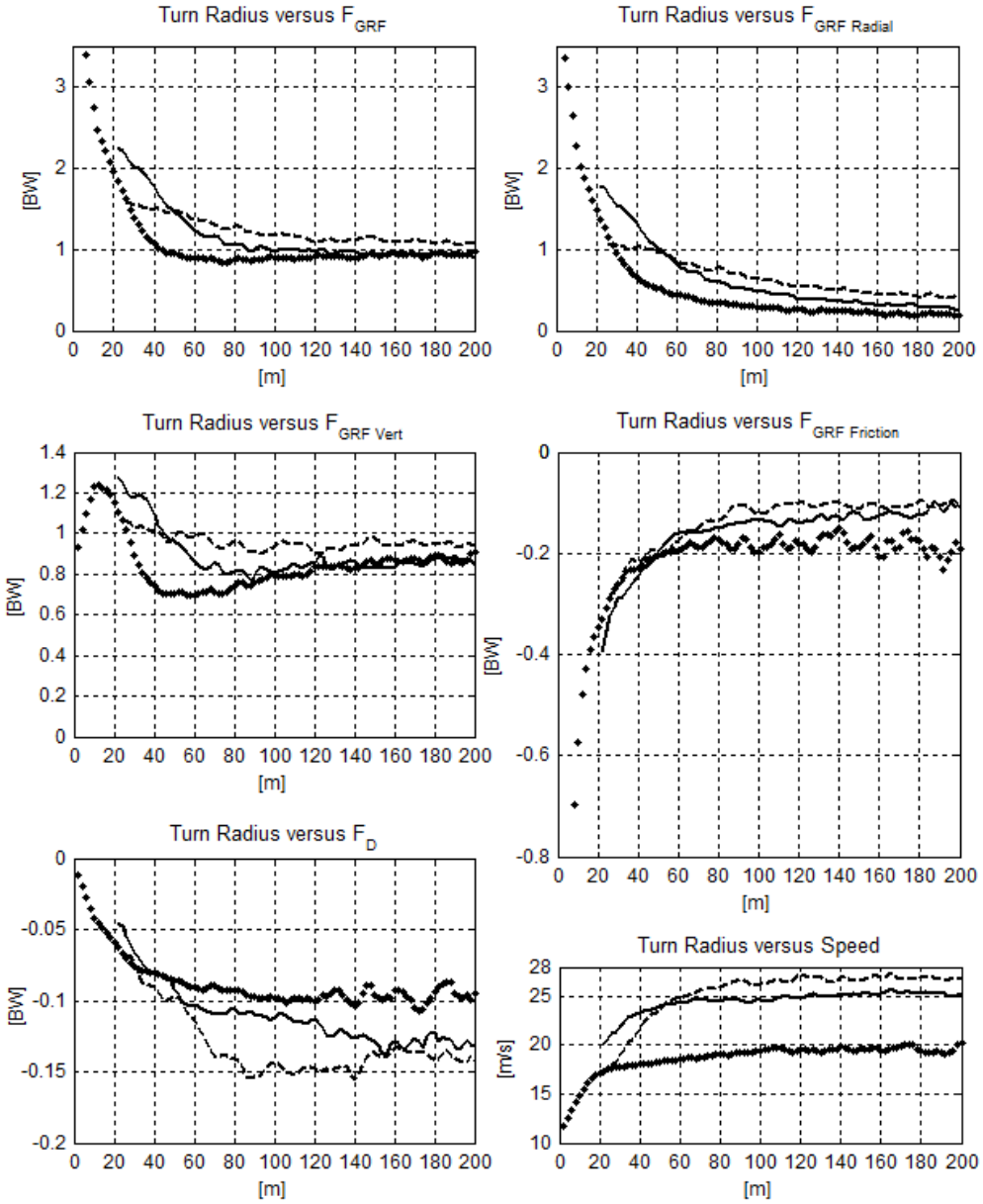

Figure 23. Illustration of the external forces and the components of the ground reaction force as a function of the turn radius for GS (dotted line), SG (solid line) and DH (dashed line). In the force graphs, the force is shown on the vertical axis and turn radius on the horizontal axis. In the speed graph, speed is shown on the vertical axis and turn radius on the horizontal axis.

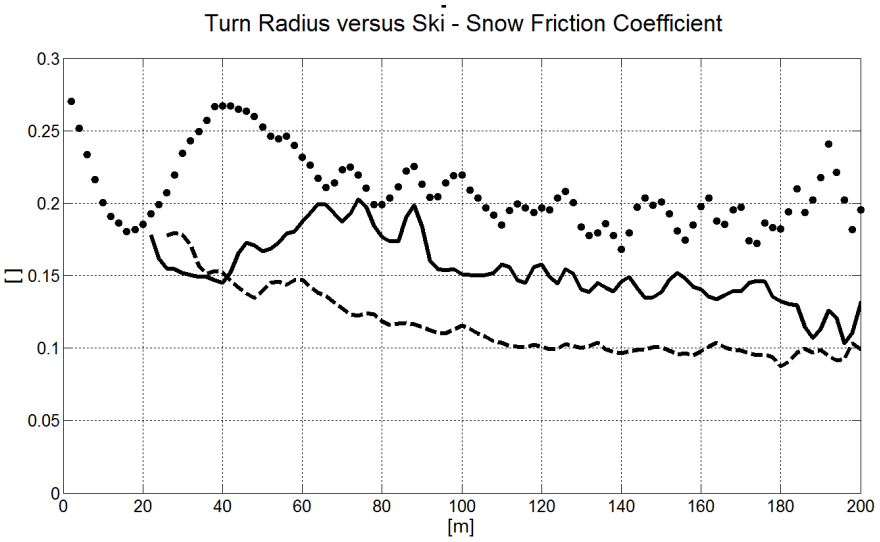

Figure 24. Illustration of the ski–snow friction coefficient as a function of the turn radius for GS (dotted line), SG (solid line) and DH (dashed line). The ski – snow friction coefficient is shown on the vertical axis and turn radius on the horizontal axis.

3.2.2.1.4 Energy dissipation

The contributions of the dissipative forces air drag and ski–snow friction to energy dissipation (E_{DISS}) are illustrated in Figure 25. There was no significant difference in the median and the distribution between GS and SG for $E_{DISS\ (FGRF\ Friction)}$. All other discipline medians were significantly different for both energy dissipation types. The median $E_{DISS\ (FGRF\ Friction)}$ was 41% (GS) and 42% (SG) larger than for DH. The median of $E_{DISS\ (FD)}$ was found to be 41% (GS) and 71% (SG) of the median for DH. DH had also the largest IQR. The median relative contribution of energy dissipation due to air drag and due to ski–snow friction was found to be 23% ($E_{DISS\ (FD)}$) and 77% ($E_{DISS\ (FGRF\ Friction)}$) for GS, 35% ($E_{DISS\ (FD)}$) and 65% ($E_{DISS\ (FGRF\ Friction)}$) for SG and 51% ($E_{DISS\ (FD)}$) and 49% ($E_{DISS\ (FGRF\ Friction)}$) in DH. In Figure 26 the percentage contribution of $E_{DISS\ (FD)}$ to total energy dissipation for the disciplines GS, SG and DH is illustrated. The horizontal axis shows the contribution of $E_{DISS\ (FD)}$ as a percentage of total energy dissipation, while the vertical axis shows how often the contribution patterns were present in time (frequency). The percentage contribution of $E_{DISS\ (FGRF\ Friction)}$ to total energy dissipation is complementary to the percentage contribution of $E_{DISS\ (FD)}$ to total E_{DISS}, since $\boldsymbol{F_{GRF\ Friction}}$ and $\boldsymbol{F_D}$ are the only sources for E_{DISS}. For more than 80% of the time $E_{DISS\ (FGRF\ Friction)}$ had a larger contribution to total E_{DISS} than $E_{DISS\ (FD)}$ in GS, while in DH the contribution of $E_{DISS\ (FGRF\ Friction)}$ was larger than the contribution of $E_{DISS\ (FD)}$ to total E_{DISS} for less than 40% of the run time.

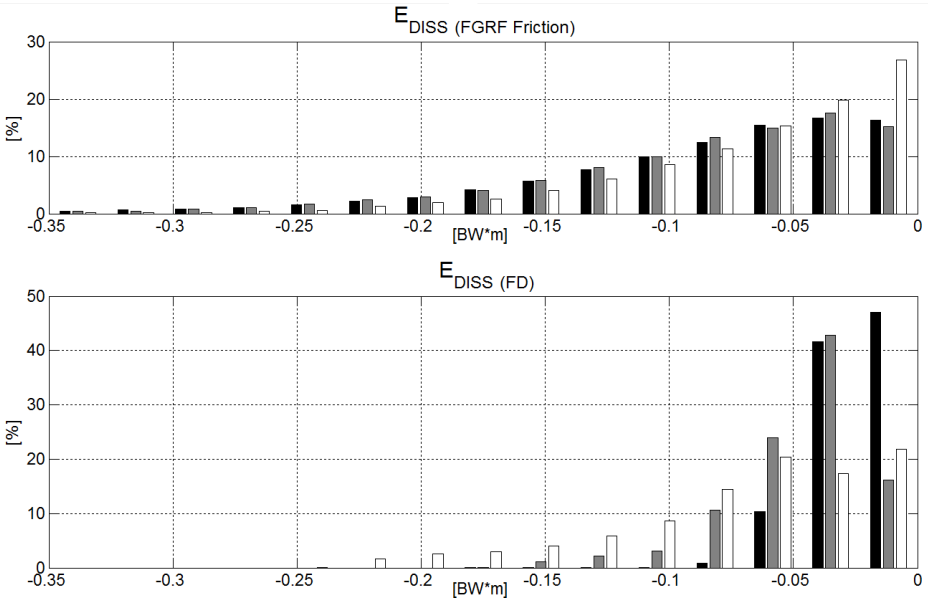

Figure 25. Histograms illustrating the distributions within and between the disciplines for energy dissipation due to air drag and due to ski–snow friction force. GS is plotted in black, SG in gray and DH in white.

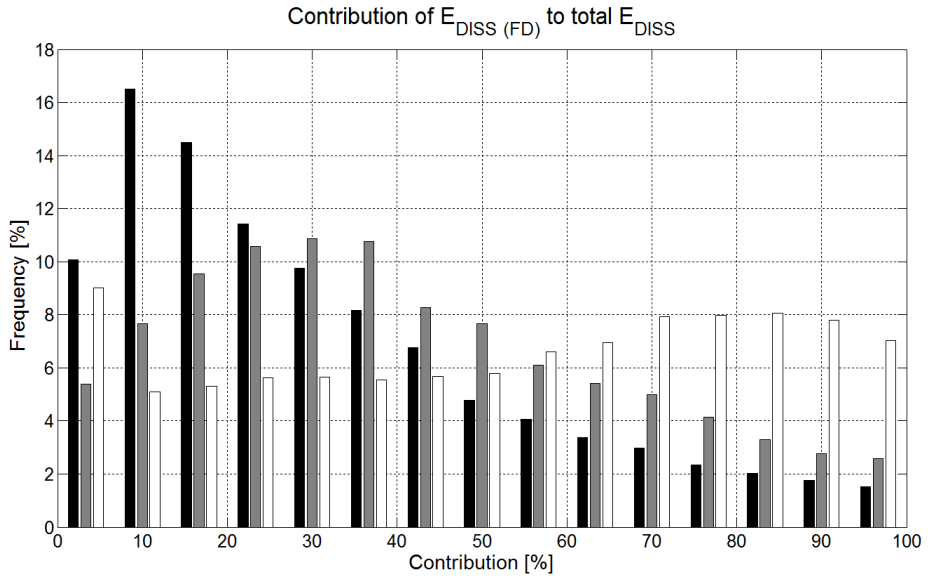

Figure 26. Histogram illustrating the percentage contribution of air drag to total energy dissipation for the disciplines GS, SG and DH. GS is plotted in black, SG in gray and DH in white. The horizontal axis shows the contribution of energy dissipation due to air drag as a percentage of total energy dissipation, while the vertical axis shows how often these contributions were present (frequency).

3.2.2.2 Discussion

The median $\boldsymbol{F_{RES}}$ decreased from GS to SG and DH and seems to reflect these differences in skiers' trajectory alterations between disciplines. Direction alteration of skier trajectory is generated by $\boldsymbol{F_{GRF}}$. Thus the fact that the median $\boldsymbol{F_{GRF}}$ was largest in GS, followed by SG and DH might mainly be a consequence of the amount of turning. This relationship seems to be supported by the fact that GS and SG, which consist of substantially more turning than DH, showed similar $\boldsymbol{F_{GRF}}$ distributions while the distribution was different for DH. The relationship between turn radius and median $\boldsymbol{F_{GRF}}$ seems to correspond with the literature: a current study found an even larger mean $\boldsymbol{F_{GRF}}$ for slalom (1.56 BW and 1.67 BW) than we found in GS (Reid, 2010), where turn radii were smaller than in GS. The combination of speed and turn radius lead to the largest $\boldsymbol{F_{GRF\ Radial}}$ in GS, followed by SG and DH. The only value for median $\boldsymbol{F_{GRF\ Radial}}$ in the literature was found to be larger (1.14 BW) than what we found in GS. The data in that study, however, were obtained from a single subject study in one turn and on steep terrain (27.5°) (Spörri et al., 2012b), while our data were obtained from all kinds of turns and terrains, with a median terrain inclination of 20.1°. Hence it might be interesting to investigate if turning in steep terrain requires a larger $\boldsymbol{F_{GRF\ Radial}}$ than in moderately steep or flat terrain. This might be of interest, since Spörri et al. (2012b) indicated that radial forces might be associated with injury risk.

Variability in the $\boldsymbol{F_{GRF\ Vert}}$ was larger in GS and SG than DH. Since the variability in the $\boldsymbol{F_{GRF\ Vert}}$ is a result of vertical movements, resulting in weighting–unweighting of the skis (Reid, 2010), it can be concluded that skiers use vertical movements to enhance turning more extensively in GS and SG than in DH. A recent study in slalom showed that the median $\boldsymbol{F_{GRF\ Vert}}$ increased with decreasing gate distance while variability decreased with decreasing gate distance (Reid, 2010). This finding might indicate that the increasing trend to deploy vertical movements in turning from DH to SG and GS is not extended to slalom. One reason for that might be shorter gate distances and time between gates which limit the execution of vertical movement in turning. In the speed disciplines, where air drag contributes to a larger extent to energy dissipation, skiers might omit vertical movements in turning as body extensions increase the frontal area exposed to wind and hence increase air drag.

$\boldsymbol{F_{GRF\ Friction}}$ is determined by $\boldsymbol{F_{GRF}}$, skiing technique, equipment and snow conditions (Lind & Sanders, 2004) and was found to be largest (median) in GS, followed by SG and DH. The difference in $\boldsymbol{F_{GRF}}$ between GS and DH was 22%, while the difference for $\boldsymbol{F_{GRF\ Friction}}$ was 102%.

Hence, 80% of the difference between GS and DH in median $\boldsymbol{F_{GRF\ Friction}}$ can be attributed to technique, equipment and snow conditions. The difference in $\boldsymbol{F_{GRF}}$ between SG and DH was 15%, while the difference for $\boldsymbol{F_{GRF\ Friction}}$ was 52%. Hence, 37% of the difference between SG and DH in median $\boldsymbol{F_{GRF\ Friction}}$ can be attributed to technique, equipment and snow conditions. The finding that 80% of the difference between GS and DH and 37% of the difference between SG and DH can be attributed to aspects other than $\boldsymbol{F_{GRF}}$ seems to make sense, since the increased amount of turning in GS and SG compared to DH requires more guiding of the skis and is therefore likely to cause more skidding and carving instead of straight gliding.

$\boldsymbol{F_D}$ was significantly larger for DH compared to GS and SG. This difference might mainly be a consequence of the increased speed in DH, since body position might be more optimal with respect to $\boldsymbol{F_D}$ for long periods of time due to the straight skiing sections which occur more frequently in DH than in the other disciplines (Paper VI). The analysis of the E_{DISS} contribution (Figures 25 and 26) confirmed the finding that E_{DISS} in GS is mainly determined by $\boldsymbol{F_{GRF\ Friction}}$ (Supej et al., 2012). In SG, $\boldsymbol{F_{GRF\ Friction}}$ was still clearly the major contributor to E_{DISS}, while the contribution was approximately balanced in DH. Hence, for the disciplines GS and SG, a certain percentage reduction of $\boldsymbol{F_{GRF\ Friction}}$ would have a larger effect on performance than a corresponding reduction of $\boldsymbol{F_D}$, while in DH the effect on performance would be about equal. This finding might have implications for the prioritization of investments in technique and equipment enhancement.

The investigation of how $\boldsymbol{F_{GRF}}$, $\boldsymbol{F_{GRF\ Vert}}$, $\boldsymbol{F_{GRF\ Friction}}$, $\boldsymbol{F_{GRF\ Radial}}$ and $\boldsymbol{F_D}$ relate to turn radius, revealed clear differences between the three disciplines. For a given turn radius larger than 60m, $\boldsymbol{F_{GRF}}$ was largest for DH, followed by SG and GS. The reason for that might be speed, which was highest in DH, followed by SG and GS, and thus caused the respective differences in $\boldsymbol{F_{GRF\ Radial}}$. Despite the fact that $\boldsymbol{F_{GRF}}$ was larger in the speed discipline than GS, GS had the largest $\boldsymbol{F_{GRF\ Friction}}$. The reason for the increased $\boldsymbol{F_{GRF\ Friction}}$ in GS compared to SG and DH is a larger c_f. The ski–snow friction coefficient was largest for GS followed by SG and DH as shown in Figure 24. The differences in c_f might be found in the equipment, skier technique, snow conditions and terrain. Shorter skis with more side-cut in GS might cause increased friction compared to the speed disciplines where longer skis with less side-cut are used. The large variations in c_f in GS for small turn radii might indicate differences between skiing techniques used in different phases of turns and radii as found in other studies (Reid, 2010; Supej & Holmberg, 2010; Spörri et al., 2012b).

For turn radii smaller than 50m, speed was lower in DH than SG and therefore, $\boldsymbol{F}_{GRF\ Radial}$ and $\boldsymbol{F}_{GRF}$ were lower in DH than SG for turn radii smaller than 50m. $\boldsymbol{F}_{GRF\ Radial}$ increased rapidly and to a larger extent than the other components with decreasing turn radius. Hence, the rapid increase in $\boldsymbol{F}_{GRF}$ with decreasing radius was mainly an effect of the increase in $\boldsymbol{F}_{GRF\ Radial}$. For small turn radii, $\boldsymbol{F}_{GRF\ Friction}$ followed a comparable increase in magnitude for decreasing turn radius for all disciplines. Consequently, turning sharply seemed to be costly in the form of increased ski–snow friction regardless of discipline. The relationships between turn radius, force and speed might be useful as input parameters to static or quasi-static simulations of equipment or ski–snow interaction (Madura, Lufkin, & Brown, 2010; Heinrich, Mossner, Kaps et al., 2010; Mossner, Heinrich, Schindelwig et al., 2005; Heinrich, Mossner, Kaps et al., 2005; Federolf, Roos, Lüthi et al., 2010; Federolf et al., 2004; Lüthi, Federolf, Fauve et al., 2006; Lüthi et al., 2004) and for simulations of trajectography in alpine ski racing (Madura et al., 2010; Schiestl et al., 2006; Kaps, Nachbauer, & Mossner, 1996).

3.2.2.3 Methodological considerations

Air drag computation might be enhanced if full-body kinematic information was applied instead of body extension. The role of lift due to $\boldsymbol{F}_{D}$ was not investigated in this study and its effect on $\boldsymbol{F}_{GRF\ Vert}$ and c_f is therefore unknown. For certain simulation studies it would be more appropriate if the relationship between turn radius and forces was expressed as a function of turn cycle, specifying the loading and unloading of skis in the different turn phases. However, such analysis was beyond the scope of this study and should therefore be conducted separately. The applied method is unable to determine the ground reaction force for single legs. Only the sum of the ground reaction force of both legs can be determined. The representations of the relationships between turn radius and forces lack a time dimension and, therefore, do not represent turn cycle courses. They represent the typical force (and speed) response for a given turn radius in a typical but virtual condition (terrain, snow condition, course setting) for each discipline.

3.2.3 Differences in injury rate and skiers' mechanics between the disciplines giant slalom, super-G and downhill

3.2.3.1 Results

The number of injuries per hour (exposure-time normalized injury rate) was highest for GS, followed by SG, DH and SL. While the differences between DH, SG and GS were less than 2%, SL had an 18% lower injury rate than DH.

The mean, SD and % of DH values for E_{KIN}, I_{GRF+D}, run time and jump characteristics for the entire runs are given in Table 10. All mean values were largest for DH, followed by SG and GS for all parameters. SG consisted of about half the number of jumps compared to DH, while GS had none. The jumps were about 20% shorter in SG compared to DH, but airtime was reduced by only 6%. The medians were significantly different ($\alpha = 0.01$) between disciplines for all parameters except the jump parameters.

Table 10. Mean and SD values for disciplines GS, SG and DH and as % of DH for GS and SG.

	Mean ± SD in absolute values			**% of DH ***	
	GS	**SG**	**DH**	**GS**	**SG**
I_{GRF+D} [kBW·s]	124.3±12.5	153.0±13.3	173.4±25.3	71	88
Run time [s]	77.4±5.2	92.9±9.7	121.4±17.7	64	76
# jumps / race	-	2.3±0.8	4.2±1.5	-	55
Jump length [m]	-	23.8±9.9	30.2±10.4	-	79
Jump airtime [s]	-	0.98±0.44	1.04±0.44	-	94

** DH is 100% for the respective measures.*

Associating skiers' mechanical characteristics with injury rates, Figure 27 shows the mean and extreme values of turn speed, turn radius and turn F_{GRF} compared to the injury rates. Injuries per hour were similar between disciplines, while injuries per 1000 runs and mean and extreme values increased from GS to SG and DH for turn speed, turn radius and for kinetic energy of the entire run. The difference in turn radius mean and minimum was substantial between GS and the speed disciplines. F_{GRF} in turns increased from DH to SG and GS.

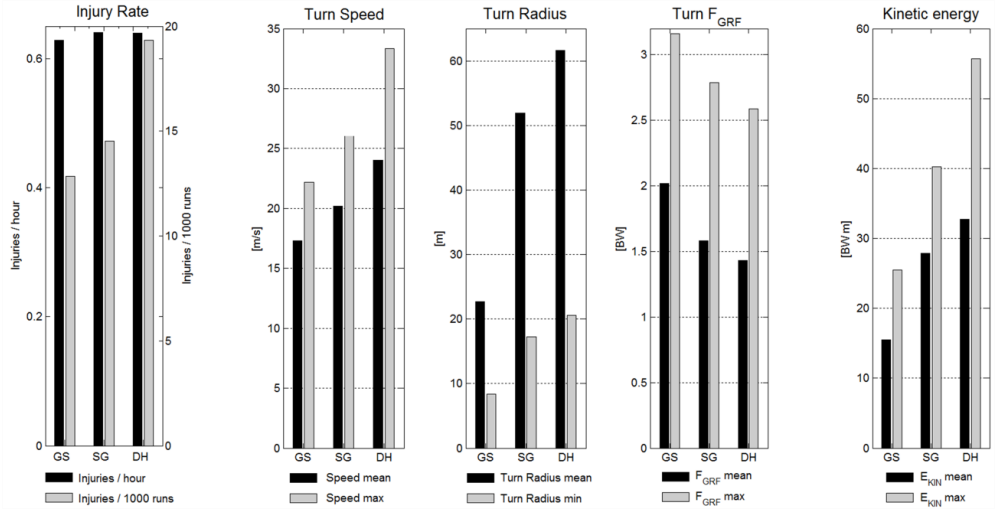

Figure 27. Comparison of injury rates (left graph), skiers' characteristics in turns (turn speed, turn radius and turn F_{GRF}, in middle) and skiers' kinetic energy for entire runs. For injury rates, injuries per hour are shown in black and injuries per 1000 runs in gray. For skiers' mechanical characteristics, mean values are shown in black and extreme values in gray.

Skier mechanical characteristics specific for turning are presented in Table 11. For the turns, limited by maximal turn radii of 30m (GS), 75m (SG) and 125m (DH), the mean and extreme values of turn speed, turn radius and turn $\boldsymbol{F_{GRF}}$ are presented. While turn speed and turn radius mean and extreme values increased from GS to SG and DH, they decreased for turn $\boldsymbol{F_{GRF}}$. The medians were significantly different ($\alpha = 0.01$) between disciplines for all parameters.

Table 11. Turn characteristics: mean values, extreme values and % of DH for the disciplines GS, SG and DH.

		Mean and extreme values for turns			**% of DH ***	
		GS	**SG**	**DH**	**GS**	**SG**
Turn Speed [m/s]	Mean	17.32	22.7	24	72	95
	Max	22.2	28.3	32.3	69	88
Turn Radius [m]	Mean	22.7	52	61.6	37	84
	Min	8.4	17.2	20.6	41	84
Turn F_{GRF} [BW]	Mean	2.02	1.58	1.43	141	110
	Max	3.16	2.79	2.59	122	108

** DH is 100% for the respective measures.*

3.2.3.2 Discussion

It has recently been found that many injuries occur while turning, without falling or being the result of a crash (Bere et al., 2013). Figure 21 shows that skiers are turning for approximately 55% of the time in DH, 80% in SG and 93% in GS. Moreover, it was shown that small turn radii might be related to an increased injury risk in GS since they provoke the skiers to use their full backward and inward leaning capacities and thus skiers have less buffer if an additional factor causes an out-of-balance situation (Spörri et al., 2012b). Out-of-balance situations themselves are known to be a critical part of typical injury mechanisms, such as the "slip-catch" and "dynamic snowplow" (Bere et al., 2013; Bere et al., 2011a). Comparing the mean and minimal turn radii between disciplines from Figure 27 and Table 11, it is evident that GS has substantially smaller turn radii than SG and DH. Additional analysis of the data showed that the radial component is the main contributor to the increased F_{GRF} in GS. Thus the combination of small turn radii and speed leads to larger mean and maximum F_{GRF} in GS compared to SG and DH. Furthermore, in GS, skiers' balance might be challenged simultaneously by small turn radii and high forces. Measures to prevent injuries in GS should therefore focus on both speed and turn radius. Suitable tools might be course setting and equipment. Furthermore, GS includes a larger number of turns (52.0 ± 3.5) compared to SG (40.0 ± 3.5) and DH. Hence skiers have to find balance in turning more frequently in a run and thus might be more often susceptible to balance-related mistakes in turn initiations.

Speed in general is considered a major injury risk factor in competitive alpine skiing (Spörri et al., 2012; Florenes et al., 2009). It has been hypothesized that the differences in speed might be the reason for the higher numbers of injuries per 1000 runs in the speed disciplines (Florenes et al., 2009). Comparing the number of injuries per hour and kinetic energy in Figure 27, no direct relationship is apparent, since speed increased from GS to SG and DH while the exposure-time normalized injury rates were almost constant across the disciplines. This finding indicates that speed might not be the sole factor explaining the differences in injury rates between disciplines. Nevertheless, speed might have several major impacts on injury risk, especially in DH and SG. In technically demanding sections (e.g. jumps, rough terrain and turns), anticipation and adaptation time decrease with speed and mistakes might be more likely to occur. Furthermore, for a given jump, jump distance and air time increase with speed and a mistake at take-off might have more severe consequences. In crash situations speed has a significant impact, since the energy which is dissipated in an impact increases with speed by the power of 2 (E_{KIN} = mass·speed^2/2) and E_{KIN} is almost doubled from GS to DH. The forces occurring in a crash impact are dependent on both

the impact energy and the timespan of the energy dissipation process. Safety barriers are therefore built so that they can give way to a certain extent in order to increase the time of the impact process and thus decrease the impact forces. Hence, the functionality (Petrone, Ceolin, & Morandin, 2010; Petrone, Pollazzon, & Morandin, 2008) and positioning of protective barriers is highly important in speed disciplines. Measures to prevent injuries in SG and DH should aim at reducing speed at spots where skiers are likely to crash. Since turn forces are generally lower compared to GS and SG it might be reasonable to use course setting to radically slow down skiers at locations where crashes are likely to occur.

Fatigue is a known injury risk factor (Spörri et al., 2012). A recent study showed that most injuries occur during the last fourth of a race (Bere et al., 2013). It is further known that fatigue has a negative effect on balance (Qu & Nussbaum, 2009; Simoneau, Begin, & Teasdale, 2006) and thus fatigued athletes might be more susceptible to out-of-balance situations and injuries (Spörri et al., 2012b). Since fatigue cannot be measured directly, in the current study race time and impulse were calculated as approximations of the work load over the entire run. I_{GRF+D} per run showed an increase from GS to SG and DH along with an increase in the number of injuries per 1000 runs. Analyses of the causes for the differences in impulse between disciplines revealed that run time contributed to a larger extent to the impulse than the forces. Consequently the fatigue related parameter impulse is strongly linked with exposure time. Exposure time (and fatigue) seems to explain the increased injury rate per 1000 runs for the speed disciplines to a large extent. Two seasons of epidemiologic data is a relatively small amount for the computation of injury rates, but the trend between run time and injury incidences per 1000 runs is apparent. If epidemiologic studies could pinpoint when accidents occur in a race for the respective disciplines, the role of fatigue could probably be better clarified.

Jumps are considered to contribute to the high injury rates (Spörri et al., 2012). The number of jumps in DH is nearly double that in SG. However, no epidemiologic study has ever pinpointed the number of injuries occurring at jumps in the respective disciplines. Hence, it has not been possible as yet to relate jump characteristics to injury risk.

An imbalance at the jump take-off can lead to an angular momentum during the time the skier is airborne. Since the angular momentum is only influenced by air drag as long as the skier is airborne, the time until landing is critical. A longer airtime leads to a larger rotation angle and a more critical body position at landing. In the current study it was found that flight distance was 21% shorter in SG compared to DH, while air time was only 6% shorter in SG compared to DH.

This finding leads to the conclusion that an angular momentum during airtime can also lead to large rotation angles in SG. Since many severe injuries (Bere et al., 2013) seem to occur at jumps, the mechanics of jumping and its relation to injury risk should be investigated in more detail.

3.2.3.3 Methodological considerations

The approach of measuring for the first time under competition conditions in WC alpine skiing adds valuable new perspectives to the investigation of injury risk factors. However, there are some limitations related to the methods used in the current study. First, the model for the computation of the F_{GRF} does not capture the high frequency force components and, therefore, might underestimate the work load (impulse), in particular for GS. Second, for the computation of impulse, the method used does not account for body position. Consequently, the work load during straight gliding sections in DH, where skiers are in a deep tuck position, might be underestimated compared to GS, where skiers are in more extended body positions. Third, the forerunners who captured the data for this study skied slightly slower than the WC skiers. The time difference between our forerunners and the median of all skiers who completed the run was 2.4±2.1% for GS, 1.3±2.3% for SG and 5.29±1.2% for DH. Hence the data in this study slightly underestimate the mechanical characteristics of a typical WC skier.

4 Conclusions

4.1 GNSS method development and validation

A GNSS-based method was proposed for the simultaneous determination of all external forces, CoM position, velocity and acceleration in competitive alpine skiing. The method was found to be technically valid for comparing turn mean values and allowed instantaneous relative comparisons between skiers with respect to certain precision boundaries. Due to its technical validity, its small equipment size/weight and geodetic GNSS measurement robustness, the system was found suitable to simultaneously determine position, velocity, acceleration and forces under WC racing conditions across large capture volumes. The method's advantage with respect to injury prevention might be that skier loading (ground reaction force) can be determined at the same time as other injury risk factors such as speed are captured, using a single device.

The only GNSS method that consistently yielded sub-decimeter position accuracy in typical alpine skiing conditions was a differential method using GPS and GLONASS satellite systems, applying the satellite signal frequencies L1 and L2.

Under conditions of minimal satellite signal obstruction, valid results were achieved when either the satellite system GLONASS or the frequency L2 was dropped from the best configuration. All other methods failed to fulfill the accuracy requirements needed to detect relevant differences in the kinematics of alpine skiers, even in conditions favorable for GNSS measurements.

Methods with good positioning accuracy had also the shortest times to compute differential solutions.

4.2 Application of GNSS methods in World Cup giant slalom, super-G and downhill

Variability in course setting was introduced by the horizontal gate distance. The horizontal gate distance tended to decrease with decreasing terrain inclination in GS and SG. Terrain was, on average, steeper in GS than SG and DH. Gates were in general set close to terrain transitions but 1 to 2m after the terrain transition apex in GS. Extreme terrain inclination changes along the skiers' trajectory per unit time skiing were overrepresented in DH, while extreme changes per unit distance were overrepresented in GS.

Mean speed was found to be 17.7 m/s in GS, 23.8 m/s in SG and 25.6 m/s in DH. Skiers skied stright (turn radis > 125m) for approximately 45% (DH), 20% (SG) and 7% (GS) of the time. The median ground reaction force was found to be 1.46 BW in GS, 1.42 BW in SG and 1.21 BW in DH. The median air drag force was 0.07 BW in GS, 0.09 BW in SG and 0.13 BW in DH.

For a given CoM turn radius between 60m and 400m ground reaction force and ski – snow friction force were largest for GS, followed by SG and DH.

Ski–snow friction was the main contributor to energy dissipation in GS and SG, while in DH the contribution of air drag and ski–snow friction was approximately equal.

The WC alpine skiing disciplines were found to be approximately equally dangerous per unit of time.

The skiers' mechanical characteristics were significantly different. Therefore, it is likely that the causes and mechanisms of injury are different for the specific disciplines. In SG and DH, injuries might be mainly related to higher speed and jumps, while injuries in the technical disciplines might be related to a combination of turn speed and turn radius resulting in high loads.

The recently reported higher number of injuries per 1000 runs in DH might not only be explained by speed, but also by a bias of total exposure time and thus potentially by fatigue.

5 Future research

5.1 GNSS based data collection method

The GNSS-based method should be improved further. Data from inertial navigation systems (INS) rigidly attached to the GNSS antenna could be used to improve the method's robustness in situations when GNSS signal reception is limited. By adding INS, skiers', segment kinematics could be captured and injury risk factors related to segment movements could be assessed. The estimate of the frontal area for the computation of the air drag force could also be improved by additional knowledge about segment movements obtained from INS or other measurement systems. In addition, high frequency ground reaction force components could be assessed using data from INS attached to the lower extremities or equipment.

5.2 The effect of course setting and terrain geomorophology on skier injury risk factors

The mechanical data from the WC monitoring project need to be deviced to investigate how course setting and terrain geomorphology influence skier parameters, such as speed, force and fatigue, which are recognised as injury risk factors (Spörri et al., 2012b; Spörri et al., 2012; Bere et al., 2013; Florenes et al., 2009). Preliminary analyses conducted for GS are presented in the following section.

5.2.1 Methods

An n-way ANOVA was conducted to investigate the effect of gate distance, horizontal gate distance and vertical gate distance on: resultant force ($\boldsymbol{F_{RES}}$); the difference in speed (Δs) between turn transition at the beginning of the turn and turn transition at the end of the turn; and the minimal turn radius. The effect size was also calculated using Cohen's d. The 572 turns were first assigned to one of three categories - flat, moderate and steep terrain. The terrain inclination categories were defined by division of the terrain inclination range across all turns into three equal parts, using the mean terrain inclination per turn. Each terrain inclination category was further divided into two turn entrance speed categories (fast and slow). The speed categories were defined by division of the speed range within the terrain inclination category into two parts.

Turn entrance speed was represented by the speed at the skier's trajectory deflection point between two turns. Spearman correlation coefficients were calculated for the relationships between horizontal gate distance and minimal turn radius, $\boldsymbol{F_{RES}}$, and Δs, for all turns in each terrain inclination category, and for all turns in each sub-category defined by terrain inclination and turn entrance speed. A principal component analysis was conducted to assess the relationship between terrain inclination, horizontal gate distance and mean speed per turn.

To investigate the effect of horizontal gate distance on the $\boldsymbol{F_{RES}}$ time series, the time series of $\boldsymbol{F_{RES}}$ of all 572 turns were time-centered at gate passage. The $\boldsymbol{F_{RES}}$ turn time series were assigned to categories of horizontal gate distance ranges and three terrain inclination categories. The mean values of the $\boldsymbol{F_{RES}}$ time series values within the respective horizontal gate distance and terrain inclination categories were calculated at 0.02s intervals from 0.4s before to 0.3s after gate passage, within the horizontal gate distance and terrain inclination categories. $\boldsymbol{F_{RES}}$ time series expressed in function of horizontal gate distance categories were also expressed for the entire turn cycle as percentage of turn cycle.

5.2.2 Results

Figure 28 illustrates the first principal component describing the relationship between terrain inclination, horizontal gate distance and turn mean speed for all 572 turns. The vector of the first principal component is shown in Figure 28. The endpoints of the vector are for endpoint A: -34.9° (terrain inclination), 10.07m (horizontal gate distance), 15.24m/s (speed); and for endpoint B -2.4° (terrain inclination), 3.66m (horizontal gate distance), 21.42m/s (speed). The vector direction was 0.96° (terrain inclination), -0.19m (horizontal gate distance), 0.18m/s (speed). The variance explained by the first component was 84.5%.

Using an n-way ANOVA and Cohens' d, large effect size was found for horizontal gate distance. Therefore, the correlation and significances between horizontal gate distance and $\boldsymbol{F_{RES}}$, Δs, and minimal turn radius were assessed using the Spearman correlation coefficients. The results are shown in Table 12.

The Spearman correlation coefficients for the relationships between horizontal gate distance and minimal turn radius, $\boldsymbol{F_{RES}}$, and Δs were weak or moderate for all terrain inclination and speed categories. The relationships were stronger if speed was high. If speed was not considered, the correlations were strongest in flat terrain. Figures 29–31 illustrate the relationships between the horizontal gate distance and minimal turn radius, Δs and $\boldsymbol{F_{RES,}}$ for all 572 turns. Figure 32 shows

the resultant force time series expressed as a percentage of the turn cycle and grouped in categories of horizontal gate offset ranges. Figure 33 illustrates the resultant force time series from 0.4s before to 0.3s after gate passage in categories of horizontal gate offset ranges.

*Table 12. Spearman correlation coefficients and significance level for the relationships between horizontal gate distance and minimal turn radius, resultant force (F_{RES}) and delta speed (Δs). * p < 0.05, ** p < 0.01, *** p < 0.001.*

Horizontal gate distance - Minimal turn radius				
All turns	**Terrain inclination**		**Speed**	
-0.56***	Flat	-0.51***	Low	-0.27
			High	-0.57***
	Moderate	-0.49***	Low	-0.30**
			High	-0.51***
	Steep	-0.39***	Low	-0.26**
			High	-0.53**
Horizontal gate distance - Resultant force (F_{RES})				
All turns	**Terrain inclination**		**Speed**	
0.51***	Flat	0.54***	Low	0.49**
			High	0.59***
	Moderate	0.37***	Low	0.19
			High	0.48***
	Steep	0.38***	Low	0.38***
			High	0.47***
Horizontal gate distance - Delta speed (Δs)				
All turns	**Terrain inclination**		**Speed**	
-0.56***	Flat	-0.31***	Low	-0.27
			High	-0.57***
	Moderate	-0.30***	Low	-0.30**
			High	-0.51***
	Steep	-0.22***	Low	-0.26**
			High	-0.53**

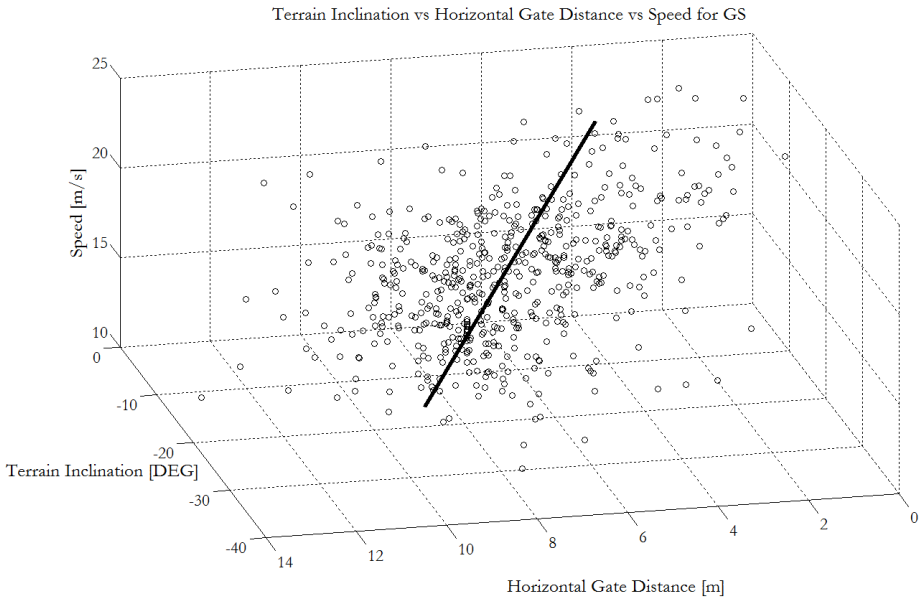

Figure 28. Illustration of the first principal component describing the relationship between terrain inclination, horizontal gate distance and turn mean speed for all 572 turns.

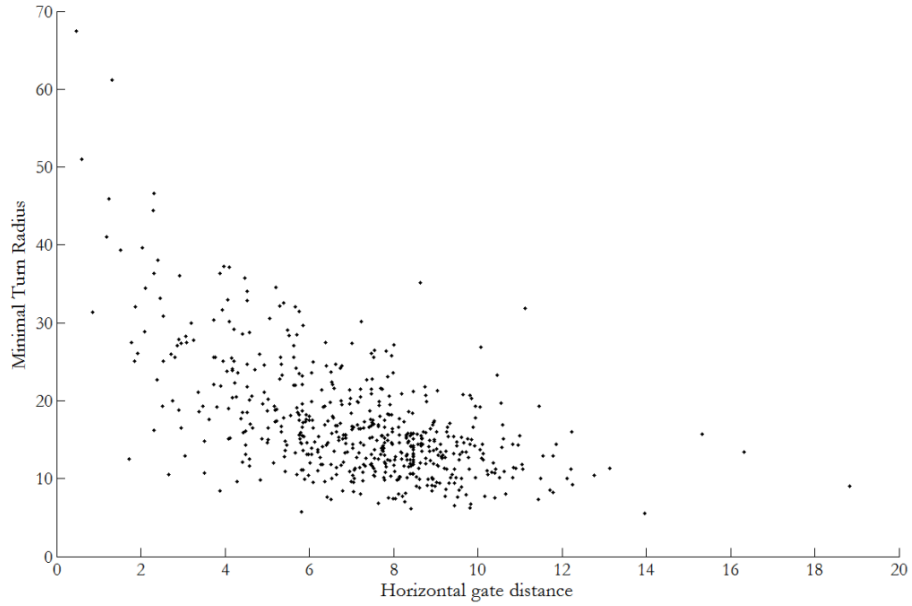

Figure 29. Illustration of the relationship between horizontal gate distance and minimal turn radius (Min Turn Radius) for all 572 turns, with the linear regression line.

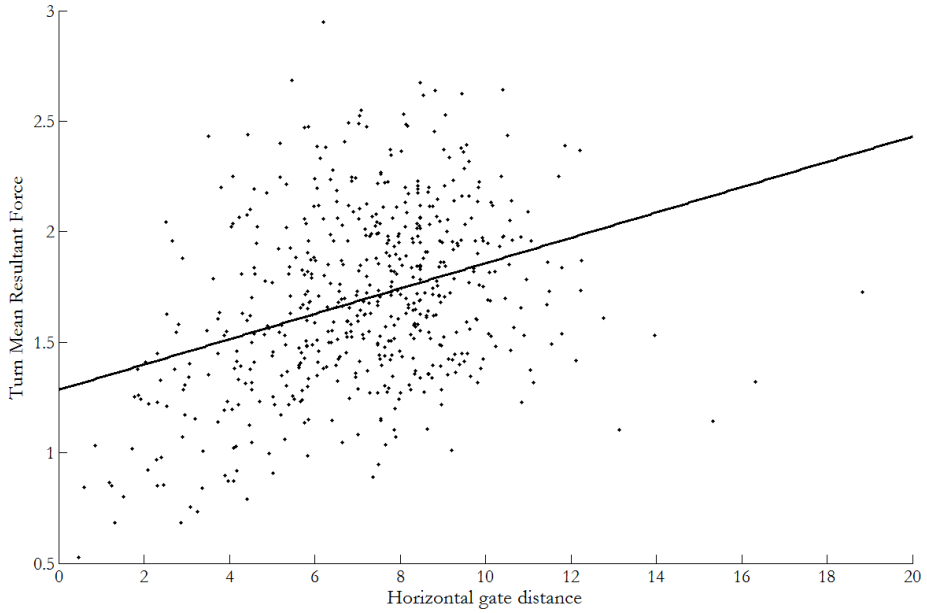

*Figure 30. Illustration of the relationship between horizontal gate distance and turn mean resultant force (Mean **Fres**) for all 572 turns, with the linear regression line.*

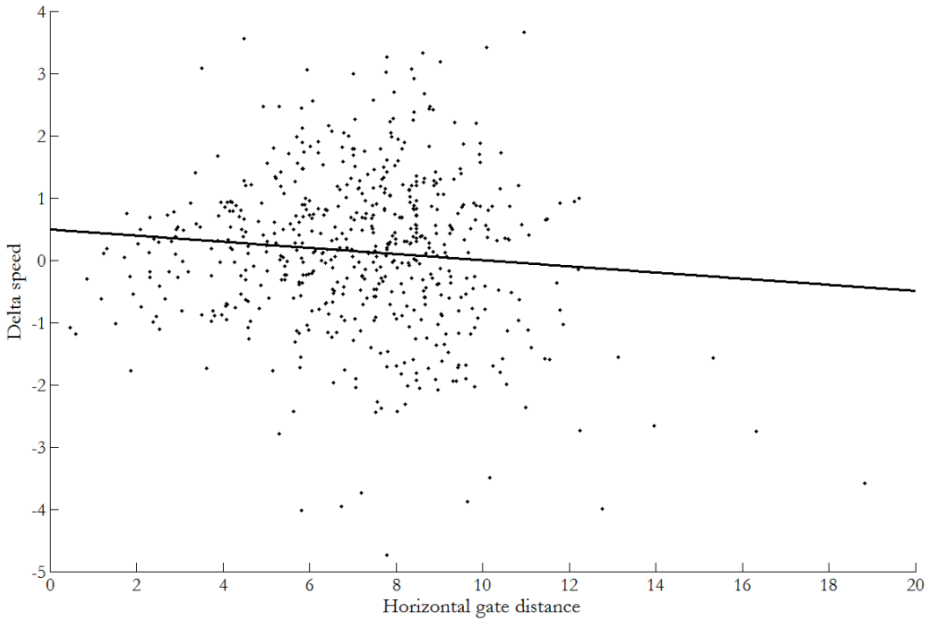

Figure 31. Illustration of the relationship between horizontal gate distance and the difference in speed from turn end to turn start (Δs) for all 572 turns, with the linear regression line.

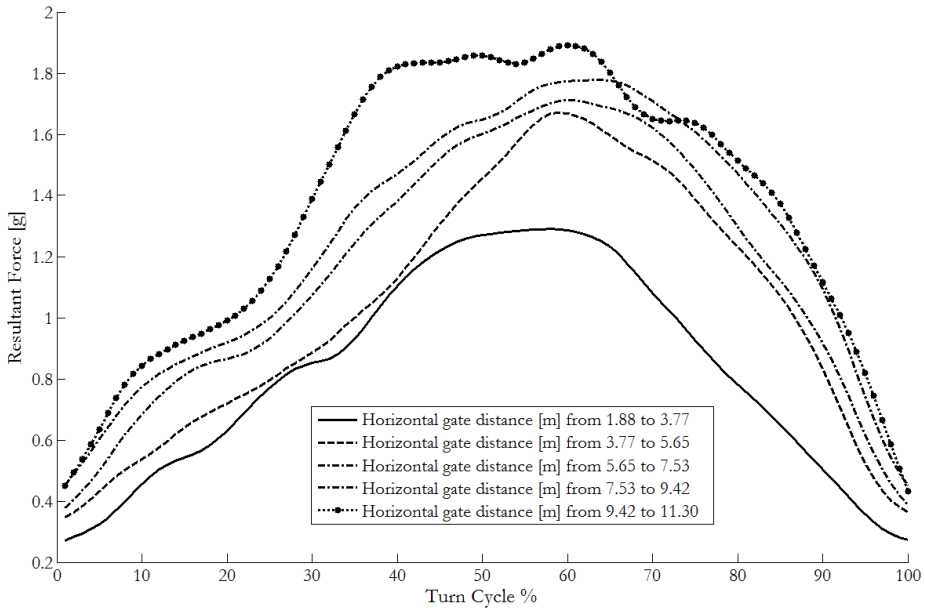

Figure 32. Illustration of the resultant force time series expressed as % of turn cycle, grouped in categories of horizontal gate offset ranges.

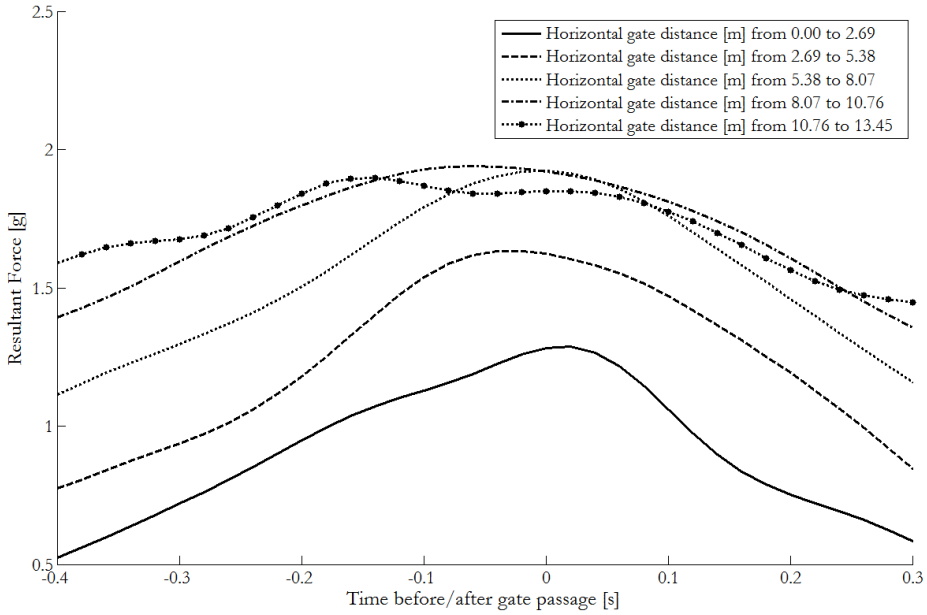

Figure 33. Illustration of the resultant force time series from 0.4s before to 0.3s after gate passage, grouped in categories of horizontal gate offset ranges.

5.2.3 Discussion

The preliminary analysis was conducted to get a first impression of the relationship between terrain geomorphology, course setting and skiers' mechanical parameters in GS. As an examples the relation between one course setting characterisitc and three potential injury risk factors were assessed. Figure 28 shows that horizontal gate distance increased and speed decreased with increasing terrain inclination. Table 12 and Figures 29–31 show only weak and moderate relationships between horizontal gate distance and minimal turn radius, turn mean $\boldsymbol{F_{RES}}$ and Δs. One reason for these results might be that the data were collected from different subjects (one per race) and in different races with different snow conditions. Such differences might cause offsets between the data from different races and the data should therefore be analysed using a statistical method which takes into account these offsets. Further a multivariate model might be suitable to capture the effects of multiple inputs. For example the extent of speed reduction or ground reaction forces might not only depend on horizontal gate distance but also turn entrance speed, dterrain inclination in course and normal to course direction, and course setting conditions ahead of the examined gate. Whether minimal turn radius is an injury risk factor remains to be investigated. However, small minimal turn radii at increased forces may challenge skiers' balance capacity.

Figures 32 and 33 show qualitatively that increased horizontal gate distances lead to longer periods of increased radial forces as it was hypothesised (Spörri et al., 2012b). The increased impulse (Force · time) might lead to increased fatigue and therefore increase injury risk.

5.3 Linking quantitative data to injury risk data

Further insight into how terrain geomorphology and course setting influence skier mechanical injury risk factors could be gained, if the quantitative data generated in this project is linked to real injury data. Devicing data from TV footage of World Cup races at locations where data was collected in this project might allow to link terrain, course setting and skier mechanical characteristics to actual accidents. Such approaches might improve insight in where and why injuries occur in World Cup alpine skiing.

6 Reference List

Atha, J. (1984). Current techniques for measuring motion. *Applied Ergonomics, 15,* 245-257.

Aughey, R. J. (2011). Applications of GPS Technologies to Field Sports. *International Journal of Sports Physiology and Performance, 6,* 295-310.

Babiel, S., Hartmann, S., Spitzenpfeil, P., & Mester, J. (1997). Groundreaction forces in alpine skiing, cross-country skiing and ski jumping. In E.Müller, D. Bacharach, R. Klika, H. Schwameder, & S. Lindinger (Eds.), *Science and Skiing III* (pp. 200-207). Spon (UK): E&FN.

Barelle, C., Ruby, A., & Tavernier, M. (2004). Experimental model of the aerodynamic drag coefficient in alpine skiing. *Journal of Applied Biomechanics, 20,* 167-176.

Bere, T., Florenes, T. W., Krosshaug, T., Haugen, P., Svandal, I., Nordsletten, L., & Bahr, R. (2013). A systematic video analysis of 69 injury cases in World Cup alpine skiing. *Scandinavian Journal of Medicine & Science in Sports*.

Bere, T., Florenes, T. W., Krosshaug, T., Koga, H., Nordsletten, L., Irving, C., Müller, E., Reid, R. C., Senner, V., & Bahr, R. (2011a). Mechanisms of anterior cruciate ligament injury in World Cup alpine skiing: a systematic video analysis of 20 cases. *American Journal of Sports Medicine, 39,* 1421-1429.

Bere, T., Florenes, T. W., Krosshaug, T., Nordsletten, L., & Bahr, R. (2011b). Events leading to anterior cruciate ligament injury in World Cup Alpine Skiing: a systematic video analysis of 20 cases. *British Journal of Sports Medicine, 45,* 1294-1302.

Bere, T., Florenes, T. W., Nordsletten, L., & Bahr, R. (2013). Sex differences in the risk of injury in World Cup alpine skiers: a 6-year cohort study. *British Journal of Sports Medicine*.

Bere, T., Mok, K. M., Koga, H., Krosshaug, T., Nordsletten, L., & Bahr, R. (2013). Kinematics of Anterior Cruciate Ligament Ruptures in World Cup Alpine Skiing: 2 Case Reports of the Slip-Catch Mechanism. *The American Journal of Sports Medicine, 41,* 1067-1073.

Brewin, M. A. & Kerwin, D. G. (2005). Accuracy of scaling and DLT reconstruction techniques for planar motion analyses. *Journal of Applied Biomechanics, 19,* 79-88.

Brodie, M., Walmsley, A., & Page, W. (2008). Fusion Motion Capture: A Prototype System Using IMUs and GPS for the Biomechanical Analysis of Alpine Ski Racing. *Journal of Sports Technology, 1,* 17-28.

Chardonnens, J., Favre, J., Gremion, G., & Aminian, K. (2012). Knee joint kinematics measurement in alpine skiing based on inertial sensors. In E. Müller, S. Lindinger, & T. Stoggl (Eds.), *5th International Congress on Science and Skiing 2010* Salzburg, Austria: Meyer & Meyer Sport.

de Berg, M., Otfried, C., van Kreveld, M., & Overmars, M. (2008). *Computational Geometry: Algorithms and Applications*. (vols. 3) Berlin: Springer Verlag.

de Leva, P. (1996). Adjustments to zatsiorsky-seluyanov's segment inertia parameters. *Journal of Biomechanics, 29,* 1223-1230.

Ducret, S., Ribot, P., Vargiolu, R., Lawrence, J., & Midol, A. (2004a). Analysis of Downhill Ski Performance Using GPS and Ground Force Recording. In D. Bacharach & J. Seifert (Eds.), *3rd International Congress on Skiing and Science* St. Cloud State University.

Ducret, S., Ribot, P., Vargiolu, R., Midol, A., & Mathia, T. (2004b). The new technology for ski performance analysis. In D. Bacharach & J. Seifert (Eds.), *3rd International Congress on Skiing and Science* (pp. 65-66). St. Cloud State University.

Federolf, P., Fauve, M., Luthi, A., Rhyner, H., Ammann, W., & Dual, J. (2004). Finite element simulation of a carving alpine ski. In D. Bacharach & J. Seifert (Eds.), *3rd International Congress on Skiing and Science* (pp. 11-12). Snowmass at Aspen (USA): St. Cloud State University.

Federolf, P., Roos, M., Lüthi, A., & Dual, J. (2010). Finite element simulation of the ski snow interaction of an alpine ski in a carved turn. *Sports Engineering, 12,* 123-133.

Federolf, P., Scheiber, P., Rauscher, E., Schwameder, H., Luthi, A., Rhyner, H. U., & Müller, E. (2008). Impact of skier actions on the gliding times in alpine skiing. *Scandinavian Journal of Medicine & Science in Sports, 18,* 790-797.

Florenes, T. W., Bere, T., Nordsletten, L., Heir, S., & Bahr, R. (2009). Injuries among male and female World Cup alpine skiers. *British Journal of Sports Medicine, 43,* 973-978.

Gilgien, M. (2008). *External forces acting in direction of travel and their relation to energy dissipation in slalom.* Master Norwegian School of Sport Sciences.

Gilgien, M., Reid, R., Haugen, P., Kipp, R., & Smith, G. (2009). External forces acting in direction of travel and their relation to energy dissipation in slalom. In *14th Annual Congress of the European College of Sport Science.*

Gilgien, M., Reid, R., Haugen, P., & Smith, G. (2008). A Method to Capture and Model the Geomorphology of Snow Surfaces for use in Biomechanical Investigations in Snow Sports. In J. Cabri (Ed.), *13th Annual Congress of the European College of Sport Science* (pp. 569). Lisboa, (Portugal): European College of Sport Sciences.

Gilgien, M., Singer, J., & Rhyner, H. (2010). Comparison of two methods to assess the choice of skier trajectories through banked turns in ski cross. In *5th International Congress on Science and Skiing 2010* Salzburg, Austria: Meyer & Meyer Sport.

Gurney, J. K., Kersting, U., & Rosenbaum, D. (2008). Between-day reliability of repeated plantar pressure distribution measurements in a normal population. *Gait & posture, 27,* 706-709.

Heinrich, D., Mossner, M., Kaps, P., & Nachbauer, W. (2010). Calculation of the contact pressure between ski and snow during a carved turn in Alpine skiing. *Scandinavian Journal of Medicine & Science in Sports, 20,* 485-492.

Heinrich, D., Mossner, M., Kaps, P., Schretter, H., & Nachbauer, W. (2005). Influence of ski bending stiffness on the turning radius of alpine skis at different edging angles and velocities - a computer simulation. In *Mountain & sport: Updating study and research from laboratory to field* (pp. 44).

Holden, M., Parker, R., & Walsh, A. (2004). Dynamic force measurement technique to evaluate skier performance. In D. Bacharach & J. Seifert (Eds.), *3rd International Congress on Skiing and Science* (pp. 13-14). St. Cloud State University.

Huber, A., Spitzenpfeil, P., Waibel, K., Debus, D., & Fozzy M.E. (2012). CRIPS - Crash recognition and injury prevention in alpine ski racing. In E. Müller, S. Lindinger, & T.

Stoggl (Eds.), *5th International Congress on Science and Skiing 2010* Salzburg, Austria: Meyer & Meyer Sport.

Hugentobler, M. (2004). *Terrain Modelling with Triangle Based Free-Form Surfaces.* dissertation Universität Zurich, Switzerland, Zürich.

Hurkmans, H. L. P., Bussmann, J. B. J., Selles, R. D., Horemans, H. L. D., Benda, E., Stam, H. J. et al. (2004). Validity of the pedar mobile system of vertical force measurement during a long-term period. In *EMED Scientific Community Proceedings 2004* (pp. 60).

Jackson, K. M. (1979). Fitting of Mathematical Functions to Biomechanical Data. *Biomedical Engineering, IEEE Transactions on, BME-26,* 122-124.

Kaps, P., Nachbauer, W., & Mossner, M. (1996). Determination of kinetic friction and drag area in alpine skiing. In C.D.Mote, R. J. Johnson, W. Hauser, & P. S. Schaff (Eds.), *Ski Trauma and Skiing Safety* (pp. 165-177). Philadelphia: American Society for Testing and Materials.

Kiefmann, A., Krinninger, M., Lindemann, U., Senner, V., & Spitzenpfeil, P. (2006). A new six component dynamometer for measuring ground reaction forces in alpine skiing. In E.F.Moritz & S. Haake (Eds.), *The engineering of sport 6* (pp. 87-92). New York: Springer.

Klous, M., Müller, E., & Schwameder, H. (2008). Knee joint loading an alpine skiing: A comparison between carved and skikked turns. In *12th Annual Congress of the European College of Sport Science.*

Klous, M., Müller, E., & Schwameder, H. (2010). Collecting kinematic data on a ski/snowboard track with panning, tilting, and zooming cameras: Is there sufficient accuracy for a biomechanical analysis? *Journal of Sports Sciences, 28,* 1345-1353.

Krüger, A. & Edelmann-Nusser, J. (2009). Biomechanical analysis in freestyle snowboarding: application of a full-body inertial measurement system and a bilateral insole measurement system. *Sports Technology, 2,* 17-23.

Krüger, A. & Edelmann-Nusser, J. (2010). Application of a full body inertial measurement system in alpine skiing: a comparison with an optical video based system. *Journal of Applied Biomechanics, 26,* 516-521.

Kumar, S. & Moore, K. (2002). The Evolution of Global Positioning System (GPS) Technology. *Journal of Science Education and Technology, 11,* 59-80.

Lachapelle, G., Morrison, A., & Ong, R. B. (2009). Ultra – precise positioning for sport applications. In *13th IAIN World Congress, 2009* Stockholm, Sweden.

Lachapelle, G., Morrison, A., Ong, R. B., & Cole, G. (2009). A High Performance GNSS-based Sensor for Elite Skier Training. *GPS World, 20,* 28-30.

Limpach, P. and Skaloud, J. (2003, July 1). Trajectographie de courses de ski alpin avec GPS. *Geomatik Schweiz, 7,* 389-391.

Lind, D. & Sanders, S. (2004). *The Physics of skiing: Skiing at the Triple Point*. (2nd ed.) New York: Springer.

Lindinger, S. (2007). Methodological aspects in cross country skiing research. In V.Linnamo, P. V. Komi, & E. Müller (Eds.), *Science and Nordic Skiing* (pp. 27-38). Meyer & Meyer Sport.

Luethi, S. & Denoth, J. (1987). The Influence of Aerodynamic and Anthropometric Factors on Speed in Skiing. *International Journal of Sport Biomechanics, 3,* 345-352.

Lüthi, A., Federolf, P., Fauve, M., Oberhofer, K., Rhyner, H., Amman, W. et al. (2004). Determination of forces in carving using three independent methods. In D. Bacharach & J. Seifert (Eds.), *3rd International Congress on Skiing and Science* (pp. 3-4). Snowmass at Aspen (USA): St. Cloud State University.

Lüthi, A., Federolf, P., Fauve, M., & Rhyner, H. (2006). Effect of bindings and plates on ski mechanical properties and carving performance. In E.F.Moritz & S. Haake (Eds.), *The engineering of sport 6* (pp. 299-304). New York: Springer.

Madura, J. M., Lufkin, T., & Brown, C. (2010). Calculated descent times for different radii in ski racing. In E. Müller, S. Lindinger, & T. Stoggl (Eds.), *5th International Congress on Science and Skiing 2010* (pp. 124). St.Christoph, (Austria): University of Salzburg.

Meyer, F. (2012). *Biomechanical analysis of alpine skiers performing giant slalom turns.* University Lausanne, Switzerland.

Meyer, F., Bahr, A., Lochmatter, T., & Borrani, F. (2011). Wireless GPS-based phase-locked synchronization system for outdoor environment. *Journal of Biomechanics*.

Meyer, F., Le Pelley, D., & Borrani, F. (2011). Aerodynamic Drag Modeling Of Alpine Skiers Performing Giant Slalom Turns. *Medicine & Science in Sports & Exercise, 44,* 1109-1115.

Morawski, J. M. (1973). Control systems approach to a ski-turn analysis. *Journal of Biomechanics, 6,* 267-279.

Moritz, E. F., Haake, S., Kiefmann, A., Krinninger, M., Lindemann, U., Senner, V. et al. (2006). A New Six Component Dynamometer for Measuring Ground Reaction Forces in Alpine Skiing

The Engineering of Sport 6. In (2 ed., pp. 87-92). New York: Springer.

Mossner, M., Heinrich, D., Schindelwig, K., Kaps, P., Schiedmayer, H. B., Schretter, H. et al. (2005). Modelling of the ski-snow contact for a carved turn. In *Mountain & Sport: Updating study and research from laboratory to field* (pp. 64). Rovereto (Italy): University of Verona.

Mossner, M., Kaps, P., & Nachbauer, W. (1995). Smoothing the DLT parameters for moved cameras. In K. Hakkinen, K. L. Keskinen, P. V. Komi, & A. Mero (Eds.), *XVth Congress of the International Society of Biomechanics* (pp. 642-643).

Mossner, M., Kaps, P., & Nachbauer, W. (1996). A method for obtaining 3-d data in alpine skiing using pan-and-tilt cameras with zoom lenses. In C.D.Mote, R. J. Johnson, W. Hauser, & P. S. Schaff (Eds.), *Skiing Trauma and Safety: Tenth Volume* (pp. 155-164). Philadelphia: American Society for Testing and Materials.

Müller, E. (1994). Analysis of the biomechanical characteristics of different swinging techniques in alpine skiing. *Journal of Sport Sciences, 12,* 261-278.

Müller, E., Bartlett, R., Raschner, C., Schwameder, H., Benko-Bernwick, U., & Lindinger, S. (1998). Comparisons of the ski turn techniques of experienced and intermediate skiers. *Journal of Sports Sciences, 16,* 545-559.

Müller, E. & Schwameder, H. (2003). Biomechanical aspects of new techniques in alpine skiing and ski-jumping. *Journal of Sports Sciences, 21,* 679-692.

Muthukrishnan, K. (2009). *Multimodal localisation : analysis, algorithms and experimental evaluation.* PhD University of Twente, Enschede.

Myklebust, G. & Bahr, R. (2005). Return to play guidelines after anterior cruciate ligament surgery. *British Journal of Sports Medicine, 39,* 127-131.

Nachbauer, W., Kaps, P., Nigg, B., Brunner, F., Lutz, A., Obkircher, G., & Mossner, M. (1996). A video technique for obtaining 3-D coordinates in Alpine skiing. *Journal of Applied Biomechanics, 12,* 104-115.

Nakazato, K., Scheiber, P., & Müller, E. (2011). A comparison of ground reaction forces determined by portable force-plate and pressure-insole systems in alpine skiing. *Journal of Sports Science and Medicine, 10,* 754-762.

Niessen, M., Müller, E., Wimmer, M. A., Schwameder, H., & Riepler, B. (1998). Force and moment measurements during alpine skiing depending on height position. In *International Symposium on Biomechanics in Sports*. Konstanz, Germany.

Orlin, M. O. & McPoil, T. G. (2000). Plantar pressure assessment. *Physical Therapy, 80,* 399-409.

Petrone, N., Ceolin, F., & Morandin, T. (2010). Full scale impact testing of ski safety barriers using an instrumented anthropomorphic dummy. *Procedia Engineering, 2,* 2593-2598.

Petrone, N., Pollazzon, C., & Morandin, T. (2008). Structural Behaviour of Ski Safety Barriers during Impacts of an Instrumented Dummy. In *The Engineering of Sport 7* (pp. 633-642). Springer Paris.

Pireaux, S., Defraigne, P., Wauters, L., Bergeot, N., Baire, Q., & Bruyninx, C. (2010). Influence of ionospheric perturbations in GPS time and frequency transfer. *Advances in Space Research, 45,* 1101-1112.

Pozzo, R., Canclini, A., Cotelli, C., Martinelli, L., & Rockmann, A. (2001). 3d kinematics of the start in the downhill at the Bormio world cup in 1995. In E.Müller, H. Schwameder, C. Raschner, S. Lindinger, & E. Kornexl (Eds.), *Science and Skiing* (pp. 95-107). Hamburg: E & FN Spon.

Qu, X. & Nussbaum, M. A. (2009). Effects of external loads on balance control during upright stance: Experimental results and model-based predictions. *Gait & posture, 29,* 23-30.

Reid, R. (2010). *A kinematic and kinetic study of alpine skiing technique in slalom.* Ph.D. Thesis Norwegian School of Sport Sciences, Oslo, Norway.

Robertson, D. G., Caldwell, G., Hamill, J., Kamen, G., & Whittlesey, S. (2004). *Research Methods in Biomechanics.* (1 ed.) Champaign: Human Kinetics.

Savolainen, S. & Visuri, R. (1994). A review of athletic energy expenditure, using skiing as a practical example. *Journal of Applied Biomechanics, 10,* 253-269.

Schiefermüller, C., Lindinger, S., Raschner, C., & Müller, E. (2004). The skier's center of gravity as a valid point in movement analyses using different reference systems. In D. Bacharach & J. Seifert (Eds.), *3rd International Congress on Skiing and Science* (pp. 69-70). St. Cloud State University.

Schiestl, M. (2005a). *DLT data reconstruction on Clough-Tocher interpolated G^1-surfaces for simulation in alpine skiing.* Diploma Thesis in Technical Mathmatics Leopold-Franzens- University of Innsbruck, Mathematical Faculty.

Schiestl, M. (2005b). Improving DLT precision with constant camera parameters.

Schiestl, M., Kaps, P., Mossner, M., & Nachbauer, W. (2006). Calculation of friction and reaction forces during an alpine world cup downhill race. In E.F.Moritz & S. Haake (Eds.), *The engineering of sport 6* (pp. 269-274). New York: Springer.

Sheynin, O. (1995). Helmert's work in the theory of errors. *Archive for History of Exact Sciences, 49,* 73-104.

Simoneau, M., Begin, F., & Teasdale, N. (2006). The effects of moderate fatigue on dynamic balance control and attentional demands. *Journal of NeuroEngineering and Rehabilitation, 3,* 22.

Skaloud, J. & Limpach, P. (2003). Synergy of CP-DGPS, Accelerometry and Magnetic Sensors for Precise Trajectography in Ski Racing. In *Conference of the ION GPS/GNSS 2003, Portland, USA.*

Spörri, J., Kröll, J., Amesberger, G., Blake, O., & Müller, E. (2012). Perceived key injury risk factors in World Cup alpine ski racing an explorative qualitative study with expert stakeholders. *British Journal of Sports Medicine, 46,* 1059-1064.

Spörri, J., Kröll, J., Schwameder, H., & Müller, E. (2012a). Turn Characteristics of a Top World Class Athlete in Giant Slalom: A Case Study Assessing Current Performance Prediction Concepts. *International Journal of Sports Science and Coaching, 7,* 647-660.

Spörri, J., Kröll, J., Schwameder, H., Schiefermüller, C., & Müller, E. (2012b). Course setting and selected biomechanical variables related to injury risk in alpine ski racing: an explorative case study. *British Journal of Sports Medicine, 46,* 1072-1077.

Stricker, G., Scheiber, P., Lindenhofer, E., & Müller, E. (2010). Determination of forces in alpine skiing and snowboarding: Validation of a mobile data acquisition system. *European Journal of Sport Science, 10,* 31-41.

Supej, M. (2010). 3D measurements of alpine skiing with an inertial sensor motion capture suit and GNSS RTK system. *Journal of Sports Sciences, 28,* 759-769.

Supej, M. & Holmberg, H. C. (2010). How gate setup and turn radii influence energy dissipation in slalom ski racing. *Journal of Applied Biomechanics, 26,* 454-464.

Supej, M. & Holmberg, H. C. (2011). A new time measurement method using a high-end global navigation satellite system to analyze alpine skiing. *Research Quarterly for Exercise and Sport, 82,* 400-411.

Supej, M., Kipp, R., & Holmberg, H. C. (2010). Mechanical parameters as predictors of performance in alpine World Cup slalom racing. *Scandinavian Journal of Medicine & Science in Sports,* 72-81.

Supej, M., Kugovnik, O., & Nemec, B. (2004a). Advanced analyzing of alpine skiing based on 3d kinematical measurements. In D. Bacharach & J. Seifert (Eds.), *3rd International Congress on Skiing and Science* (pp. 7-8). St. Cloud State University.

Supej, M., Kugovnik, O., & Nemec, B. (2004b). Modelling and simulation of two competition slalom techniques. *Kinesiology, 36,* 206-212.

Supej, M., Kugovnik, O., & Nemec, B. (2005). Energy principle used for estimating the quality of a racing ski turn. In E. Müller, D. Bacharach, S. Klika, S. Lindinger, & H. Schwameder (Eds.), *3rd international congress on science in skiing* (pp. 228-237). Adelaide: Meyer & Meyer Sport Ltd..

Supej, M., Nemec, B., & Kugovnik, O. (2005). Changing conditions on the slalom ski course affect competitors' performances. *Kinesiology, 37,* 151-158.

Supej, M., Saetran, L., Oggiano, L., Ettema, G., Saarabon, N., Nemec, B., & Holmberg, H. C. (2012). Aerodynamic drag is not the major determinant of performance during giant slalom skiing at the elite level. *Scandinavian Journal of Medicine & Science in Sports, 23,* 38-47.

Terrier, P., Ladetto, Q., Merminod, B., & Schutz, Y. (2000). High-precision satellite positioning system as a new tool to study the biomechanics of human locomotion. *Journal of Biomechanics, 33,* 1717-1722.

Terrier, P., Turner, V., & Schutz, Y. (2005). GPS analysis of human locomotion: Further evidence for long-range correlations in stride-to-stride fluctuations of gait parameters. *Human Movement Science, 24,* 97-115.

Tranquilla, J. & Collpits, B. (1989). GPS antenna design characteristics for high – precision applications. *Journal of Surveying Engineering, 115,* 2-14.

Van Mechelen, W., Hlobil, H., & Kemper, H. (1992). Incidence, Severity, Aetiology and Prevention of Sports Injuries. *Sports Medicine, 14,* 82-99.

Waegli, A. (2009, January 23). Trajectory Determination and Analysis in Sports by Satellite and Inertial Navigation. *Geodätisch-geophysikalische Arbeiten in der Schweiz, 77,* 175.

Waegli, A. and Skaloud, J. (2007). Turning Point - Trajectory Analysis for Skiers. *Inside GNSS, 2,* 24-34.

Waegli, A. & Skaloud, J. (2009). Optimization of two GPS/MEMS-IMU integration strategies with application to sports. *GPS Solutions, 13,* 315-326.

Wunderly, G. S. & Hull, M. L. (1989). A biomechanical approach to alpine ski binding design. *International Journal of Sport Biomechanics, 5,* 308-323.

Wunderly, G. S., Hull, M. L., & Maxwell, S. (1988). A second generation microcomputer controlled binding system for alpine skiing research. *Journal of Biomechanics, 21,* 299-318.

Yeadon, M. R. & King, M. A. (1999). A method for synchronizing digitised video data. *Journal of Biomechanics, 32,* 983-986.

Papers I – VI

Paper I

Paper II

Sensors **2013**, *13*, 9821-9835; doi:10.3390/s130809821

OPEN ACCESS

sensors

ISSN 1424-8220

www.mdpi.com/journal/sensors

Article

Determination of External Forces in Alpine Skiing Using a Differential Global Navigation Satellite System

Matthias Gilgien [1,*], Jörg Spörri [2], Julien Chardonnens [3], Josef Kröll [2] and Erich Müller [2]

[1] Department of Physical Performance, Norwegian School of Sport Sciences, Sognsveien 220, Oslo 0806, Norway

[2] Department of Sport Science and Kinesiology, University of Salzburg, Schlossallee 49, Hallein/Rif 5400, Austria; E-Mails: joerg.spoerri@sbg.ac.at (J.S.); josef.kroell@sbg.ac.at (J.K.); erich.mueller@sbg.ac.at (E.M.)

[3] Laboratory of Movement Analysis and Measurement, Ecole Polytechnique Fédérale de Lausanne, Station 11, Lausanne 1015, Switzerland; E-Mail: julien.chardonnens@epfl.ch

***** Author to whom correspondence should be addressed; E-Mail: matthias.gilgien@nih.no; Tel.: +47-456-766-56.

Received: 1 July 2013; in revised form: 22 July 2013 / Accepted: 29 July 2013 / Published: 2 August 2013

Abstract: In alpine ski racing the relationships between skier kinetics and kinematics and their effect on performance and injury-related aspects are not well understood. There is currently no validated system to determine all external forces simultaneously acting on skiers, particularly under race conditions and throughout entire races. To address the problem, this study proposes and assesses a method for determining skier kinetics with a single lightweight differential global navigation satellite system (dGNSS). The dGNSS kinetic method was compared to a reference system for six skiers and two turns each. The pattern differences obtained between the measurement systems (offset ± SD) were −26 ± 152 N for the ground reaction force, 1 ± 96 N for ski friction and −6 ± 6 N for the air drag force. The differences between turn means were small. The error pattern within the dGNSS kinetic method was highly repeatable and precision was therefore good (SD within system: 63 N ground reaction force, 42 N friction force and 7 N air drag force) allowing instantaneous relative comparisons and identification of discriminative meaningful changes. The method is therefore highly valid in assessing relative differences between skiers in the same turn, as well as turn means between different turns. The system is suitable to measure large capture volumes under race conditions.

Keywords: force; kinetics; kinematics; GPS; global navigation satellite system; technical validation; precision; alpine skiing

1. Introduction

Alpine ski racing is a highly dynamic sport. Skiers move at high speed across large areas, adjusting their momentum at relatively high rates [1–4]. Differential global navigation satellite system technology (dGNSS), an efficient method to capture skier trajectories, has been applied by several researchers to investigate performance-related issues [5–8]. To understand the underlying mechanisms governing skiers' momentum (*i.e.*, the direction of the trajectory and the speed along the trajectory) the external forces acting on the skiers (air drag, gravity and ground reaction forces) have to be determined [2,3,9,10]. So far, video-based 3D kinematic systems have been applied to compute the external forces [1,11–14]. This methodology allows accurate reconstruction of the air drag [15] and the resultant force acting on the center of mass. However, video-based 3D kinematic systems are limited in capture volume and need extensive processing time, which is unfortunate since the number of conditions to be investigated in alpine skiing is large [16]. Therefore, combinations of non-differential GNSS and inertial measurement data [17,18] as well as dGNSS [9] have been applied to reconstruct skier center of mass (CoM) position, velocity and acceleration (CoM_{PVA}) as well as segment kinematics in racing situations more efficiently. However, none of these wearable system-based methods has been validated against a reference system which has been proven valid and has been extensively used. The current wearable systems might further be optimized with respect to robustness for applications in obstructed terrain and under racing conditions (factors can include GNSS signal obstruction by the skier's own body, geodetic methodology and measurement frequency). Therefore, the aim of the current study was to propose a non-invasive and robust dGNSS based method to determine the forces acting on the CoM in demanding alpine ski racing settings and to validate the method with a video and body segment parameter-based 3D kinematic system as suggested [9].

2. Methods

2.1. Data Acquisition

A giant slalom course was set with a 27 m gate distance and an offset of 8 m on a 26 ° incline, water-injected slope (Figure 1). The snow surface was captured by terrestrial surveillance with a tachymeter (Leica TPS 1200, Leica Geosystems AG, Heerbrugg, Switzerland). The surveyed points (on average 12 points per m^2) were (a) triangulated using the method of Delaunay [19] and (b) gridded (grid spacing of 0.3 m) and smoothed with a bi-cubic spline function [20,21]. The analysis was based on data from turn eight of the course, allowing the skiers to pick up race- like speed before entering the analysis section. The analyzed section was short (one turn) due to the limitations in capture volume and the extensive processing time of the reference system. Analysis and turn start and end were defined as the point where the CoM and the mean ski trajectory crossed each other in the horizontal plane [22]. The entire turn including the straight phase at turn initiation and completion was named

turn cycle. The phase in the turn where the turn radius of the reference trajectory was below 30 m was named turning phase [3]. Six male racers ranging from European Cup to former World Cup level volunteered to participate. Two runs per skier were selected for analysis and thus in total 12 runs were monitored. The current study was approved by the Ethics Committee of the Department of Sport Science and Kinesiology at the University of Salzburg.

Figure 1. Illustration of the experimental setup at turn eight. The gates are plotted in blue, the calibration points for the video-based 3D kinematic system in black, skier CoM trajectory in red, the analyzed area in yellow, the analyzed turn cycle in green and the analyzed turning phase in pink.

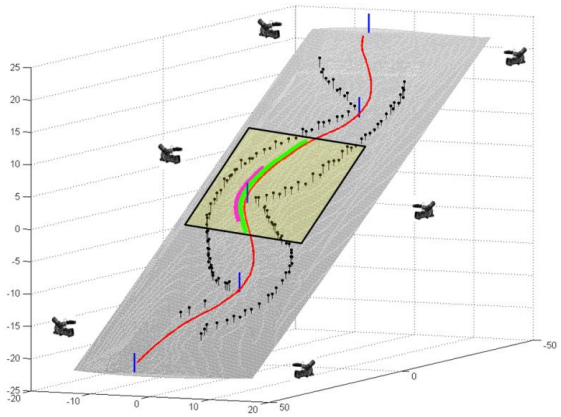

2.2. dGNSS Based Method

GNSS is the umbrella term for global navigation satellite systems, while the more widely used term GPS is the name of the American global navigation satellite system. The current study makes use of both the Russian (GLONASS) and the American (GPS) system. We therefore use GNSS as the collective term for both.

2.2.1. Computation of the Center of Mass

The skiers' head trajectories were captured using a dGNSS system consisting of a G5Ant-2AT1 antenna (160 g, Antcom, Torrence, CA, USA) mounted on the helmet (Figure 2) and an Alpha-G3T receiver (430 g, Javad, San Jose, CA, USA) carried in a small cushioned backpack. Dual frequency (L1 and L2) data of the GPS and the GLONASS satellite systems were logged at 50 Hz. Short baseline differential dGNSS solution computation was enabled by using two base stations at the start of the course. The ambiguities of the differential geodetic position solution could be solved for all trials using the kinematic KAR algorithm of the GrafNav (Waypoint, NovAtel Inc., Calgary, AB, Canada) post-processing software.

Figure 2. Left side: The pendulum model approximating the CoM in the dGNSS model. CoM position (⊗), antenna position (□). Right side: Skier with GNSS antenna mounted on the helmet.

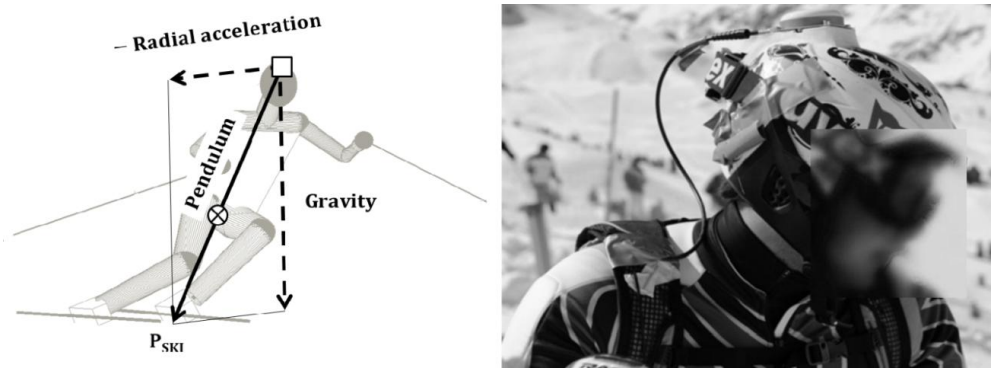

Typical errors for dGNSS systems are 10 mm ± 1 ppm in horizontal and 20 mm ± 1 ppm in vertical direction [9]. The dGNSS head trajectory ($\mathbf{P}_{\mathbf{dGNSS}}$) was filtered with a cubic spline function weighting each 3D position with its accuracy estimate from the differential position solution [5]. The tolerance factor (lambda) was 0.5 for the horizontal and 0.7 for the vertical component. For the approximation of the CoM based on the trajectory of the dGNSS antenna, the biomechanical phenomenon that skiers incline laterally in order to balance the radial force during the turn was used. The skier's inclination was modeled by an inverted pendulum [9,23] which was attached to the dGNSS antenna. The neutral position of the pendulum was given by the normal projection of the dGNSS antenna onto the snow surface. The pendulum was in neutral position during straight skiing, when the radial acceleration was zero. During turning the pendulum was deflected from its neutral position. The deflection representing the skier's lateral tilt was calculated as a linear combination of the gravitational and the dGNSS antenna radial acceleration. The intersection of the pendulum vector with the snow surface yielded the ski position ($\mathbf{P}_{\mathbf{SKI}}$). Finally, the approximation of the CoM ($\mathbf{CoM}_{\mathbf{dGNSS}}$) was modeled at 53% of the pendulum length measured from the dGNSS antenna (Figure 2). The computation of the $\mathbf{CoM}_{\mathbf{dGNSS}}$ at 53% of the pendulum length was determined on a full body segment kinematic dataset [2]. $\mathbf{CoM}_{\mathbf{dGNSS}}$ was low-pass filtered (second-order Butterworth filter; cut-off frequency of 4 Hz). Instantaneous CoM velocity ($\mathbf{v}_{\mathbf{dGNSS}}$) and acceleration ($\mathbf{a}_{\mathbf{dGNSS}}$) were computed as the first and second time derivatives using the finite central difference formulae [24]. The pendulum model was described in detail in [25].

2.2.2. Computation of the External Forces

The resultant force ($\mathbf{F}_{\mathbf{RES,dGNSS}}$) and the gravitational force ($\mathbf{F}_{\mathbf{G}}$) were calculated using the skier's mass (including equipment) and the $\mathbf{CoM}_{\mathbf{dGNSS}}$ acceleration and gravitational acceleration respectively. The air drag force ($\mathbf{F}_{\mathbf{D,dGNSS}}$) was computed according to Equation (1), where ρ is the air density. Air density was calculated from temperature and air pressure measurements taken at a meteorological station mounted along the slope. The effect of air humidity was neglected [26]. The line of action of the drag force was assumed to be opposite to $\mathbf{v}_{\mathbf{dGNSS}}$. The ambient wind velocity field ($\mathbf{v}_{\mathbf{WIND}}$) was

based on two meteorological stations positioned on the top and the bottom part of the slope respectively. Wind speed was lower than 0.6 m/s during the measurement and at about right angles to the main course direction. The drag area $(C_DA)_{BARELLE}$ was computed by adapting the model of Barelle (2004) [27], where the drag area was expressed as a function of reduced body extension (D) and arm position. For this study the arms were omitted from the model, and only the body extension was considered. Barelle [27] computed D (the distance between neck and feet) as the projections of the segment lengths L_1 (leg), L_2 (thigh) and L_3 (chest) into the frontal plane using the angles θ_1, θ_2 and θ_3 (Equation (2)). In the dGNSS method dataset D was computed along the vector between the feet position ($\mathbf{P_{SKI}}$) and the dGNSS antenna position ($\mathbf{P_{GNSS}}$) as shown in Figure 3a. The length of D was determined by the reduction of the distance between $\mathbf{P_{SKI}}$ and $\mathbf{P_{GNSS}}$ by 17% to accommodate for the distance between $\mathbf{P_{GNSS}}$ and the neck in order to follow the definition of Barelle [27]. Drag area was computed according to Equation (3):

$$F_{D,dGNSS} = \frac{\rho \cdot (-v_{dGNSS} + v_{WIND})^2}{2} \cdot (C_D A)_{BARELLE} \quad (1)$$

$$(C_D A)_{BARELLE} = 0.0003 \cdot (L_1 \cdot \sin\theta_1 + L_2 \cdot \sin\theta_2 + L_3 \cdot \sin\theta_3) - 0.026 \quad (2)$$

$$(C_D A)_{BARELLE} = 0.0003 \cdot D - 0.026 \quad (3)$$

Figure 3. (**a**) Illustration of the reduced skier amplitude (D) applied for the drag area calculation. $\mathbf{P_{GNSS}}$ (□), intersection point of the pendulum and the snow surface ($\mathbf{P_{SKI}}$); (**b**) Illustration of the ski friction force ($\mathbf{F_F}$) calculation. The direction of $\mathbf{F_F}$ is defined by the vertical projection of the velocity vector ($\mathbf{v_{dGNSS}}$) onto the snow surface ($\mathbf{v_{dGNSS}}$'). $\mathbf{F_F}$ is finally calculated by projection of the ground reaction ($\mathbf{F_{GRF,dGNSS}}$) onto $\mathbf{v_{dGNSS}}$'.

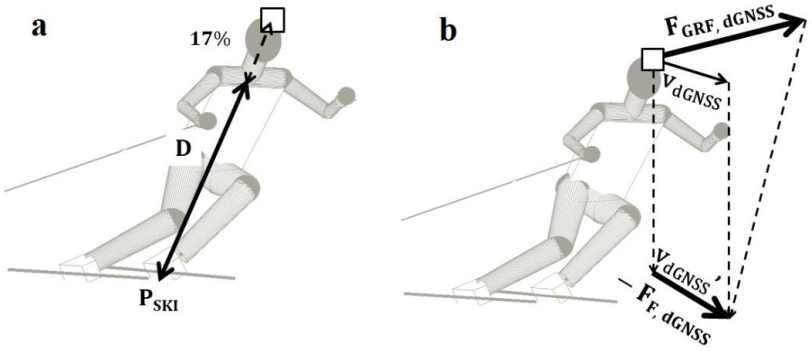

The ground reaction force ($\mathbf{F_{GRF,dGNSS}}$) was calculated according to Equation (4) and therefore includes all components of the ground reaction force:

$$F_{GRF,dGNSS} = F_{RES,dGNSS} - F_G - F_{D,dGNSS} \quad (4)$$

The ski friction force ($\mathbf{F_{F,dGNSS}}$) is the component of $\mathbf{F_{GRF,dGNSS}}$ in the tangent direction to the direction of motion. $\mathbf{F_{F,dGNSS}}$ therefore measures the braking effect of the entire ski manipulation (loading, angulation, angle of attack, etc.) and interaction with the snow on the $\mathbf{CoM_{dGNSS}}$ in the global spatial reference frame and might thus be relevant for performance related analysis. The direction of

$\mathbf{F_{F,dGNSS}}$ was defined as the vertical projection along the gravitational vector of $\mathbf{v_{dGNSS}}$ onto snow surface ($\mathbf{v_{dGNSS}}$'). The negative component of $\mathbf{F_{F,dGNSS}}$ ($-\mathbf{F_{F,dGNSS}}$) was computed by projecting $\mathbf{F_{GRF,dGNSS}}$ normal onto $\mathbf{v_{dGNSS}}$'. $\mathbf{F_{F,dGNSS}}$ was finally determined as the inverse of ($-\mathbf{F_{F,dGNSS}}$) [2]. The construction of ($-\mathbf{F_{F,dGNSS}}$) is illustrated in Figure 3b.

2.3. Reference System

2.3.1. Computation of the Center of Mass

The reference force method was derived from video-based 3D kinematic data. Skiers' segment kinematics were captured using six panned, tilted and zoomed HDV cameras (PMW-EX3, Sony, Tokyo, Japan) positioned around the capture volume. The capture frequency of the reference system was 50 Hz and was time-synchronized electronically with the dGNSS system. A standard video-based 3D kinematic system was used as the reference system [28]. Twenty-two joint centers and landmarks on the skier's body (head, neck, right and left (r/L) shoulder, (r/L) elbow, (r/L) hand, (r/L), stick's tail, (r/L) hip, (r/L) knee, (r/L) ankle, (r/L) ski's tip and tail) were reconstructed in 3D using a DLT-based panning algorithm developed by Drenk [29]. CoM position was computed using the Zatsiorsky body segment parameter model [30] with de Leva adjustments [31]. Instantaneous CoM velocity ($\mathbf{v_{CoM}}$) and acceleration ($\mathbf{a_{CoM}}$) were calculated similarly to the dGNSS method.

2.3.2. Computation of the External Forces

The resultant force ($\mathbf{F_{RES,REF}}$) and the gravitational force ($\mathbf{F_G}$) were calculated using the skier's mass (including equipment) and the ($\mathbf{a_{CoM}}$) acceleration and gravitational acceleration respectively. The air drag force ($\mathbf{F_{D,REF}}$) was computed according to Equation (5). The drag area ($(C_DA)_{MEYER}$) was computed by applying the "GM1" model of Meyer *et al.* [15] to the video-based segment kinematics method (Equation (6)), where UpH is the body length, A_F is the frontal area, and H and W are the skier's instantaneous height and width. The frontal area was calculated using the orthonormal projection of the skier's silhouette on the plane normal to $\mathbf{v_{COM}}$. The silhouette was generated by attaching geometric bodies to the reconstructed body landmarks and line segments. The frontal area (A_F) was technically determined by counting the pixels within the skier's silhouette [2,17,32]. H and W were computed from segment kinematics in the frontal plane. The air drag model was found valid with respect to wind tunnel testing. (R^2 = 0.972, p < 0.001, SD of the dragarea = 0.016) with wind-tunnel tests [15]. The ground reaction force ($\mathbf{F_{GRF,REF}}$) was calculated according to Equation (7). $\mathbf{F_{GRF,REF}}$ was decomposed into the component parallel to the direction of motion ($\mathbf{F_{F,REF}}$) with the same method as in the dGNSS method, but using $\mathbf{v_{CoM}}$ instead of $\mathbf{v_{dGNSS}}$.

$$F_{D,REF} = \frac{\rho \cdot (v_{COM} + v_{WIND})^2}{2} \cdot (C_D A)_{MEYER} \quad (5)$$

$$(C_D A)_{MEYER} = 0.046 - 0.155 \cdot UpH + 0.649 \cdot A_F + 0.181 \cdot H + 0.039 \cdot W \quad (6)$$

$$F_{GRF,REF} = F_{RES,REF} - F_G - F_{D,REF} \quad (7)$$

2.4. Comparison of the dGNSS Based Method and the Reference System

For comparison of the dGNSS based method and the reference system, each trial was time-normalized. The dGNSS-based method was then compared with the reference system for the vector amplitude of the ground reaction force ($\mathbf{F_{GRF}} = \mathbf{F_{GRF,REF}} - \mathbf{F_{GRF,dGNSS}}$), the ski friction ($\mathbf{F_F} = \mathbf{F_{F,REF}} - \mathbf{F_{F,dGNSS}}$), the air drag force ($\mathbf{F_D} = \mathbf{F_{D,REF}} - \mathbf{F_{D,dGNSS}}$) and the resultant force ($\mathbf{F_{RES}} = \mathbf{F_{RES,REF}} - \mathbf{F_{RES,dGNSS}}$). The vectorial differences between the dGNSS-based method and the reference system were calculated for each time point of each trial. For each trial the offsets of these vectorial differences were calculated. Thereafter the offsets were averaged over the twelve trials and named average vectorial difference offset (AVD-Offset). In order to obtain a precision measure for between-measurement system comparisons (dGNSS and reference system) the standard deviation (precision, SD) of the vectorial differences was calculated for the entire turn cycle for each trial separately and then averaged across the twelve trials. This precision measure was named average vectorial difference between SD (AVD-Offset-Between-SD). To assess the precision of the dGNSS method for relative comparisons between skiers and/or different turns (within-measurement system precision) the SD of the twelve trials was calculated at each time point across the turn cycle (instantaneous AVD-Within-SD) and then averaged for all time points across the turn cycle. This precision measurement was called the average vectorial difference within SD (AVD-Within-SD). The described SD and offset procedures were performed for: (a) the entire turn cycle and (b) the turning phase, the section of the turn where the turn radius of the reference system was below 30 m [28] except for AVD-Within-SD. The average vectorial difference offsets and SD's were also expressed in relation to the respective turn mean forces in order to put the measurement errors into perspective with the size of the forces. These differences were expressed in percentage and computed as division of the vectorial difference offset or SD and the turn mean force of the reference system. Mean force and maximal force were extracted for each trial and averaged across the twelve trials with both the dGNSS method and the reference system for each force. The differences between the dGNSS and the reference system of the turn cycle mean and turn cycle maxima computation were assessed by calculation of the mean error and the SD between the methods. The normality of the data was verified prior to applying parametric statistics using the Lilliefors test ($p < 0.05$).

3. Results and Discussion

3.1. Results

Using the method described previously the force differences were monitored for twelve trials. Table 1 shows the results of the assessment. The average vectorial difference offset obtained from the dGNSS and the reference system was largest for $\mathbf{F_{GRF}}$ but substantially smaller for $\mathbf{F_F}$ and $\mathbf{F_D}$.

The average vectorial difference offset for $\mathbf{F_{GRF}}$ and $\mathbf{F_D}$ was smaller for the turning phase when the turn radius was below 30 m than for the entire turn cycle both in absolute values and relative to the size of the respective turn cycle mean and turning phase mean forces. The average vectorial difference offset of $\mathbf{F_F}$ was larger for the turning phase than the turn cycle.

Table 1. Average vectorial difference offset, between and within standard deviation (SD) and percent difference of the ground reaction force ($\mathbf{F_{GRF}}$), ski-snow friction ($\mathbf{F_F}$) and air drag ($\mathbf{F_D}$) for the entire turn cycle and the turning phase (turn radius < 30 m). Comparisons of the turn mean and maximum values (typical feature of turn cycle) are given in the bottom part of the table (N = 12).

Differences		$\mathbf{F_{GRF}}$	$\mathbf{F_F}$	$\mathbf{F_D}$
Average Vectorial Difference (AVD) for Turn Cycle	Offset [N]	−25.8	1.3	−6.4
	Offset [%]	−1.9	0.3	−8.9
	Offset-between SD [N]	151.7	96.2	6.1
	Offset-between SD [%]	11	26.3	8.5
	Within SD [N]	63.2	41.5	7.0
	Within SD [%]	4.6	11.4	9.8
Average Vectorial Difference (AVD) for Turning Phase (R < 30 m)	Offset [N]	7.7	−16.6	3.1
	Offset [%]	0.5	−3.8	4.8
	Offset-between SD [N]	124.2	81.3	5.8
	Offset-between SD [%]	7.5	18.5	9.1
Typical Turn Cycle Feature	Mean [N]	−22.2	1.1	−4.4
	SD of Mean [N]	24	6.8	2.9
	Maxima [N]	−71.7	−23.2	−18.7
	SD of Maxima [N]	63.1	76.2	5.8

Figure 4. Comparison of the ground reaction force computed from the dGNSS method ($\mathbf{F_{GRF,dGNSS}}$, solid line) and the reference system ($\mathbf{F_{GRF,REF}}$, thick dashed line) with their standard deviations ($\mathbf{F_{GRF,dGNSS}}$, gray area; $\mathbf{F_{GRF,REF}}$, thin dashed lines) in the upper part of the graph. The bottom part of the graph shows the instantaneous average vectorial difference (solid line) and its instantaneous AVD-Within-SD (dashed lines) across the turn cycle. Gate passage and the points where the turn radius is less than 30 m are marked as turn start and turn end.

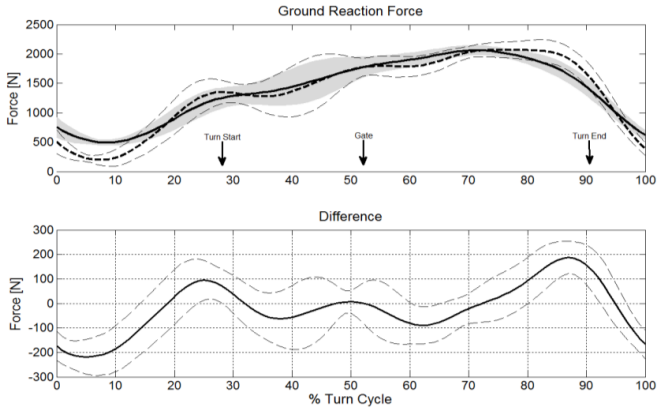

The precision offsets for comparison within the dGNSS system (AVD-Within-SD) for $\mathbf{F_{GRF}}$ and $\mathbf{F_F}$ were less than half of the precision offsets between the dGNSS and the reference system

(AVA-Between-SD) while this was nearly unchanged for $\mathbf{F_D}$. During the turning phase when the turn radius was below 30 m the AVA-Between-SD was reduced in both absolute and relative terms compared to the entire turn cycle for $\mathbf{F_{GRF}}$ and $\mathbf{F_F}$ but not for $\mathbf{F_D}$.

Comparing the typical features of turn cycles, the differences in the turn mean were substantially smaller than the AVD-Within-SD and AVD-Between-SD for all forces. The maximum values were underestimated for all forces with the largest error for $\mathbf{F_{GRF}}$.

The upper parts of Figures 4–6 illustrate $\mathbf{F_{GRF}}$, $\mathbf{F_F}$ and $\mathbf{F_D}$ obtained from the reference and the dGNSS method in time-normalized format across the examined turn cycle. The lower parts of Figures 4–6 show the progression of the vectorial difference and its AVD-Within-SD for $\mathbf{F_{GRF}}$, $\mathbf{F_F}$ and $\mathbf{F_F}$ graphically. All three forces have a variability of the offset. The largest offsets occur in the initiation and completion phase for $\mathbf{F_{GRF}}$ and in the initiation phase for $\mathbf{F_D}$.

Figure 5. Comparison of the ski friction force computed from the dGNSS method ($\mathbf{F_{F,dGNSS}}$, solid line) and the reference system ($\mathbf{F_{F,REF}}$, thick dashed line) with their standard deviation ($\mathbf{F_{F,dGNSS}}$, gray area; $\mathbf{F_{F,REF}}$, thin dashed lines) is provided in the upper part of the graph. The bottom part of the graph shows the instantaneous average vectorial difference (solid line) and instantaneous AVD-Within-SD (dashed lines) across the turn cycle. Gate passage and the points where the turn radius is less than 30 m are marked as turn start and turn end.

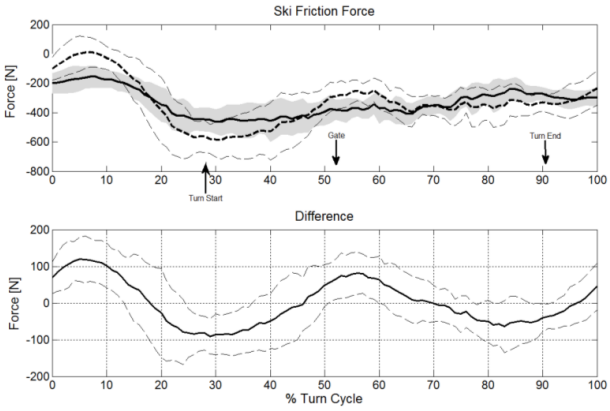

3.2. Discussion

The current study proposed a new approach for the reconstruction of the external forces acting on alpine skiers using a dGNSS-based method. Compared to previous dGNSS-based force modeling [9] the dGNSS antenna was mounted on the helmet instead of the back. The dGNSS method was compared to a kinetic reference system constructed from a video-based 3D kinematic segment model, allowing precise reconstruction of center of mass and air drag. Among the field methods applied to determine air drag in alpine skiing [2,9,14,15,17,27], [15] was chosen as the reference system, since this model most probably accounts best for the different body positions, speed and clothing in giant slalom skiing. The reference system allowed a precise reconstruction of the CoM (mean error 23 mm, SD 10 mm) and thus the resultant force acting on the CoM [33].

A repeatable instantaneous vectorial difference pattern was observed between the dGNSS method and reference system for $\mathbf{F_{GRF}}$, $\mathbf{F_F}$ and $\mathbf{F_D}$ (Figures 4–6). These patterns oscillated above and below zero and therefore the instantaneous AVD-offsets and the turn mean error compensate across the entire turn cycle and thus differ little from the reference values. Similarly the instantaneous average vectorial difference of $\mathbf{F_F}$ followed a harmonic pattern around zero (Figure 5) and was approximately compensated in the phase before and after gate passage. Therefore, the offsets of the section before gate passage (−2 N) and after gate passage (5 N) were also small. These findings suggest that comparisons of turn means (typical features of the turn cycle as given in Table (1) between skiers or between different turns are valid as long as they are larger than these precision (SD) boundaries of the method.

Figure 6. The comparison of the air drag force calculated from the dGNSS method ($\mathbf{F_{D,dGNSS}}$, solid line) and the reference system ($\mathbf{F_{F,REF}}$, thick dashed line) with their standard deviations ($\mathbf{F_{D,dGNSS}}$, gray area; $\mathbf{F_{D,REF}}$, thin dashed lines) is provided in the upper part of the graph. The bottom part of the graph shows the instantaneous average vectorial difference (solid line) and instantaneous AVD-Within-SD (dashed lines) across the turn cycle. Gate passage and the points where the turn radius is less than 30 m are marked as turn start and turn end.

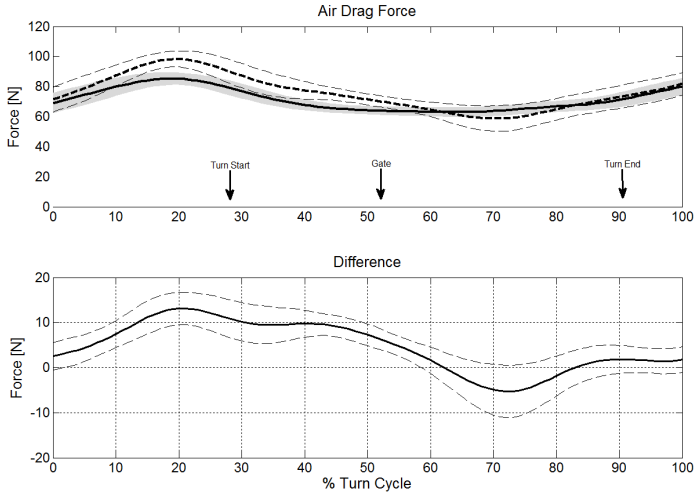

The AVD-Offset-Between-SDs represent the precision of the dGNSS method with respect to the reference system in predicting the absolute values of the forces at random time points in the turn cycle. These were relatively large for $\mathbf{F_{GRF}}$ and $\mathbf{F_F}$ but were reduced both in absolute values and relative to the acting forces in the turning phase, when the turn radius was below 30 m.

Because the instantaneous vectorial difference patterns were repeatable for the twelve trials, the AVD-Within-SDs were relatively small: smaller than the AVD-Offset-Between-SDs for $\mathbf{F_{GRF}}$ and $\mathbf{F_F}$ but about equal for $\mathbf{F_D}$. The AVD-Offset-SDs describe the precision within the dGNSS method and therefore apply for relative comparisons between skiers or turns when both components are determined with the dGNSS method. In a study investigating slalom skiing [2] it was found that the ground

reaction force was 253 N higher at gate passage on a course with a 10 m gate distance compared to a course with a 13 m gate distance. The AVD-Within-SD of the dGNSS method for $\mathbf{F_{GRF}}$ was 63 N and thus the dGNSS method is valid to identify such discriminative meaningful changes for the ground reaction force. Similarly the air drag was increased, at 15 N at gate passage in the 13 m course [2], while the AVD-Within-SD for $\mathbf{F_D}$ was 7 N. As long as the AVD-Within-SD's are smaller than the differences to be investigated, the method is valid for identifying discriminative meaningful changes at random instances in a turn cycle.

The dGNSS method underestimated the turn cycle maxima of all three forces. However, the offset and SD were acceptable with respect to the size of the maximal ground reaction forces [34,35]. Air drag might be maximal in the initiation phase of the turn (Figure 6), when skiers are in a relatively extended body position [2,36]. It is likely that skiers had their arms abducted in that phase of the turn cycle and that these contributed to $\mathbf{F_D}$. The underestimation of both maximum and AVD-offset in that phase of the turn may thus partly be caused by the lack of inclusion of the arms in the dGNSS method.

The AVD-offset of $\mathbf{F_{GRF}}$ might be caused by the offset in the resultant force, since the offset of the resultant force follows a similar pattern (see results of $\mathbf{F_{RES}}$ in the electronic supplementary information) and is substantially larger than the offset of the air drag force. Consequently, the offsets in the first and the last phase of the turn of $\mathbf{F_{GRF}}$ might be caused by deficient CoM reconstruction in the dGNSS method. Thus the offset and precision values presented in this study may be valid for the applied dGNSS method and CoM modelling, but may be different for other methods.

3.3. Limitations

The attachment of the measurement device on the head leads to exclusion of the high frequency ground reaction force components. The skier's body acts as a damper [34] and the measurement frequency of the GNSS of 50 Hz is too low to capture the remaining high frequency components transmitted to the head. The same phenomenon is present for the reference system applied in this study. A previous study [11] showed that CoMs reconstructed from video-based 3D kinematic motion capture systems lack the high frequency components due to damping by the lower extremities and the low capture frequency. However, the overall course of the ground reaction force was well reconstructed. Therefore, our reference system seems valid to assess the low frequency component of the ground reaction force. For the assessment of high frequency components or left and right leg ground reaction force information, other types of measurement systems should be applied, such as pressure insoles [11,37–40], force plates [11,37,41–44] or accelerometers [45]. The air drag force model might be improved by adding a model for the arms.

4. Conclusions

This study introduced a dGNSS-based method for the simultaneous determination of all external forces in competitive alpine skiing. The method was found to be technically valid for comparing turn mean forces and allowed instantaneous relative comparisons between skiers with respect to the precision boundaries of 63 N for the ground reaction force, 42 N for the ski friction force and 7 N for the air drag force. Due to its technical validity, its small equipment size/weight and geodetic GNSS measurement robustness the system was found suitable to simultaneously capture CoM_{PVA} [46] and the

forces acting on the CoM under racing conditions across large capture volumes. The proposed method might therefore be applied to efficiently investigate competitive alpine skiing and bring better insight to performance and injury-related aspects. The methods strength with respect to performance might be that the ski friction force is expressed in direction of travel and is therefore directly linked to speed regulation. The methods advantage with respect to injury prevention might be that skier loading (ground reaction force) can be determined at the same time as other injury risk factors such as speed are captured with one device.

Acknowledgments

The authors thank Jan Cabri, Geo Boffi and Philip Crivelli for their contribution to this study. This study was partly supported by the International Skiing Federation (FIS).

Conflict of Interest

The authors declare no conflict of interest.

References

1. Schiestl, M.; Kaps, P.; Mossner, M.; Nachbauer, W. Calculation of Friction and Reaction Forces during an Alpine World Cup Downhill Race. In *The Engineering of Sport*, 6th ed.; Moritz, E.F., Haake, S., Eds.; Springer: New York, NY, USA, 2006; Volume 1, pp. 269–274.
2. Reid, R. A Kinematic and Kinetic Study of Alpine Skiing Technique in Slalom. Ph.D. Thesis, Norwegian School of Sport Sciences: Oslo, Norway, 1 January 2010.
3. Spörri, J.; Kröll, J.; Schwameder, H.; Müller, E. Turn characteristics of a top world class athlete in giant slalom: A case study assessing current performance prediction concepts. *Int. J. Sports Sci. Coach* **2012**, *7*, 647–659.
4. Supej, M.; Kipp, R.; Holmberg, H.C. Mechanical parameters as predictors of performance in alpine World Cup slalom racing. *Scand. J. Med. Sci. Sports* **2011**, *21*, 72–81.
5. Skaloud, J.; Limpach, P. Synergy of CP-DGPS, Accelerometry and Magnetic Sensors for Precise Trajectography in Ski Racing. In Proceedings of the Conference of the ION GPS/GNSS, Portland, OR, USA, 9–12 September 2003.
6. Supej, M.; Holmberg, H.C. A new time measurement method using a high-end global navigation satellite system to analyze alpine skiing. *Res. Q. Exerc. Sport* **2011**, *82*, 400–411.
7. Supej, M. 3D measurements of alpine skiing with an inertial sensor motion capture suit and GNSS RTK system. *J. Sports Sci.* **2010**, *28*, 759–769.
8. Gilgien, M.; Singer, J.; Rhyner, H. Comparison of Two Methods to Assess the Choice of Skier Trajectories through Banked Turns in Ski Cross. In Proceedings of the 5th International Congress on Science and Skiing, St. Christoph, Austria, 14–19 October 2010.
9. Supej, M.; Saetran, L.; Oggiano, L.; Ettema, G.; Saarabon, N.; Nemec, B.; Holmberg, H.C. Aerodynamic drag is not the major determinant of performance during giant slalom skiing at the elite level. *Scand. J. Med. Sci. Sports* **2013**, *23*, e38–e47.

10. Federolf, P. Quantifying instantaneous performance in alpine ski racing. *J. Sports Sci*. **2012**, *30*, 1063–1068.
11. Lüthi, A.; Federolf, P.; Fauve, M.; Oberhofer, K.; Rhyner, H.; Amman, W.; Stricker, G.; Schiefermüller, C.; Eitzlmair, E.; Schwameder, H.; *et al*. Determination of Forces in Carving Using Three Independent Methods. In Proceedings of the 3rd International Congress on Science and Skiing, St. Cloud State University, Aspen, CO, USA, 28 March 2004.
12. Schiestl, M.; Kaps, P.; Mossner, M.; Nachbauer, W. Snow Friction and Drag during the Downhill Race in Kitzbuhel. In Proceedings of the Program and Abstracts, Mountain and Sport: Updating Study and Research from Laboratory to Field, Rovereto, Italy, 11–12 November 2005.
13. Reid, R.; Gilgien, M.; Haugen, P.; Kipp, R.; Smith, G. Force and Energy Characteristics in Competitive Slalom. In Proceedings of the 5th International Congress on Science and Skiing, St.Christoph, Austria, 14–19 October 2010; Müller, E., Lindinger, S., Stoggl, T., Eds.; Meyer & Meyer Sport: Aachen, Germany.
14. Gilgien, M.; Reid, R.; Haugen, P.; Kipp, R.; Smith, G. External Forces Acting in Direction of Travel and Their Relation to Energy Dissipation in Slalom. In Proceedings of the 14th Annual Congress of the European College of Sport Science, Oslo, Norway, 13 July 2009.
15. Meyer, F.; Le Pelley, D.; Borrani, F. Aerodynamic drag modeling of alpine skiers performing giant slalom turns. *Med. Sci. Sports Exerc*. **2011**, *44*, 1109–1115.
16. Madura, JM.; Lufkin, T.; Brown C. Calculated Descent Times for Different Radii in Ski Racing. In Proceedings of 5th International Congress on Science and Skiing, St. Christoph, Austria, 14–19 October 2010.
17. Brodie, M.; Walmsley, A.; Page, W. Fusion motion capture: A prototype system using IMUs and GPS for the biomechanical analysis of alpine ski racing. *Sports Tech*. **2008**, *1*, 17–28.
18. Huber, A.; Spitzenpfeil, P.; Waibel, K.; Debus, D.; Fozzy, M.E. CRIPS-Crash Recognition and Injury Prevention in Alpine Ski Racing. In Proceedings of the 5th International Congress on Science and Skiing, St. Christoph, Austria, 14–19 October 2010.
19. De Berg, M.; Otfried, C.; van Kreveld, M.; Overmars, M. *Computational Geometry: Algorithms and Applications*, 3rd ed.; Springer-Verlag: Berlin, Germany, 2008.
20. Gilgien, M.; Reid, R.; Haugen, P.; Smith, G. Digital Terrain Modelling of Snow Surfaces for Use in Biomechanical Investigations in Snow Sports. In Proceedings of the 13th Annual Congress of the European College of Sport Science, Lisboa, Portugal, 9–12 July 2008.
21. Hugentobler, M. Terrain Modelling with Triangle Based Free-Form Surfaces. Ph.D. Thesis, ETH Zurich, Zurich, Switzerland, 2004.
22. Supej, M.; Kugovnik, O.; Nemec, B. Kinematic determination of the beginning of a ski turn. *Kinesiol. Slov*. **2003**, *9*, 11–17.
23. Morawski, J.M. Control systems approach to a ski-turn analysis. *J. Biomech.* **1973**, *6*, 267–279.
24. Gilat, A.; Subramaniam, V. *Numerical Methods for Engineers and Scientists*, 2nd ed.; Wiley & Sons Inc.: Hoboken, NJ, USA, 2008.
25. Gilgien, M.; Spörri, J.; Kröll, J.; Chardonnens, J.; Cabri, J.; Müller, E. Speed as an Injury Risk Factor in Competitive Alpine Ski Racing Depends on Events. In Proceedings of the 17th Annual Congress of the European College of Sport Science, Bruges, Belgium, 4–7 July 2012.
26. Van Ingen, S.G.J. The influence of air friction in speed skating. *J. Biomech.* **1982**, *15*, 449–458.

27. Barelle, C.; Ruby, A.; Tavernier, M. Experimental model of the aerodynamic drag coefficient in alpine skiing. *J. Appl. Biomech.* **2004**, *20*, 167–176.
28. Spörri, J.; Kröll, J.; Schwameder, H.; Schiefermuller, C.; Müller, E. Course setting and selected biomechanical variables related to injury risk in alpine ski racing: An explorative case study. *Br. J. Sports Med*. **2012**, *46*, 1072–1077.
29. Drenk, V. Bildmeßverfahren für schwenk und neigbare sowie in der Brennweite variierbare Kameras; Institut für Angewandte Trainingswissenschaft, Bundesinstitut für Sportwissenschaft, Köln, Germany, 1994; pp. 130–142.
30. Zatsiorsky, V.M. *Kinetics of Human Motion*, 1st ed.; Human Kinetics Inc.: Champaign, IL, USA, 2002.
31. De Leva, P. Adjustments to Zatsiorsky-Seluyanov's segment inertia parameters. *J. Biomech.* **1996**, *29*, 1223–1230.
32. Gilgien, M. External Forces Acting in Direction of Travel and Their Relation to Energy Dissipation in Slalom. M.Sc. Thesis, Norwegian School of Sport Sciences: Oslo, Norway, 1 November 2010.
33. Klous, M.; Müller, E.; Schwameder, H. Collecting kinematic data on a ski/snowboard track with panning, tilting, and zooming cameras: Is there sufficient accuracy for a biomechanical analysis? *J. Sports Sci*. **2010**, *28*, 1345–1353.
34. Babiel, S.; Hartmann, S.; Spitzenpfeil, P.; Mester, J. Ground Reaction Forces in Alpine Skiing, Cross-Country Skiing and Ski Jumping. In *Science and Skiing III*; Müller, E., Bacharach, D., Klika, R., Schwameder, H., Lindinger, S., Eds.; E&FN Spon: London, UK, 1997; pp. 200–207.
35. Federolf, P.; Fauve, M.; Luthi, A.; Rhyner, H.; Ammann, W.; Dual, J. Finite Element Simulation of a Carving Alpine Ski. In Proceedings of the 3rd International Congress on Science and Skiing, Saint Cloud, MN, USA, 28 March 2004.
36. Müller, E.; Schwameder, H. Biomechanical aspects of new techniques in alpine skiing and ski-jumping. *J. Sport Sci*. **2003**, *21*, 679–692.
37. Nakazato, K.; Scheiber, P.; Müller, E. A comparison of ground reaction forces determined by portable force-plate and pressure-insole systems in alpine skiing. *J. Sports Sci. Med*. **2011**, *10*, 754–762.
38. Holden, M.; Parker, R.; Walsh, A. Dynamic Force Measurement Technique to Evaluate Skier Performance. In Proceedings of the 3rd International Congress on Science and Skiing, Saint Cloud, MN, USA, 28 March 2004.
39. Kruger, A.; Edelmann-Nusser, J. Biomechanical analysis in freestyle snowboarding: Application of a full-body inertial measurement system and a bilateral insole measurement system. *Sports Technol*. **2009**, *2*, 17–23.
40. Klous, M.; Müller, E.; Schwameder, H. Knee Joint Loading an Alpine Skiing: A Comparison between Carved and Skidded Turns. In Proceedings of the 13th Annual Congress of the European College of Sport Science, Lisboa, Portugal, 9–12 July 2008.
41. Niessen, M.; Müller, E.; Wimmer, M.A.; Schwameder, H.; Riepler, B. Force and Moment Measurements during Alpine Skiing Depending on Height Position. In Proceedings of the 16th International Symposium on Biomechanics in Sports, Konstanz, Germany, 21–25 July 1998.

42. Wunderly, G.S.; Hull, M.L.; Maxwell, S. A second generation microcomputer controlled binding system for alpine skiing research. *J. Biomech.* **1988**, *21*, 299–318.
43. Wunderly, G.S.; Hull, M.L. A biomechanical approach to alpine ski binding design. *Int. J. Sport Biomech.* **1989**, *5*, 308–323.
44. Federolf, P.; Scheiber, P.; Rauscher, E.; Schwameder, H.; Luthi, A.; Rhyner, H.U.; Müller, E. Impact of skier actions on the gliding times in alpine skiing. *Scand. J. Med. Sci. Sports* **2008**, *18*, 790–797.
45. Chardonnens, J.; Favre, J.; Gremion, G.; Aminian, K. Knee Joint Kinematics Measurement in Alpine Skiing Based on Inertial Sensors. In Proceedings of the 5th International Congress on Science and Skiing, St. Christoph, Austria, 14–19 October 2010.
46. Gilgien, M. GNSS-Anwendungen im Schneesport-Leistungsoptimierung und Verletzungs-Prophylaxe. *AHORN, Der Alpenraum und seine Herausforderungen im Bereich Orientierung, Navigation und Informationsaustausch*; Schweizerisches Institut für Navigation (ION-CH): Davos, Switzerland, 2012.

Paper III

Paper IV

Paper V

Paper VI

Mechanical parameters related to injury risk in World Cup alpine skiing – a comparison between the competition disciplines.

Matthias Gilgien,[1] Jörg Spörri,[2] Josef Kröll,[2] Philip Crivelli,[3] Erich Müller,[2]

[1]Norwegian School of Sport Sciences, Department of Physical Performance, Oslo, Norway

[2]University of Salzburg, Department of Sport Science and Kinesiology, Hallein-Rif, Austria

[3]WSL - Institute for Snow and Avalanche Research SLF, Group for Snowsports, Davos, Switzerland

Keywords:

Alpine Skiing; Injury; Injury Prevention; Biomechanics; Global Navigation Satellite System

What are the new findings

This is the first study comprehensively quantifying the mechanical characteristics of World Cup Alpine Skiing under real race conditions.

This study reveals that World Cup Alpine Skiing is equally dangerous per unit time for the disciplines giant slalom, super-G and downhill

Injuries in giant slalom seem to be linked to high loads while turning; injuries in downhill and super-G to jumps and high speed and the mechanical energy involved in crashing

How might it impact on clinical practice in the near future

The quantification of World Cup ski racing mechanics might allow future studies to use the correct order of magnitude of skier mechanical parameters.

The study showed that future research should be conducted discipline specific.

The role of exposure time is highlighted and might influence future research.

ABSTRACT

Background / Aim In alpine ski racing, there is limited information about skiers' mechanical characteristics and their relation to injury risk, in particular for World Cup (WC) competitions. Hence, current findings from epidemiologic and qualitative research cannot be linked to skiers' mechanics. This study was undertaken to investigate whether recently reported differences in numbers of injuries per 1000 runs for competition disciplines can be explained by differences in the skiers´ mechanics.

Methods During 7 giant slalom, 4 super-g and 5 downhill WC competitions, mechanical characteristics of a forerunner were captured using differential global navigation satellite technology and a precise terrain surface model. Finally, the discipline-specific skiers´ mechanics were compared to the respective number of total exposure-time normalized injuries (injuries per hour).

Results While the number of injuries per hour skiing was approximately equal for all disciplines, kinetic energy, impulse, run time, turn radius and turn speed were significantly different and increased from giant slalom to super-G and downhill. Turn ground reaction forces were largest for giant slalom, followed by super-G and downhill. The number of jumps was doubled from super-G to downhill.

Conclusions Associating the number of injuries per hour in WC skiing with skiers' mechanical characteristics, injuries in super-G and downhill seem to be related to increased speed and jumps, while injuries in giant slalom may be related to high loads in turning. The reported differences in numbers of injuries per 1000 runs might be explained by a bias in total exposure time per run and thus potentially by emerged fatigue.

INTRODUCTION

Competitive alpine skiing is considered to be a sport with a high injury risk [1;2]. Injury rates per competition season and per 100 World Cup (WC) athletes were reported to be 36.7, with the knee the most frequently affected body part [1;3]. Injury rates were found to be dependent on the discipline (for males: slalom: 7.5 injuries per 1000 runs, giant slalom: 12.8, super-G: 14.5, and downhill: 19.3) [1]. Based on these findings it was hypothesized that injury risk increases with speed [1]. In a qualitative study based on expert stakeholders´ opinions, high speed was also considered as an injury key risk factor leading to large impact energies and high turn forces [2]. However, as recently illustrated, speed might not be the only factor related to injury risk: out-of-balance situations while turning or landing and fatigue might be other important factors increasing injury risk [4;5]. Moreover, a recent experimental study in giant slalom showed that speed, the risk of out-of-balance situations, turn force and probably fatigue might be dependent on course setting [6]. Hence, these factors might serve as additional explanatory approaches for the differences in the number of injuries per 1000 runs among the disciplines.

Despite the large body of knowledge about injury rates [1;3;7;8] and injury risk factors [2;4-6;9], current knowledge about mechanical parameters and their relation to injury risk is limited and is lacking data collected during WC competitions .However, since injury rates per 1000 runs are higher during competitions than during normal training sessions on snow [1], these data are essential in order to associate the known injury rates with the mechanical characteristics of the disciplines. Consequently, the aims of this study were firstly to establish a quantitative understanding of the mechanical characteristics of WC Alpine skiing for the disciplines giant slalom, super-G and downhill, and secondly to investigate whether the differences in the number of injuries per 1000 runs among the disciplines can be explained by differences in the skiers´ mechanics.

METHODS

Measurement protocol

Seven WC giant slalom (GS) races, (14 runs in total at Sölden, Beaver Creek, Adelboden, Hinterstoder, Crans Montana), 4 super-G (SG) races, (4 runs in total at Kitzbühel, Hinterstoder, Crans Montana) and 5 downhill (DH) races, (16 runs in total at Lake Louise, Beaver Creek, Wengen, Kitzbühel, Åre) were monitored during the WC season 2010/11 and 2011/12. In the GS discipline each single run was included in the analysis. In DH official competition training runs were also used. If several DH runs were measured in one race location they were treated as repeated measures in the analysis. At each race one forerunner, who was part of the official forerunner group, was equipped to collect data for this study. All of those forerunners were former WC or current European Cup racers.

This study was approved by the Ethics Committee of the Department of Sport Science and Kinesiology at the University of Salzburg.

Data collection methodology

The forerunner's trajectory was captured using a differential global navigation satellite system (dGNSS). The dGNSS antenna (G5Ant-2AT1, Antcom, USA) was mounted on the skier's helmet and a GPS/GLONASS dual frequency (L1/L2) receiver (Alpha-G3T, Javad, USA) recorded position signals at 50Hz. The receiver was carried in a small cushioned backpack. Differential position solutions of the skier trajectory were computed using the data from two base stations (antennas (GrAnt-G3T, Javad, USA) and Alpha-G3T receivers (Javad, USA)) and the geodetic post-processing software GrafNav (NovAtel Inc., Canada).

The snow surface geomorphology was captured using static dGNSS (Alpha-G3T receivers with GrAnt-G3T antenna (Javad, USA) and Leica TPS 1230+ (Leica Geosystems AG, Switzerland)). Using the surveyed snow surface points, a digital terrain model (DTM) was computed by Delaunay triangulation [10] and smoothing with bi-cubic spline functions [11;12].

Parameter computation

The antenna trajectory and the DTM were used as input parameters for a mechanical model [13;14] from which the instantaneous skier turn radius, speed, air drag force (F_D) and ground reaction force (F_{GRF}) were reconstructed. The applied data capture and parameter reconstruction method was validated against reference methods for position, speed and forces [13;14]. Using speed and the skier's mass the skier kinetic energy (E_{kin}) was computed. The impulse of F_{GRF} and F_D were calculated for the entire race and added (I_{GRF+D}) as shown in equation 1. I_{GRF+D} might account for the major part of the processes causing fatigue. The race time was measured with the official race timing system.

The jump frequency per race (J_f), air time (J_t) and distance (J_d) per jump were determined from the skier trajectory and the DTM. The time of take-off was determined from the distance over ground and the touch-down from the peak of the vertical acceleration. J_d and J_t were computed from the spatial and temporal difference between take-off and touch-down locations.

$$I_{GRF+D} = \int_{Start}^{Finish} F_{GRF} \cdot dt + \int_{Start}^{Finish} F_D \cdot dt \qquad (1)$$

Epidemiologic injury data from the FIS ISS injury surveillance system[1] were used to compute exposure-time independent injury rates. Exposure time was defined as the average race time per discipline and was calculated as the mean of all race medians involving all racers who finished the race. The data for the exposure time analysis were taken from the fis-ski.com webpage and represented the same two seasons (2006/7 and 2007/8) in which the injury data was collected. Finally, exposure-time normalized incidence rates, injuries per hour, were computed for each discipline as the (number of injuries in WC races) / (average run time * number of runs in WC races) and were compared to the skier's mechanical characteristics.

Statistical Analysis

For Ekin, I_{GRF+D}, run time, J_f, J_t, and J_d, the mean and SD were calculated within each discipline and compared as a percentage of the DH values. The medians of each discipline were compared using a Kruskal - Wallis test ($\alpha = 0.01$). The distributions between and within disciplines were illustrated in histograms for speed, turn radius and F_{GRF}. Straight skiing was defined by a minimum turn radius of 125m for all disciplines. To compare turn characteristics between the disciplines, the phases with substantial direction change were defined and analyzed based on a maximal turn radius criterion: 30m in GS [6] and proportional criteria for SG (75m) and DH (125m). The mean of the turn means was calculated for turn speed, turn F_{GRF} and turn radius within each discipline. The extreme values (minimum for turn radius, maximum for turn speed and F_{GRF}) were calculated for each single turn and the values of the turns with the 10% most extreme values were averaged within each discipline. The median of each discipline was compared using a Kruskal - Wallis test ($\alpha = 0.01$).

RESULTS

The exposure-time normalized injury rates are given in Table 1. The number of injuries per hour was highest for GS, followed by SG, DH and SL. While the differences between DH, SG and GS were less than 2%, SL had an 18% lower injury rate than DH.

Table 1 *Calculation of the exposure time normalized injury rates. The number of injuries and the number of runs were taken from Florenes et al.[1]. The exposure time normalized injury risk rate was calculated as number of injuries divided by the exposure time.*

Discipline	# Injuries	# Runs	Mean Run time [s]	Exposure time [h]	Incidence (injuries/hour)	% of DH *
SL	14	1864	53.00	27.44	0.510	81.7
GS	14	1090	75.40	22.83	0.613	98.3
SG	9	620	83.38	14.36	0.627	100.4
DH	25	1292	111.62	40.06	0.624	100.0

* DH is 100% for the respective measures.

The distributions within and between disciplines for turn speed, turn radius and F_{GRF} are shown in Figure 1. For F_{GRF} distributions between disciplines were similar, with the largest variance for GS and the smallest for DH. Turn speed and turn radius had larger distribution differences between disciplines. DH had the largest mean turn radius, while GS had the smallest mean turn radius. Straight skiing (turn radius of >125m) occurred for approximately 45% of the time in DH, 20% of the time in SG and 7% of the time in GS.

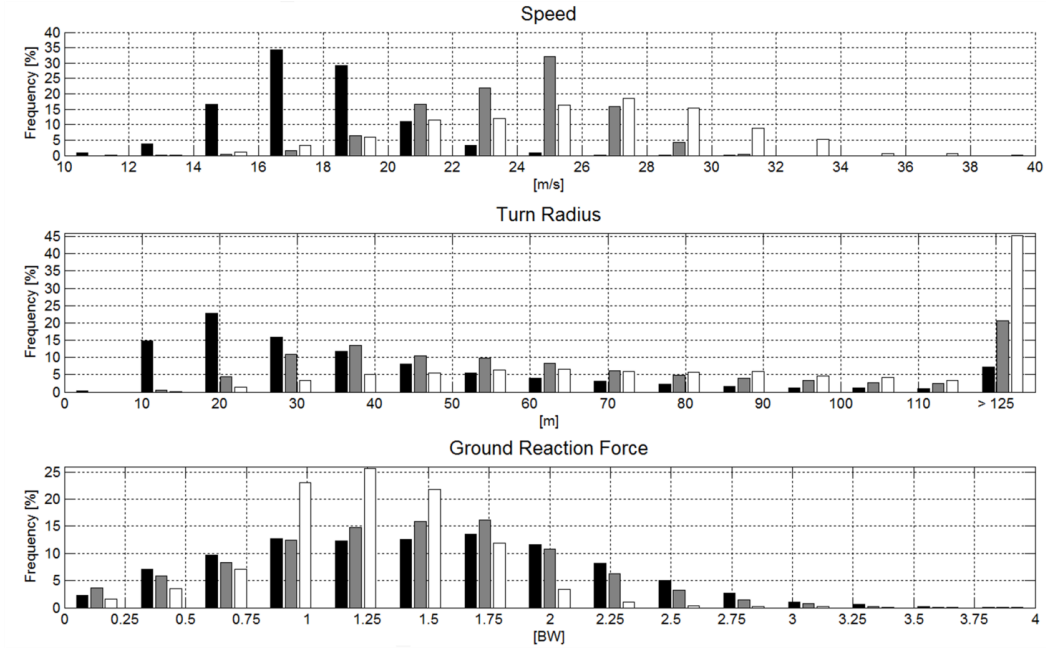

Figure 1. *Histograms for speed, turn radius and ground reaction force. GS is shown in black, SG in gray and DH in white*

Skier mechanical characteristics specific for turning are presented in Table 2. For the turns, limited by maximal turn radii of 30m (GS), 75m (SG) and 125m (DH), the mean and extreme values of turn speed, turn radius and turn F_{GRF} are presented. While turn speed and turn radius mean and extreme values increased from GS to SG and DH, they decreased for turn F_{GRF}. The medians were significantly different ($\alpha = 0.01$) between disciplines for all parameters.

Table 2 *Turn characteristics: mean values, extreme values and % of DH for the disciplines GS, SG and DH.*

		Mean and extreme values for turns			**% of DH** *	
		GS	**SG**	**DH**	**GS**	**SG**
Turn Speed [m/s]	Mean	17.32	22.7	24.0	72	95
	Max	22.2	28.3	32.3	69	88
Turn Radius [m]	Mean	22.7	52.0	61.6	37	84
	Min	8.4	17.2	20.6	41	84
Turn F_{GRF} [BW]	Mean	2.02	1.58	1.43	141	110
	Max	3.16	2.79	2.59	122	108

* DH is 100% for the respective measures.

The mean, SD and % of DH values for E_{KIN}, I_{GRF+D}, run time and jump characteristics for the entire runs are given in Table 3. All mean values were largest for DH, followed by SG and GS for all parameters. SG consisted of about half the number of jumps compared to DH, while GS had none. The jumps were about 20% shorter in SG compared to DH, but airtime was reduced by only 6%. The medians were significantly different ($\alpha = 0.01$) between disciplines for all parameters except the jump parameters.

Table 3 *Mean and SD values for disciplines GS, SG and DH and as % of DH for SL, GS and SG.*

	Mean ± SD in absolute values			**% of DH** *	
	GS	**SG**	**DH**	**GS**	**SG**
E_{KIN} [BW·m]	15.5±4.0	27.9±6.1	32.7±10.7	47	85
I_{GRF+D} [kBW·s]	124.3±12.5	153.0±13.3	173.4±25.3	71	88
Run time [s]	77.4±5.2	92.9±9.7	121.4±17.7	64	76
# jumps / race	-	2.3±0.8	4.2±1.5	-	55
Jump length [m]	-	23.8±9.9	30.2±10.4	-	79
Jump airtime [s]	-	0.98±0.44	1.04±0.44	-	94

* DH is 100% for the respective measures.

Associating skiers' mechanical characteristics with injury rates, Figure 2 shows the mean and extreme values of turn speed, turn radius and turn F_{GRF} compared to the injury rates. Injuries per hour were similar between disciplines, while injuries per 1000 runs and mean and extreme values increased from GS to SG and DH for turn speed, turn radius and for kinetic energy of the entire run. The difference in turn radius mean and minimum was substantial between GS and the speed disciplines. F_{GRF} in turns increased from DH to SG and GS.

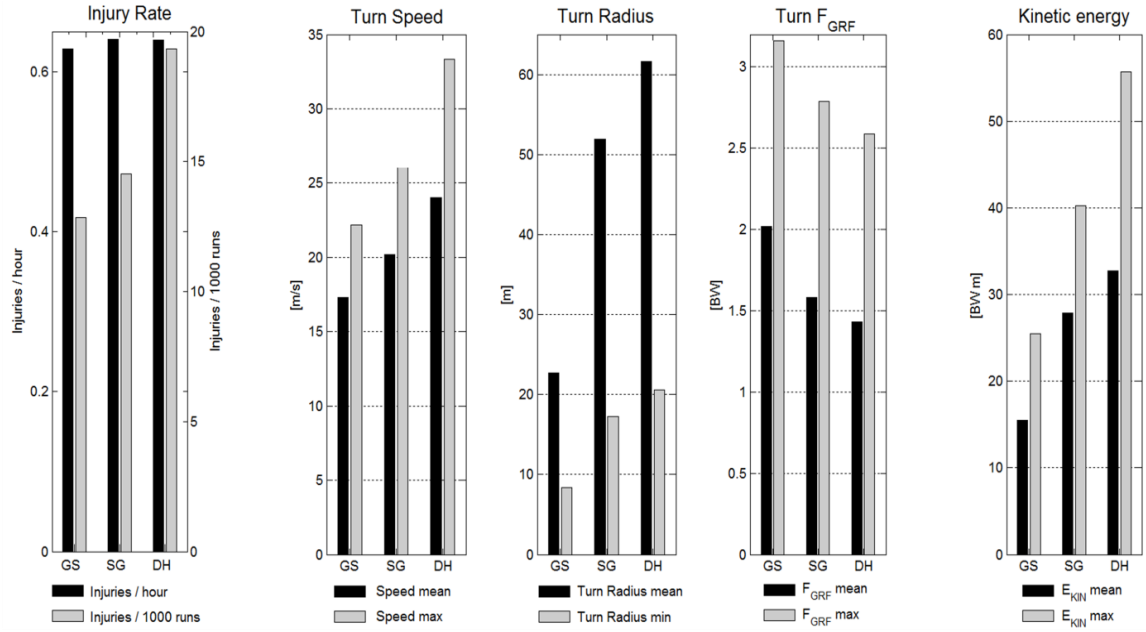

Figure 2. *Comparison of injury rates (left graph), skiers' characteristics in turns (turn speed, turn radius and turn FGRF, in middle) and skiers' kinetic energy for entire runs. For injury rates, injuries per hour are shown in black and injuries per 1000 runs in gray. For skiers' mechanical characteristics, mean values are shown in black and extreme values in gray.*

DISCUSSION

The main findings of this study were that 1) the exposure-time normalized injury rate (injuries per hour) was similar for GS, SG and DH; 2) DH consisted of 45% straight skiing, SG of 20% and GS of 7%; 3) in turns, turn speed and turn radius were largest in DH, followed by SG and GS, while the ranking was inverse for F_{GRF}; 4) kinetic energy, impulse due to F_{GRF} and air drag and run time were largest for DH, followed by SG and GS; 5) jump frequency, jump length and airtime were larger for DH than SG.

Mechanics of Turning

It has recently been found that many injuries occur while turning, without falling or being the result of a crash [4]. Figure 1 shows that skiers are turning for approximately 55% of the time in DH, 80% in SG and 93% in GS. Moreover, it was shown that small turn radii might be related to an increased injury risk in GS since they provoke the skiers to use their full backward and inward leaning capacities and thus skiers have less buffer if an additional factor causes an out-of-balance situation [6]. Out-of-balance situations themselves are known to be a critical part of typical injury mechanisms, such as the "slip-catch" and "dynamic snowplow" [4;5;13]. Comparing the mean and minimal turn radii between disciplines from Figure 2 and Table 3, it is evident that GS has substantially smaller turn radii than SG and DH. Additional analysis of the data showed that the radial component is the main contributor to the increased F_{GRF} in GS. Thus the combination of small turn radii and speed leads to larger mean and maximum F_{GRF} in GS compared to SG and DH. Furthermore, in GS, skiers' balance might be challenged simultaneously by small turn radii and high forces. Measures to prevent injuries in GS should therefore focus on both speed and turn radius. Suitable tools might be course setting and equipment. Furthermore, GS includes a larger number of turns (52.0 ± 3.5) compared to SG (40.0 ± 3.5) and DH. Hence skiers have to find balance in turning more frequently in a run and thus might be more often susceptible to balance-related mistakes in turn initiations.

Speed and Kinetic Energy

Speed in general is considered a major injury risk factor in competitive alpine skiing [1;2]. It has been hypothesized that the differences in speed might be the reason for the higher numbers of injuries per 1000 runs in the speed disciplines [1]. Comparing the number of injuries per hour and kinetic energy in Figure 2, no direct relationship is apparent, since speed increased from GS to SG and DH while the exposure-time normalized injury rates were almost constant across the disciplines. This finding indicates that speed might not be the sole factor explaining the differences in injury rates between disciplines. Nevertheless, speed might have several major impacts on injury risk, especially in DH and SG. In technically demanding sections (e.g. jumps, rough terrain and turns), anticipation and

adaptation time decrease with speed and mistakes might be more likely to occur. Furthermore, for a given jump, jump distance and air time increase with speed and a mistake at take-off might have more severe consequences. In crash situations speed has a significant impact, since the energy which is dissipated in an impact increases with speed by the power of 2 (E_{KIN} = mass·speed^2/2) and E_{KIN} is almost doubled from GS to DH. The forces occurring in a crash impact are dependent on both the impact energy and the timespan of the energy dissipation process. Safety barriers are therefore built so that they can give way to a certain extent in order to increase the time of the impact process and thus decrease the impact forces. Hence, the functionality [15;16] and positioning of protective barriers is highly important in speed disciplines. Measures to prevent injuries in SG and DH should aim at reducing speed at spots where skiers are likely to crash. Since turn forces are generally lower compared to GS and SG it might be reasonable to use course setting to radically slow down skiers at locations where crashes are likely to occur.

Fatigue

Fatigue is a known injury risk factor [2]. A recent study showed that most injuries occur during the last fourth of a race [4]. It is further known that fatigue has a negative effect on balance [17;18] and thus fatigued athletes might be more susceptible to out-of-balance situations and injuries [6]. Since fatigue cannot be measured directly, in the current study race time and impulse were calculated as approximations of the work load over the entire run. I_{GRF+D} per run showed an increase from GS to SG and DH along with an increase in the number of injuries per 1000 runs. Analyses of the causes for the differences in impulse between disciplines revealed that run time contributed to a larger extent to the impulse than the forces. Consequently the fatigue related parameter impulse is strongly linked with exposure time. Exposure time (and fatigue) seems to explain the increased injury rate per 1000 runs for the speed disciplines to a large extent. Two seasons of epidemiologic data is a relatively small amount for the computation of injury rates, but the trend between run time and injury incidences per 1000 runs is apparent. If epidemiologic studies could pinpoint when accidents occur in a race for the respective disciplines, the role of fatigue could probably be better clarified.

Jumps

Jumps are considered to contribute to the high injury rates [2]. The number of jumps in DH is nearly double that in SG. However, no epidemiologic study has ever pinpointed the number of injuries occurring at jumps in the respective disciplines. Hence, it has not been possible as yet to relate jump characteristics to injury risk.

An imbalance at the jump take-off can lead to an angular momentum during the time the skier is airborne. Since the angular momentum is only influenced by air drag as long as the skier is airborne, the time until landing is critical. A longer airtime leads to a larger rotation angle and a more critical body position at landing. In the current study it was found that flight distance was 21% shorter in SG compared to DH, while air time was only 6% shorter in SG compared to DH. This finding leads to the conclusion that an angular momentum during airtime can also lead to large rotation angles in SG. Since many severe injuries [4] seem to occur at jumps, the mechanics of jumping and its relation to injury risk should be investigated in more detail.

LIMITATIONS

The approach of measuring for the first time under competition conditions in WC alpine skiing adds valuable new perspectives to the investigation of injury risk factors. However, there are some limitations related to the methods used in the current study.

First, the model for the computation of the F_{GRF} does not capture the high frequency force components and, therefore, might underestimate the work load (impulse), in particular for GS.

Second, for the computation of impulse, the method used does not account for body position. Consequently, the work load during straight gliding sections in DH, where skiers are in a deep tuck position, might be underestimated compared to GS, where skiers are in more extended body positions.

Third, the forerunners who captured the data for this study skied slightly slower than the WC skiers. The time difference between our forerunners and the median of all skiers who completed the run was 2.4±2.1% for GS, 1.3±2.3% for SG and 5.29±1.2% for DH. Hence the data in this study slightly underestimate the mechanical characteristics of a typical WC skier.

CONCLUSIONS

This study showed that the disciplines in WC alpine skiing are approximately equally dangerous per time unit. In contrast, the skiers' mechanical characteristics were significantly different. Therefore, it is likely that the causes and mechanisms of injury are different for the specific disciplines. In SG and DH, injuries might be mainly related to higher speed and jumps, while injuries in the technical disciplines might be related to a combination of turn speed and turn radius resulting in high loads. Therefore, future epidemiologic and qualitative studies should pinpoint types of injuries and injury mechanics in each discipline in order to facilitate suitable injury-prevention measures for the specific disciplines.

Another interesting finding of this study is the fact that the number of injuries per 1000 runs showed a similar increase (from GS to DH) to the parameters of race duration and impulse. Hence, the recently reported higher number of injuries per 1000 runs in downhill might not only be explained by speed, but also by a bias of total exposure time and thus potentially by emerged fatigue.

ACKNOWLEDGMENTS

We would like to thank Geo Boffi, Rüdiger Jahnel, Julien Chardonnens, Jan Cabri, the International Ski Federation staff and race organizers for their support.

COMPETING INTERESTS

None

FUNDING

This study was financially supported by the International Ski Federation (FIS) Injury Surveillance System (ISS). The funding source had no involvement in the study design; in the collection, analysis and interpretation data; in the writing of the report; or in the decision to submit this paper for publication.

CONTRIBUTORSHIP STATEMENT

JS, JK and EM conceptualized and coordinated the study. MG, JS, JK and EM contributed to study design and data collection. MG contributed the data collection methodology. MG and PC conducted data processing and analysis. All authors contributed to the intellectual content and manuscript writing and approved its content.

REFERENCES

(1) Florenes TW, Bere T, Nordsletten L,et al. Injuries among male and female World Cup alpine skiers. Br J Sports Med 2009;43(13):973-8.

(2) Spörri J, Kröll J, Amesberger G, et al. Perceived key injury risk factors in World Cup alpine ski racing an explorative qualitative study with expert stakeholders. Br J Sports Med 2012;46(15):1059-64.

(3) Florenes TW, Nordsletten L, Heir S, et al. Injuries among World Cup ski and snowboard athletes. Scand J Med Sci Sports 2012;22(1):58-66.

(4) Bere T, Florenes TW, Krosshaug T, et al. A systematic video analysis of 69 injury cases in World Cup alpine skiing. Scand J Med Sci Sports 2013;Published Online First Jan 10. doi: 10.1111/sms.12038.

(5) Bere T, Florenes TW, Krosshaug T, et al. Mechanisms of anterior cruciate ligament injury in World Cup alpine skiing: a systematic video analysis of 20 cases. Am J Sports Med 2011;39(7):1421-9.

(6) Spörri J, Kröll J, Schwameder H, et al. Course setting and selected biomechanical variables related to injury risk in alpine ski racing: an explorative case study. Br J Sports Med 2012 ;46(15):1072-7.

(7) Ekeland A, Nordsletten L. Equipment related injuries in skiing. Recommendations. Sports Med 1994;17(5):283-7.

(8) Pujol N, Blanchi M, Chambat P. The incidence of anterior cruciate ligament injuries among competitive Alpine skiers: A 25-year Investigation. Am J Sports Med 2007;35(7):1070-4.

(9) Raschner C, Platzer H, Patterson C, et al. The relationship between ACL injuries and physical fitness in young competitive ski racers: a 10-year longitudinal study. Br J Sports Med 2012;46(15):1065-71.

(10) de Berg M, Otfried C, van Kreveld M, Overmars M. Computational Geometry: Algorithms and Applications. Berlin: Springer Verlag; 2008.

(11) Hugentobler M. Terrain Modelling with Triangle Based Free-Form Surfaces. Zürich: Universität Zurich, Switzerland; 2004.

(12) Gilgien M, Reid R, Haugen P, et al. Digital terrain modelling of snow surfaces for use in biomechanical investigations in snow sports. 2008. 13th Annual Congress of the European College of Sport Science; Lisboa, Portugal.

(13) Gilgien M, Spörri J, Chardonnens J, et al. Determination of the centre of mass kinematics in alpine skiing using differential global navigation satellite systems. Submitted to J Sports Sci.

(14) Gilgien M, Spörri J, Chardonnens J, et al. Determination of External Forces in Alpine Skiing Using a Differential Global Navigation Satellite System. Sensors (Basel) 2013;13(8):9821-35.

(15) Petrone N, Ceolin F, Orandin T. Full scale impact testing of ski safety barriers using an instrumented anthropomorphic dummy. Procedia Engineering 2010;2(2):2593-8.

(16) Petrone N, Pollazzon C, Morandin T. Structural Behaviour of Ski Safety Barriers during Impacts of an Instrumented Dummy. The Engineering of Sport 7. Springer Paris; 2008. p. 633-42.

(17) Qu X, Nussbaum MA. Effects of external loads on balance control during upright stance: Experimental results and model-based predictions. Gait Posture 2009;29(1):23-30.

(18) Simoneau M, Begin F, Teasdale N. The effects of moderate fatigue on dynamic balance control and attentional demands. J Neuroeng Rehabil 2006;3(1):22.

Ethics

UNIVERSITÄT SALZBURG

Department of Sport Science and Kinesiology
Ethic Committee

Schlossallee 49 · 5400 Hallein-Rif
Austria · Europe
Tel.: +43/(0)662/8044-4850
Fax: +43/(0)662/8044-614
www.uni-salzburg.at/spo

Salzburg, 2009 01 15

Ethic Committee

Department of Sport Science and Kinesiology

Applicants: 1 MSc ETH Jörg Spörri (University of Salzburg, AT), video-based 3D kinematic methods, main-author

2 Dr. Josef Kröll (University of Salzburg, AT), Pedar and EMG methods, main-author

3 MSc Matthias Gilgien (Norwegian School of Sport Science, NOR), GPS methods, main-author

4 MSc EPFL Julien Chardonnens (EPFL Lausanne, SUI), IMU methods, main-author

(principal investigators)

Project leader: Prof. Dr. Erich Müller

Date of submission: 2010-1-20

Title of the Project:

Part 1: Equipment and biomechanical variables related to injury risk

Part 2: Validation and enhancement of measurement methods

Part 3: Performance analysis

Decision of the ethic committee:

There is no objection to the study “FIS Injury Prevention Studies”.

Date of decision: 2010.02. 08

EC_NR. 2010_03

The decision is based on the following documents: Application

The decision is valid up to the end of the study.

Head of the ethic committee

Prof. Dr. Günter Amesberger